ILLINOIS

UNIVERSITY OF ILLINOIS AT URBANA-CHAMPAIGN

-

PRODUCTION NOTE

UNIVERSITY OF ILLINOIS ENGINEERING EXPERIMENT STATION

Bulletin Series No. 399

A STUDY OF COMBINED BENDING AND AXIAL LOAD IN REINFORCED CONCRETE MEMBERS

Eivind Hognestad

UNIVERSITY OF ILLINOIS BULLETIN

A REPORT OF AN INVESTIGATION

Conducted by

THE ENGINEERING EXPERIMENT STATION
UNIVERSITY OF ILLINOIS

Under auspices of

THE ENGINEERING FOUNDATION

Through

THE REINFORCED CONCRETE
RESEARCH COUNCIL

Price: One Dollar

UNIVERSITY OF ILLINOIS BULLETIN

Volume 49, Number 22; November, 1951. Published seven times each month by the University of Illinois. Entered as second-class matter December 11, 1912, at the post office at Urbana, Illinois, under the Act of August 24, 1912. Office of Publication, 358 Administration Building, Urbana, Illinois.

UNIVERSITY OF ILLINOIS ENGINEERING EXPERIMENT STATION

Bulletin Series No. 399

A STUDY OF COMBINED BENDING AND AXIAL LOAD IN REINFORCED CONCRETE MEMBERS

EIVIND HOGNESTAD
Research Assistant Professor
of Theoretical and Applied Mechanics

Published by the University of Illinois, Urbana

This study was deemed worthy by Norway's Institute of Technology to be defended for the degree *doctor technicae,* doctor of the technical sciences.

Trondheim, Norway
June 4, 1951

Harald Dahl
Rektor

4500—11-51—46924

UNIVERSITY
OF ILLINOIS
PRESS

Dedicated to the memory of
my father
Hans E. Hognestad

ABSTRACT

This bulletin presents the methods and results of an experimental and analytical investigation undertaken in an attempt to throw new light on the behavior of reinforced concrete members subject to combined bending and axial load. It is the purpose of this report to describe observations regarding the basic behavior of such members and to develop mathematical expressions for ultimate loads.

A total of 120 column specimens were tested, 90 of which were 10-in. square tied columns with 1.46 to 4.8 percent reinforcement, and 30 were 12-in. cylindrical spiral columns with 4.25 percent longitudinal reinforcement. The concrete quality was varied from 1500 to 5500 p.s.i., and the eccentricity of loading varied from 0 to 1¼ times the lateral dimension of the columns.

An inelastic flexural theory was developed, by means of which the behavior of the test columns may be explained and the measured ultimate loads may be predicted with a satisfactory accuracy.

CONTENTS

FIGURES

TABLES

I. INTRODUCTION

1. Historical Review

The subject of strength of materials has from the earliest developments, due to the very nature of the problems involved, been a science of empirical character. This is particularly so in the case of concrete and reinforced concrete. The first attempts to establish a mathematical design procedure for reinforced concrete were all aimed at an agreement with load carrying capacities determined in tests. In modern terms, several of these early theories may be referred to as the *inelastic* or *ultimate* theories.

A rational analysis of simple reinforced concrete slabs subject to bending was first published by M. Koenen in 1886[1]*, and many other theories were published shortly after.[2, 3, 4, 5, 6, 7, 8, 9] Some characteristic basic assumptions of these early theories are reviewed in Fig. 1.

Navier's theory of bending, based on Bernoulli's assumption regarding plane sections remaining plane and Hooke's Law, was well known in the 1890's. Thus, it is a reasonable fact that the Coignet-Tédesco theory (Fig. 1) became generally accepted almost immediately after its publication in 1894.[3] The majority of the authors referred to in Fig. 1 conceded that this latter theory was accurate enough for design purposes and had great advantages in its mathematical simplicity. Hence, the "straight-line" or "standard" theory became established at the turn of the century, and a very rapid development in the use of reinforced concrete as a construction material followed.

The scientific studies of reinforced concrete were continued on a steadily broadening scope through the work of such men as Bach, Considère, Emperger, Graf and Mörsch. In this country, the researches of Talbot and Withey may have made the most important contributions. Much experimental work was done in these first decades of our century, but few new ideas of importance regarding the basic assumptions involved in reinforced concrete design were developed.

The standard theory, on the other hand, became so widely used that the approximative character of this theory was forgotten, and applications beyond its range of validity resulted. When beams were designed with an allowable concrete compressive stress, f_c, equal to

* Parenthesized superscript numbers refer to the bibliography at the end of this bulletin.

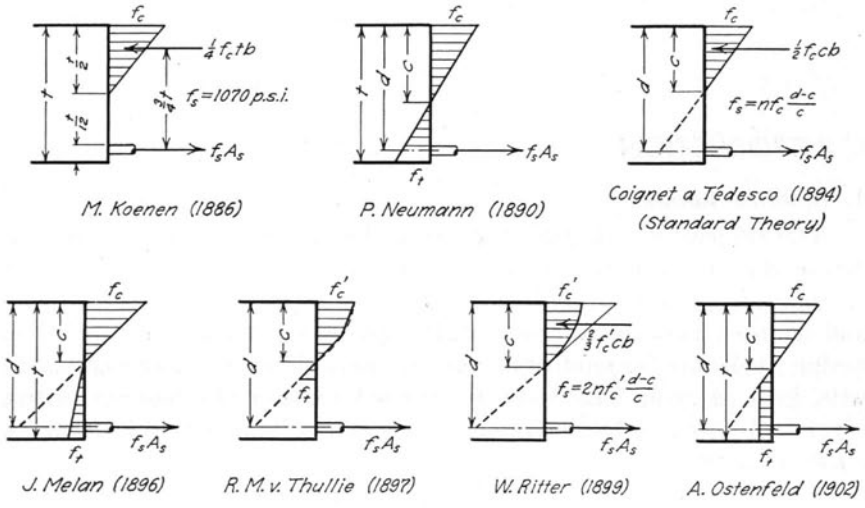

Fig. 1. Early Assumptions in Flexural Analysis

0.325 times the strength of 6- by 12-in. cylinders, f_c', it was at times erroneously concluded that the safety factor against a compression failure was near three. In the period from 1920 to 1930, Slater, Zipprodt and Lyse made valuable contributions in pointing out that the safety factor in the case mentioned above generally is considerably larger than that indicated by the ratio f_c'/f_c, thus re-emphasizing the actual inelastic behavior of concrete.[16, 24]

Another important development took place in the decade from 1920 to 1930. Before that time, bending stresses were generally neglected in the design of concrete building columns, and such stresses were assumed to be provided for, together with other effects, in an all-inclusive factor of safety. This neglect was mainly due to the lack of suitable methods for structural analysis of monolithic structures. Two major methods were developed to meet this lack of information. The Slope-Deflection Method appeared in 1918,[15a] and the Moment Distribution Method followed.[23a, 35a] The moments of inertia used in these methods have generally been based on the uncracked section. Recent extensive tests of structures[65, 69a] have shown that this application of P. Neumann's 60-year-old theory (Fig. 1) is satisfactory for the structural analysis of indeterminate reinforced concrete structures at working loads if proper values of the modulus ratio are chosen.

About 1900, centrically loaded reinforced concrete columns were generally designed after the following formula for the allowable load:

$$P = f_c A_c + f_s A_{st} \tag{1}$$

where f_c and f_s were allowable stresses, and A_c and A_{st} were areas of concrete and steel, respectively. Later the standard theory was used, and the transformed area formula resulted

$$P = A_c f_c [1 + (n - 1)\, p_{st}] \tag{2}$$

in which p_{st} is the ratio of effective longitudinal reinforcement area to the gross area of concrete, and n is the modular ratio.

In 1921, McMillan made a study of column test data[17] which showed that building columns under load may develop steel stresses, due to plastic action, considerably higher than those predicted by the standard theory, Eq. (2). This study led to the ACI Column Investigation in the 1930's which was carried out by Lyse, Slater, and Richart. Through their work, rational equations for the strength of centrically loaded reinforced concrete columns were developed.[23, 25, 26, 27, 28, 30, 31, 32, 33, 36, 40, 43] The ultimate load of tied columns and the yield point of spiral columns were expressed as

$$P = 0.85 f_c' A_c + f_{yp} A_{st}. \tag{3}$$

For the ultimate load of spiral columns, the following equation was developed

$$P = 0.85 f_c' A_{\text{core}} + f_{yp} A_{st} + 2.0 p_{sp} A_{\text{core}} f_{sp} \tag{4}$$

in which

f_{yp} = yield point stress of longitudinal reinforcement

f_{sp} = useful limit stress of spiral reinforcement, generally assumed as the stress at a strain of 0.005

A_{core} = area of the column core (out-to-out of spiral)

p_{sp} = ratio of volume of spiral reinforcement to the volume of concrete core.

Following the publication of the results of this investigation, an inelastic design formula of the same form as Eq. (1) became much used in this country as well as in several countries abroad. The basic formula of the 1947 ACI Building Code[93] may be written

$$P = 0.225 f_c' A_c + 0.4 f_{yp} A_{st}. \tag{5}$$

This design equation is, however, characterized by a larger "factor of safety" for the concrete than for the steel. Furthermore, the inelastic design is used only for columns loaded centrically or with small eccentricities. Beams and columns with large eccentricities are still being

designed after the standard theory. In beams, however, the inelastic properties of concrete are recognized to some extent by allowing the effectiveness of compression reinforcement in resisting bending to be taken as twice the value obtained from the standard theory.

Another milestone of progress in the theory of reinforced concrete was passed in 1931 when Emperger wrote a critical study of the modular ratio and the allowable stresses.[29] This paper initiated intense studies of the ultimate strength of reinforced concrete beams in bending, which soon spread over the world. A large number of ultimate theories, some of which are described in detail in Section 10, were developed.

In recent years it has been claimed repeatedly that our knowledge of the entire field of reinforced concrete design has advanced so far that a transition to inelasticity rather than elasticity and to ultimate loads rather than working stresses is necessary in order to continue progress. It has also been argued that equal factors of safety should be used for concrete and steel, and that different safety factors should be used for live and dead loads. A transition to ultimate design has been made in some countries such as USSR and Brazil, and several European authors have claimed that the ultimate theories are "ripe for the specification form now."

There are two major phases involved in an ultimate design of reinforced concrete structures: (1) the structural analysis of indeterminate structures, and (2) the process of dimensioning sections. In the past, the major interest has been focused on the dimensioning problem. Hence, the ultimate design methods adopted in USSR and Brazil, while specifying dimensioning procedures based on ultimate loads, have still maintained the theory of elasticity for most purposes of structural analysis. In recent years, some studies have been devoted to the inelastic analysis of reinforced concrete structures. Examples of such studies are the Fracture Line Theory for slabs,[99a] the Stringer Theory for cylindrical shells,[110b] and the Method of Partial Restraints for continuous beams.[39] The present Danish specifications for reinforced concrete structures[110a] permit an inelastic analysis of indeterminate structures, while the dimensioning methods are based on the standard theory.

In this country it is generally felt, however, that the ultimate dimensioning theory is worthy of primary interest. For concentrically loaded columns, and beams failing in bending, this theory has been rather well established as the result of a large number of tests. Our knowledge of some other types of members, among them eccentrically loaded columns, is incomplete because tests made on such members of large dimensions are too few to be conclusive.

Thus, the investigation reported herein was undertaken in order

to throw new light on the behavior of reinforced concrete members subject to combined bending and axial load. It is the purpose of this bulletin to describe observations regarding the basic behavior of such members and to express this behavior, as far as possible, in mathematical terms. Hence, the present bulletin deals with two major problems. First, simple approximate expressions for ultimate capacities suitable for design purposes are studied. Secondly, a general theory is developed with the aim of predicting behavior of eccentrically loaded reinforced concrete members from the smallest loads through the entire range of loading to failure, including the mode of failure. Only by expressing this general behavior in mathematical terms can we determine appropriate factors of safety under various conditions, develop equations suitable for design, study variables not included in existing test data, and advance our knowledge pertaining to the inelastic theory of reinforced concrete structures.

2. Outline of Tests

The total number of 120 test specimens was divided into four groups, three of tied columns and one of spirally reinforced columns. An outline of the tests is given in Table 1, which indicates that the major variables were: amount of reinforcement, concrete quality and eccentricity of load.

Table 1

Outline of Tests*

Group No.	Col. No.†	Eccentricity, in.	Col. Size	Longitudinal Reinforcement	Concrete Quality	Total No. of Columns
I	1	0	Tied Col. 10 in. square	Tens. 4 ⅝ in.rd. A_s =1.24 sq in. Compr. 2 ⅜ in.rd. A_s' =0.22 sq in.	A,B,C	30
	2	2.5				
	3	5.0				
	4	7.5				
	5	12.5				
II	6	0	Tied Col. 10 in. square	Tens. =Compr. 4 ⅝ in.rd. A_s =A_s' =1.24 sq in.	A,B,C	30
	7	2.5				
	8	5.0				
	9	7.5				
	10	12.5				
III	11	0	Tied Col. 10 in. square	Tens. =Compr. 4 ⅞ in.rd. A_s =A_s' =2.40 sq in.	A,B,C	30
	12	2.5				
	13	5.0				
	14	7.5				
	15	12.5				
IV	16	0	Spiral Col. 12 in. round	8 ⅞ in.rd. A_{st} =4.80 sq in.	A,B,C	30
	17	3.0				
	18	6.0				
	19	9.0				
	20	15.0				

* The columns were made with intermediate grade Hi-Bond longitudinal bars and drawn wire spirals. Groups I to III were made with plain ¼-in. ties at 8-in. spacing. The spiral size varied with concrete strength: Concrete A, USSWG No. 1; Concrete B, No. 3; Concrete C, No. 7; all at 1½-in. pitch. The three grades of concrete were: A =5000, B =3500, and C =2000 p.s.i. Two companion specimens were made throughout. The total column length was 7.5 times the least lateral dimension.

† Columns are completely designated by a capital letter, a numeral, and a small letter. The capital letter — A, B or C — indicates the grade of concrete; the numeral — 1 through 20 — indicates the column number; the small letter — a or b — indicates one of two companion specimens. Thus B-4a indicates 3500 p.s.i. concrete, column No. 4, the first companion specimen.

The tied columns were all 10 in. square with a total length of 6 ft 3 in., while the spirally reinforced columns were 12 in. round and 7 ft 6 in. long.

All specimens were tested in 15 to 20 increments of load to failure, the total testing time being about an hour. Strains in the reinforcement and on the concrete surface as well as deflections were measured after each increment of load.

3. Acknowledgment

The investigation reported herein was carried out at the Talbot Laboratory in the University of Illinois Engineering Experiment Station, under the auspices of the Engineering Foundation through the Reinforced Concrete Research Council, and was supported by the Portland Cement Association and the Concrete Reinforcing Steel Institute. The research program was under the general administrative guidance of Dean W. L. Everitt, director of the Station, and Professor F. B. Seely, head of the Department of Theoretical and Applied Mechanics.

Credit for initiating the investigation must be given to the ASCE Sub-committee on Ultimate Load Design and especially to the late A. J. Boase who planned the tests in cooperation with the late Professor F. E. Richart. The tests were carried out under the general supervision of Professor Richart and the Council, consisting of the following:

Chairman
R. F. Blanks, U. S. Bureau of Reclamation
Secretary
J. M. Garrelts, Columbia University
Special Adviser
B. A. Bakhmeteff, representing the Engineering Foundation
Members
Raymond Archibald, U. S. Bureau of Public Roads
J. R. Ayers, Bureau of Yards and Docks
R. L. Bloor, Corps of Engineers
L. H. Corning, Portland Cement Association
A. E. Cummings, ASCE Research Committee
O. W. Irvin, Rail Steel Bar Association
H. D. Jolly, Concrete Reinforcing Steel Institute
Douglas McHenry, U. S. Bureau of Reclamation
C. T. Morris, Ohio State University
D. E. Parsons, National Bureau of Standards
Harry Posner, American Railway Engineering Association
F. E. Richart, University of Illinois
E. J. Ruble, Association of American Railroads

The steel for the spirals used in Group IV was furnished by the American Steel and Wire Company, Chicago. These spirals were fabricated by the Ceco Steel Products Corporation, Chicago.

The manuscript of this bulletin was critically studied by C. P. Siess and I. M. Viest of the University staff and by a review committee of the Council consisting of L. H. Corning, chairman, R. Archibald and E. J. Ruble. Their helpful comments and criticisms are gratefully acknowledged.

4. Notation

The letter symbols used in this bulletin are generally defined when they are first introduced. The most common symbols are listed below for convenient reference.

A = area
A_c = concrete gross area
A_{core} = area of column core (out-to-out of spiral)
A_s = area of tension reinforcement
A_s' = area of compression reinforcement
A_{st} = total area of longitudinal reinforcement
a = depth of a rectangular stress-block in the concrete
b = width of a rectangular member
C = total internal compressive force in concrete
c = distance from neutral axis to compression edge of member
c/w = cement-water ratio by weight
D = diameter
d = distance from centroid of tension reinforcement to compression edge of member
d' = distance between centroids of tension and compression reinforcements
E_c = modulus of elasticity of concrete
E_s = modulus of elasticity of reinforcing steel
E_{cc} = secant modulus computed from deflections with moment of inertia of concrete only
E_{ct} = secant modulus computed from deflections with moment of inertia of transformed section
e = eccentricity with respect to mid-depth of section
e' = eccentricity with respect to centroid of tension reinforcement
Δe = increase in eccentricity due to deflection
f_c = compressive stress in concrete; also allowable compressive stress
f_c' = compressive strength of 6- by 12-in. cylinders or prisms of similar dimensions
f_{cu}' = compressive strength of cubes
f_c'' = compressive strength of concrete in flexure
f_{ct} = tensile strength of concrete
f_s = stress in tension reinforcement; also allowable stress in reinforcement
f_s' = stress in compression reinforcement
f_{yp} = yield point of reinforcement, especially tension reinforcement
f_{yp}' = yield point of compression reinforcement
f_{sp} = useful limit stress of spiral reinforcement, generally assumed as the stress at a strain of 0.005
I = moment of inertia
I_c = moment of inertia of concrete
I_s = moment of inertia of steel
$k = c/d$ = ratio indicating position of neutral axis
k_1, k_2 = coefficients related to magnitude and position of internal compressive force in concrete
L = length
M = bending moment

M_o = moment of all internal compressive forces about centroid of tension reinforcement for balanced section
m = inelastic "modular ratio"
$n = E_s/E_c$ = modular ratio
P = load; also ultimate load
P_o = ultimate load of concentrically loaded column
$p = A_s/bd$
$p' = A_s'/bd$
$p_{st} = A_{st}/A_c$ = ratio of total reinforcement area to gross area of concrete
p_{sp} = ratio of volume of spiral reinforcement to volume of concrete core
T = internal force in tension reinforcement
t = depth of section
V = coefficient of variation
x = distance to centroid of an area
Z = section modulus
z = internal moment arm
$\alpha = k_2/k_1$; also a coefficient
β = Jensen's plasticity ratio
δ = deflection
ϵ = strain
ϵ_c = strain in concrete
ϵ_o = compressive strain in concrete corresponding to maximum stress
ϵ_u = ultimate concrete strain in flexure
ϵ_s = strain in reinforcement
ϵ_v = volume strain
σ = standard deviation
% = percent (hundredths)
‰ = per mill (thousandths)

Columns are designated by a capital letter, a numeral, and a small letter. The capital letter—A, B or C—indicates the grade of concrete; the numeral—1 through 20—indicates the column number; the small letter—a or b—indicates one of two companion specimens. Thus B-4a indicates 3500 p.s.i. concrete, column No. 4, the first companion specimen.

II. MATERIALS, FABRICATION AND TEST METHODS

5. Materials

a. Cement

Lehigh Portland Cement Type I was used throughout the tests. The cement was purchased in paper bags in two lots from a local dealer and stored under proper conditions.

b. Fine and Coarse Aggregates

The fine aggregate used was a Wabash River torpedo sand having an average fineness modulus of about three. The coarse aggregate was a Wabash River gravel of 1-in. maximum size. Both aggregates have been in use at this laboratory for years and they passed the usual specification tests. Aggregate sieve analyses are given in Table 2. The specific gravities were 2.65 and 2.70 for sand and gravel, respectively. The absorption of both fine and coarse aggregate was about one percent by weight of surface-dry aggregate.

Table 2

Sieve Analysis of Aggregates*

Kind of Aggregate	Percentage Retained on Sieve No.											Fineness Modulus
	1½ in.	1 in.	¾ in.	½ in.	⅜ in.	4	8	16	30	50	100	
Sand	...	...	....	....	0	2.4	11.3	28.3	64.6	91.0	98.4	2.96
Gravel	0	3.8	34.3	64.9	91.8	98.7	100	100	100	100	100	7.25

* Average of four lots of each aggregate.

The origin of these aggregates is a glacial outwash, mainly of the Wisconsin glaciation. The major constituents of the gravel were limestone and dolomite; minor quantities of quartz, granite, gneiss, etc., were present. The sand consisted mainly of quartz with a character similar to the gravel in the coarser fractions.

c. Concrete Mixtures

The three concrete mixtures used were designed to have 28-day cylinder strengths of about 2000, 3500 and 5000 p.s.i. The second lot of cement, however, gave about 20 percent higher strengths than the first. The mixtures were therefore adjusted slightly as the tests proceeded. The average properties of the mixtures are given in Table 3,

Table 3
Concrete Mixtures

Concrete	Mix (By Weight)*	Average Slump, in.	Percent Sand, (By Wt.)	Cement, lbs per cu yd	Water, lbs per cu yd	c/w (By Wt.)	w/c (By Wt.)
A	1:2.2:3.1	5.9	41.5	594	323	1.83	0.55
B	1:3.1:4.3	6.3	42.0	450	311	1.45	0.69
C	1:4.8:6.4	6.6	43.0	308	313	0.98	1.02

* Surface dry basis.

and the relations between strength, c/w and curing procedures are given in Fig. 2. The strengths of 6- by 12-in. control cylinders are listed with the results of the column tests.

All concrete was mixed in a non-tilting drum mixer of 6.5-cu ft capacity, and was placed in the forms by means of vibration.

d. Reinforcing Steel

Three sizes of deformed bars were used as longitudinal reinforcement in these tests: $\frac{3}{8}$ in., $\frac{5}{8}$ in., and $\frac{7}{8}$ in. For the $\frac{5}{8}$- and $\frac{7}{8}$-in. sizes, the Hi-Bond bar, which is representative of modern deformed bars meeting ASTM Designation A305-49, was chosen in intermediate grade billet steel, and the quantity necessary for the complete investigation was purchased from a commercial firm and received in one shipment. The laboratory's stock of old deformed bars was used for the $\frac{3}{8}$-in. compressive reinforcement in Group I. The ties for the square columns were manufactured by hand from the laboratory's stock of $\frac{1}{4}$-in. plain bars. The drawn wire spirals were received as gifts. Properties of the reinforcement as determined from tension tests are given in Table 4. Since no uncoiled wire was furnished with the spirals, no strain measurements were made during the tension tests of the wires.

Electric SR-4 gages were used to measure strain in the longitudinal steel of all columns. In order to attach such gages to the Hi-Bond bars, the lugs were removed on one side of the bars over a length of about 2 in. By testing pairs of 2-ft specimens cut from the same reinforcing bar and attaching SR-4, A-11 gages to one specimen of each pair, it was found that yield point and ultimate strength were little affected by the local removal of lugs, as indicated in Table 4. The modulus of elasticity as measured by a mechanical gage over an 8-in. length was also practically unaffected. The local strains as measured by the SR-4, A-11, 1-in. gages were, however, 10 to 15 percent larger than the corresponding strains measured over an 8-in. length, as shown in Fig. 3a and 3b. This difference is believed to be due mainly to the eccentricity introduced by the removal of lugs. Thus, all strains measured by SR-4, A-11 gages during the column tests were corrected to an 8-in. length by using Fig. 3.

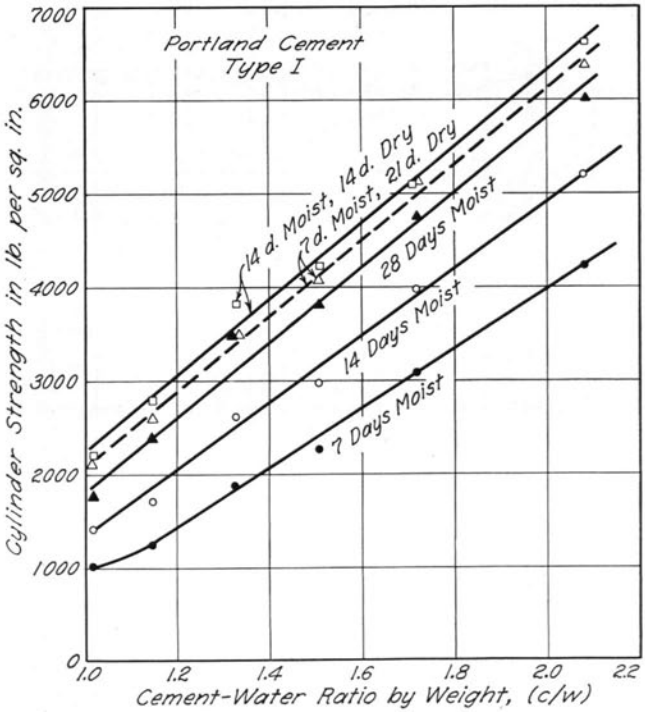

Fig. 2. Strength Relations for Concrete

The properties of the deformations of the Hi-Bond bars are given in Table 5. The details of the lug measurements and the computation of the various significant properties are presented in an earlier paper by C. P. Siess and the writer.[114]

6. Types of Specimens

Tests of 120 reinforced concrete columns are reported herein, of which 90 were square tied columns and 30 cylindrical spiral columns. Since the investigation was confined to the combined stress problem, the specimens were purposely kept fairly short, so that the results would not be confused by the occurrence of buckling failures. The two types of columns with four types of longitudinal reinforcement are shown in Fig. 4. Cylinders, 6 by 12 in. were used as auxiliary specimens.

7. Fabrication and Curing

The reinforcement was assembled into a unit or cage before it was placed in the forms for casting. The longitudinal steel, which was placed inside the ties or spirals and securely wired to them, was carried straight

Table 4
Tension Tests of Reinforcement

Bar	Size	Average* Stress at Yield Point, p.s.i.	Max. and Min. Yield Point, p.s.i.	Average Ultimate Strength, p.s.i.	Average Elongation in 10 in. at Ult. Load, per cent	Average Reduction in Area† at Ult. Load, per cent	Average Modulus of Elasticity, p.s.i.×10^6
Hi-Bond	⅝-in.	43,900	47,100 40,000	74,800	19.5	27.9	28.0
	⅝-in. lugs rem.	43,400	47,100 38,700	73,800	14.5	31.9	28.0
Hi-Bond	⅞-in.	43,800	45,800 42,300	77,500	12.1	24.6	29.0
	⅞-in. lugs rem.	43,500	45,500 41,700	76,300	11.6	32.9	29.0
Old Deformed	⅜-in.	60,000	66,800 52,900	87,400	18.5	....	....
Ties	¼-in.	61,600	73,600 59,100	84,000	16.7	56.0	....
Spirals	USSWG No. 1 No. 3 No. 7			 110,000 129,000 108,000		 45.7 37.1 37.6	 ....

All stresses, including the modulus of elasticity, are based on the nominal cross-sectional area.
* Average of five specimens for the ⅞-in. Hi-Bond bars, four specimens for the remaining bars.
† For the deformed bars, the diameter from gap to gap, d_1, was measured before testing and after failure. The minimum diameter, d_2, perpendicular to d_1 was also measured twice. The reduction in area is computed as the change in $(d_1 + d_2)^2$.

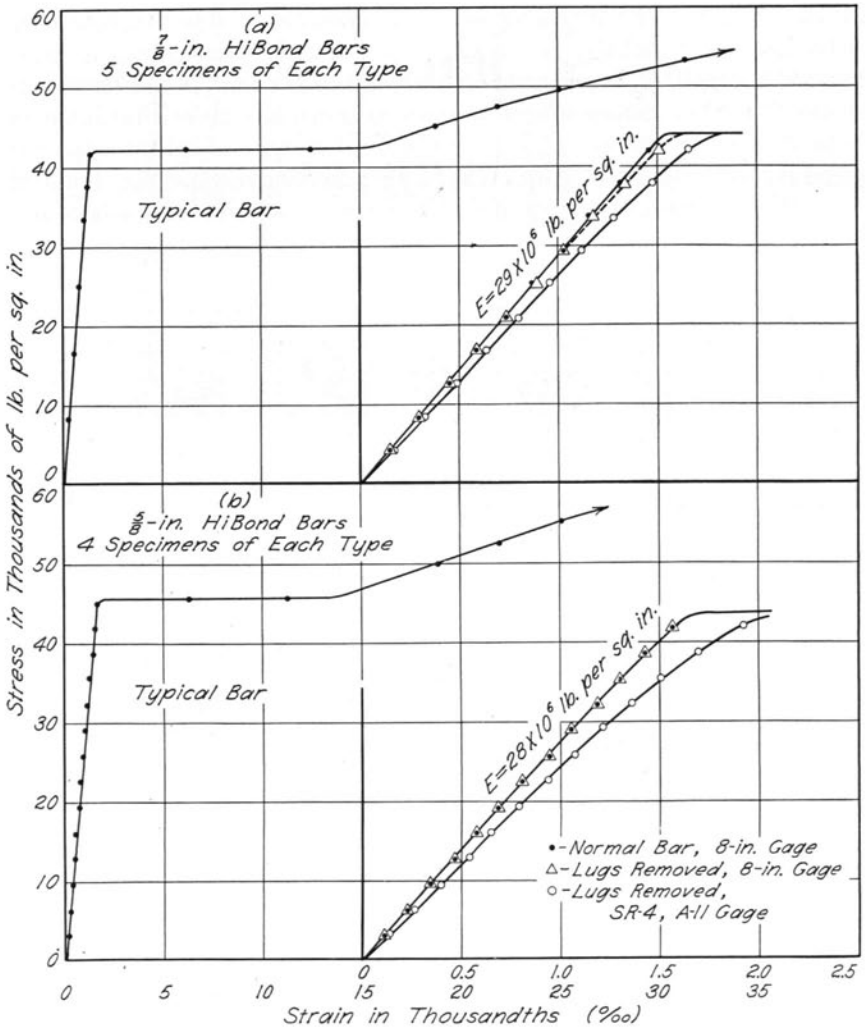

Fig. 3. Stress-Strain Relations for Reinforcement

through the entire length of the columns. Spacing blocks were used to provide accurate spacing of these bars. Additional reinforcement was provided in the brackets or capitals, the purpose of which was to transfer the eccentric load and its moment to the prismatic shaft of the columns. For the small eccentricities this was achieved with a light reinforcement

Table 5
Lug Measurements, Hi-Bond Bars

Bar Diam, in.	Average Actual Weight, lb per ft	Dimensions of Bars					Requirements of ASTM Designation A305-49			Bearing Area		Shearing Area, Sq in. per in.
		Height (h), in.	Spacing (s), in.	Gap (g), in.	Diam (d), in.	Width (w), in.	Min. Height, in.	Max. Av Spacing, in.	Max. Gap, in.	Sq in. per in.	Sq in. per Sq in. of Nom. Surf. Area	
3/8	2.048	0.055	0.380	0.121	0.969	0.071	.044	.612	.334	.381	.138	2,280
5/8	0.997	0.046	0.298	0.089	0.670	0.061	.028	.437	.239	.275	.140	1,510

bent around the longitudinal bars as shown to the left in Fig. 5a. In the cases of large eccentricities, however, a heavy reinforcement welded to the longitudinal bars was necessary to prevent tension, diagonal tension, or bond failures in the capitals. Such a reinforcement unit is shown to the right in Fig. 5a. Except for the top capital of one column which failed in bond, all capitals proved to be satisfactory, as they were perfectly sound after the prismatic part of the columns had failed.

The columns were cast in a vertical position. Some previous investigators[44, 51, 94] cast their specimens horizontally in order to avoid a differential in concrete quality along the column length. Such a differential

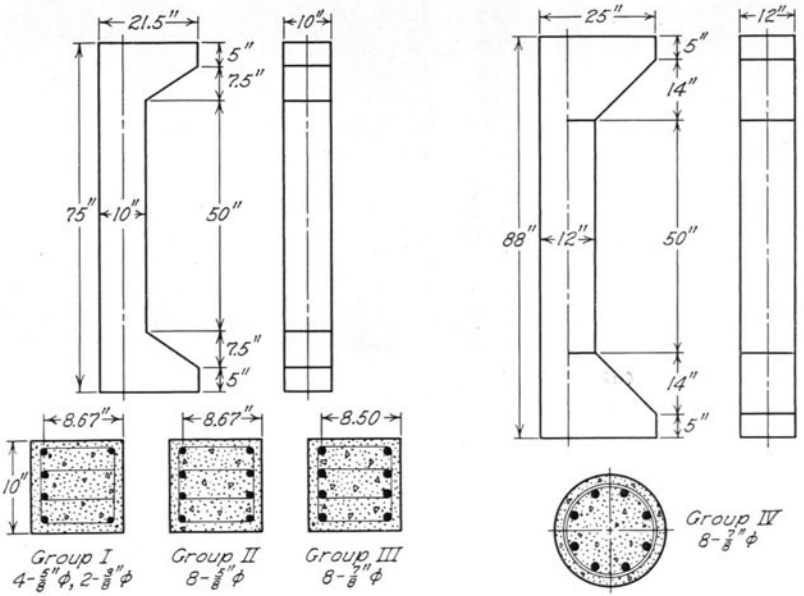

Fig. 4. Types of Specimens

will exist in a vertically cast column because the concrete in the bottom part generally will be compacted better than in the top part. Also, even a moderate water gain or bleeding will decrease the c/w ratio and hence the strength of the concrete in the upper part. Horizontal casting, on the other hand, will cause a strength differential across the cross section of the columns.

Furthermore, the orientation of the members during casting will determine whether the longitudinal stresses during testing will be parallel or perpendicular to the direction of casting. Since all columns tested at

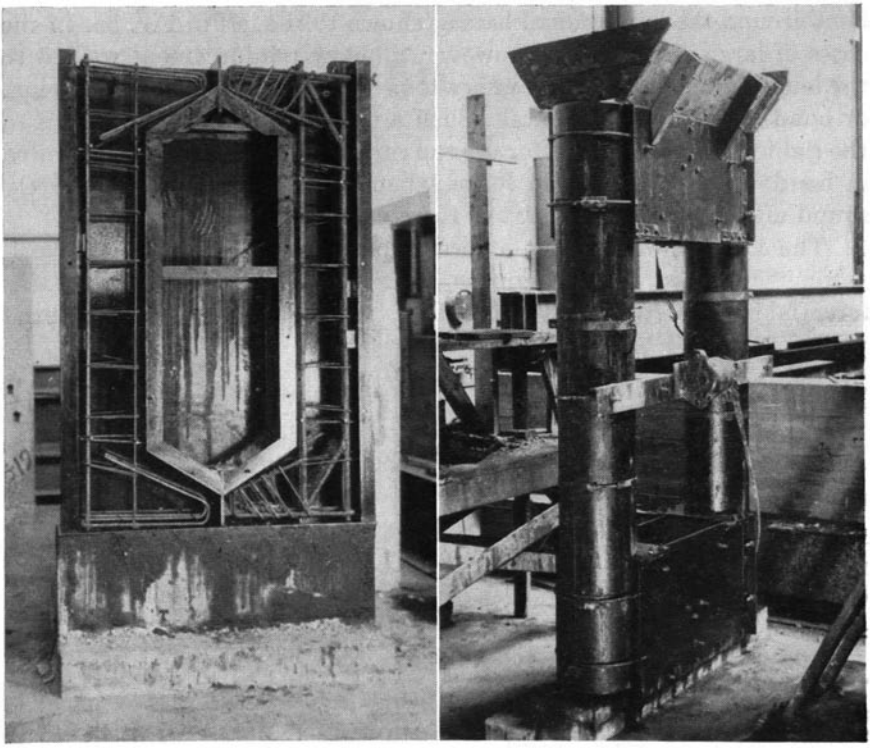

(a) (b)

Fig. 5. Types of Forms

this laboratory in earlier investigations[22, 43, 95] were cast vertically, since most columns in practice are cast vertical or inclined, and since it is very difficult to cast cylindrical columns horizontally, all columns described herein were cast and tested in a vertical position.

A view of the two types of steel forms is given in Fig. 5a and 5b. It can be seen that the columns were cast in pairs in forms built from plates, shapes, and split pipes bolted together. The lateral dimensions of the prismatic parts of the columns were found to be true to ± 0.1 in. at the time of testing. Spacers were provided to keep the reinforcement units centered in the forms with a 1-in. cover over the longitudinal bars of the tied columns, and a 1-in. cover over the spirals of the cylindrical columns. Since a heavy external vibrator was attached to the forms to compact the concrete, this spacing was found to vary about $\pm \frac{3}{8}$ in. The forms were carefully leveled and plumbed.

In all columns a reasonably fluid consistency of concrete was used to facilitate its placing around the heavy capital reinforcements and to

provide a smooth surface which is desirable for the application of electric strain gages. The forms were removed the day after the columns were cast, and the columns were stored in a fog room at 75–80 deg F for seven days after casting. They were then stored in the air of the laboratory until testing took place at an age of 28 days. This curing process is reasonably similar to practical conditions, and it was also chosen because, as yet, no methods are known of applying electric gages to a wet concrete surface.

In all cases 9 to 12 cylinders (6 by 12 in.) were made, stored and tested with each pair of columns.

8. Attachment of Electric SR-4 Gages

Electric gages were used throughout these tests to measure strains in the reinforcement as well as on the concrete surface. The manner of attaching the SR-4 gages to the reinforcement varied in the tests. Attachment of gages to bars to be embedded in fresh concrete requires careful waterproofing of the gages and leads. For compression gages in the square columns and for all gages in the spiral columns this was considered necessary. However, for tension measurements in the square columns, it was considered satisfactory, and very much simpler, to provide core holes in the concrete during casting and to attach the gages to the reinforcement after the concrete had hardened and cured. The core holes may have slightly influenced the formation of tension cracks; but such cracks would form in any event before the steel stresses became large.

Even though the errors introduced by the attachment of gages are small, it was decided to avoid attaching all gages at the same cross section of the columns. Thus, for the compression as well as the tension side of the square columns, one gage was attached at midheight of the column and the other two gages 8 in. above or below midheight. In the spiral columns gages were attached to all longitudinal bars alternately at midheight and 12.5 in. above midheight.

Due to the heterogeneous character of concrete, strains measured over a short length on a concrete surface cannot be expected to yield satisfactory results. Thus SR-4, A-9 gages with 6-in. gage lengths were used for measurements of strains in the concrete. In some preliminary tests these gages were checked against an 8-in. Berry gage, and the agreement was very good. Generally about five gages were used to determine the strain distribution across the cross section. The majority of these gages were placed where the columns were expected to fail, near the upper quarterpoint of the column shaft. One SR-4, A-9 gage was also used to measure lateral strain on the compression face of the column in order to obtain information regarding volume strains.

The electric gages gave very satisfactory service throughout these tests and their easy operation facilitated the testing considerably. A detailed description of the methods involved in the use of these gages as applied to reinforced concrete is given in an earlier publication by I. M. Viest and the writer.[111]

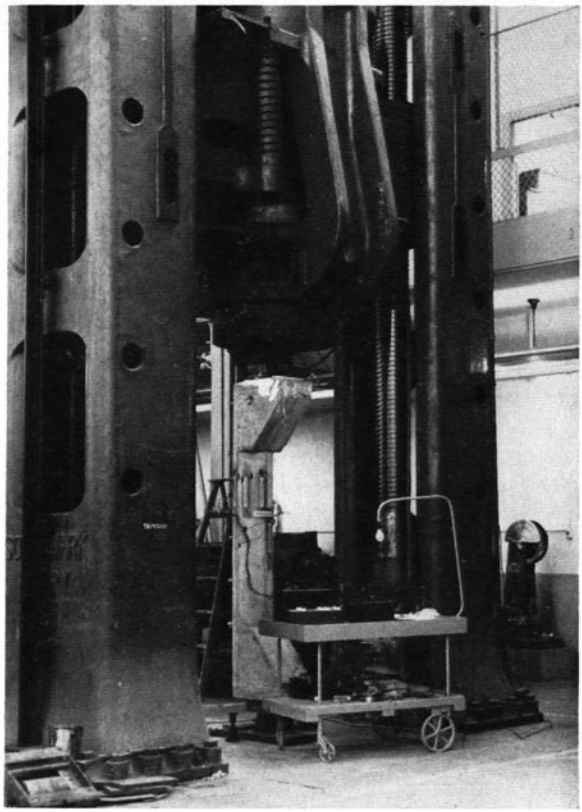

Fig. 6. Test of Cylindrical Column

9. Testing Procedure

All columns were tested in a 3,000,000-lb capacity Southwark-Emery hydraulic testing machine. A view of the machine during the test of a cylindrical column is shown in Fig. 6. Load was applied through "knife edges" at the top and bottom support of all columns, except the concentrically loaded spiral columns which were tested with "flat ends." A sketch of the testing equipment with knife edges is given in Fig. 7 which

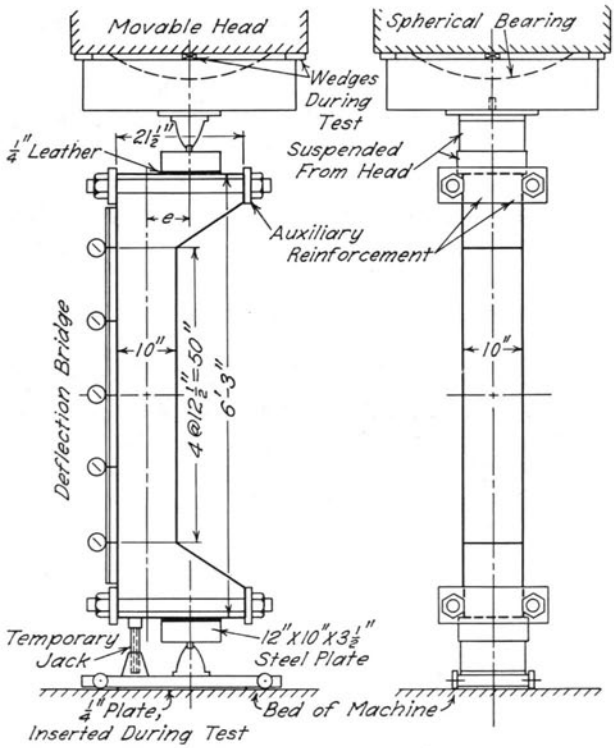

Fig. 7. Testing Arrangement

shows a square column. The bottom knife edge rested on a wheeled carriage, thus permitting easy placing, centering, and removal of the columns in the testing machine. The upper knife edge and base plate were suspended from the movable head of the machine. Two auxiliary tension rods were attached to each capital of the square columns, because it was found impracticable to reinforce these capitals sufficiently with only embedded bar reinforcement. A deflection bridge, carrying five dial indicators, furnished deflection readings in the plane of eccentricity.

The arrangement for testing the spirally reinforced columns was very similar; however no auxiliary rods were used. The concentrically loaded spiral columns were tested with flat ends.

All columns were carefully centered and plumbed in the testing machine. However, since the knife edges were ½ in. thick and since no optical instruments were used to center the columns, the actual eccentricities of loads during testing probably deviated up to $\pm \frac{1}{4}$ in. from

the nominal values. Initial readings of all gages were taken immediately before application of any load. Then a load of about 3.5 kips, which corresponds to the weight of the spherically seated block in the movable head of the testing machine, was applied. During this loading, the block was allowed to adjust itself by movements in the spherical bearing. Before further load was applied, however, this block was fixed by wedges and the temporary jacks under the column were removed. Loading proceeded to failure in 15 to 20 increments, the time between the first and last increments being about one hour. After each increment of load, the machine was operated in small increments until the immediate creep had taken place and the load came to rest at a reading about one percent over the nominal load. Then, all gages were read in a cyclic manner, returning to the first gage for control purposes. After all gages were read, the load had generally dropped to about one percent under the nominal load. This may have been caused by creep of the specimen and by a slight leaking of oil from the pressure cylinders of the machine.

III. INELASTIC FLEXURAL THEORIES

10. Historical Development of Inelastic Dimensioning Theories

It was mentioned in the introduction to this bulletin that a great number of theories relating to the flexural analysis of reinforced concrete have been published since M. Koenen's basic note in 1886.[1] Generally, it has been agreed that the "standard" theory, using the concepts of a transformed section and a modular ratio, is sufficiently accurate for estimating stresses and for dimensioning sections with reference to safe loads.

Many authors have argued, however, that the safety and economy of reinforced concrete structures are not controlled satisfactorily by this "classical elastic theory" and that a consideration of the plastic character of concrete near ultimate loads is necessary to achieve such control. In order to review the most important inelastic theories presented before 1950, it is convenient to group the basic types of assumptions as follows:

1. Distribution and magnitude of the compressive stresses in the concrete
2a. The ultimate strain in the concrete, or
2b. The limiting depth of the neutral axis
3. Tension stresses in the concrete
4. Bernoulli's hypothesis regarding a linear distribution of strains
5. The stress-strain relation of the reinforcing steel
6. The absence of a general slip between concrete and steel.

Most earlier investigators have assumed that the concrete resists no tension, that Bernoulli's hypothesis is valid, and that no slip occurs between concrete and steel. The stress-strain relation for mild steel reinforcement has generally been assumed trapezoidal with the yield level at the yield-point stress. These assumptions will apply to all theories discussed below unless a statement to the contrary is made.

The modes of failure of reinforced concrete members subject to flexure either without or combined with axial load are generally characterized by one of the following five groups:

1. Failure by excessive compressive strain in the concrete *before* the tension steel reaches yielding — *compression failure*

2. A failure *initiated* by yielding of the tension steel at the *yield point of the member*, with a resulting movement of the neutral axis which leads to excessive compressive strain in the concrete — *tension failure*

3. A balanced condition between (1) and (2) where the tension reinforcement reaches yielding exactly at the ultimate load, at which the concrete also fails at the compression edge — *balanced failure*

4. Compression failure of the concrete with tension steel stresses greater than the yield point

5. A brittle mode of failure caused by rupture of the tension steel immediately after the formation of tension cracks in the concrete.

The majority of previous theories consider compression and tension failures only, thus neglecting the effect of strain hardening in the tension steel as unreliable for practical purposes. The brittle mode of failure takes place only for very small reinforcement percentages and is therefore of secondary importance for practical purposes.

All inelastic theories advanced with reference to reinforced concrete subject to bending have been limited to the uni-axial state of stress. Thus, two equations of equilibrium and one compatibility equation involving strain relationships are available for a flexural analysis. All three equations have generally been used by past investigators in studies of compression failures and yield points of members. The compatibility equation then served the purpose of determining the tension steel stress for compression failures and the concrete stress for yield points. When tension failures are discussed, however, the tension steel stress is generally assumed to be at the yield point and the stress-block in the concrete will be that corresponding to failure of the concrete. Thus, the compatibility equation need not be used, nor is it necessary to assume an ultimate strain in the concrete, the validity of Bernoulli's hypothesis, and the absence of slip.

a. E. Suenson, 1912[13]

The writer believes that Suenson originated the use of the rectangular stress-block, Fig. 8, which has been much used later, directly or indirectly. Suenson's analysis covers the case of tension failures in a rectangular beam or slab only. Therefore no compatibility equation is needed.

An equation for dimensioning the reinforcement of a slab was developed in the following manner (Fig. 8).

From the equilibrium of forces $f_c''ab = A_s f_s$

and the equilibrium of moments $M = A_s f_s \left(d - \frac{a}{2}\right)$ (6)

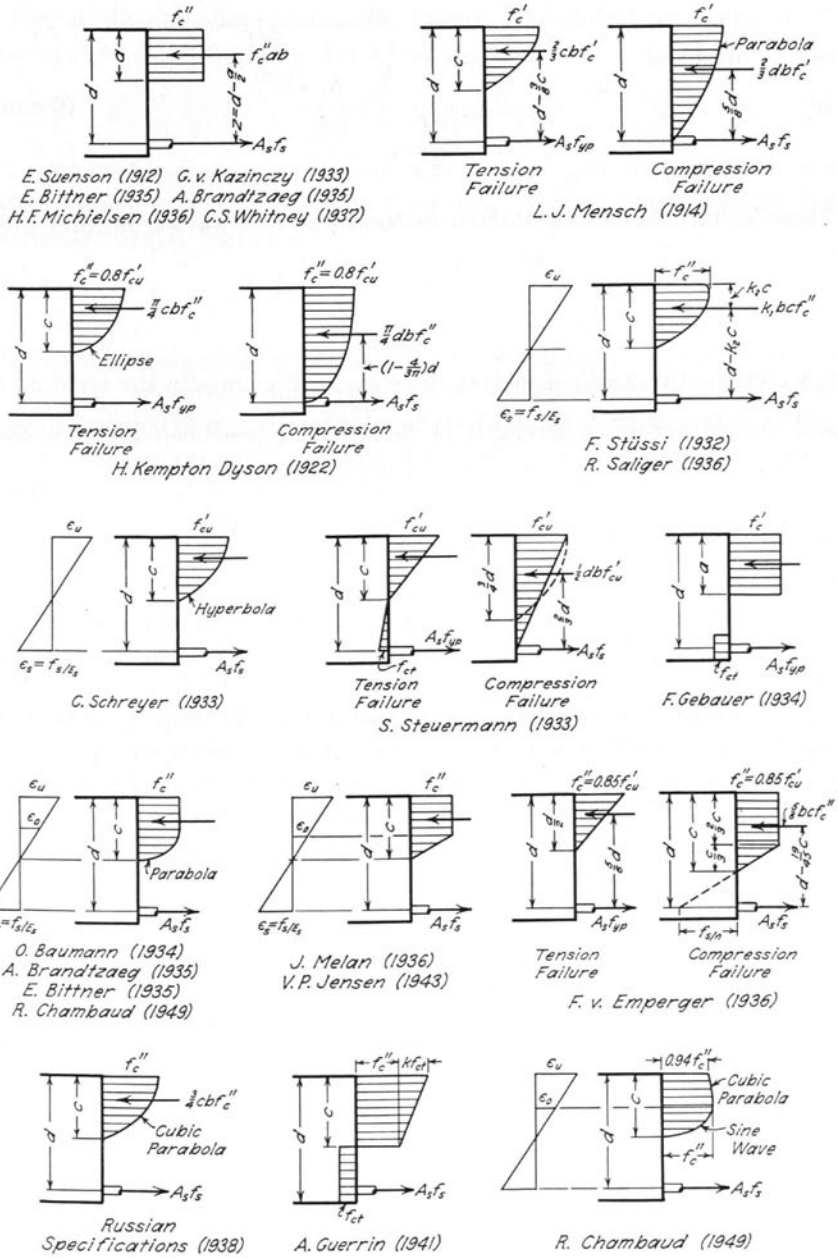

Fig. 8. Assumptions in Flexural Analysis

can be obtained

$$\frac{a}{d} = 1 - \sqrt{1 - \frac{2M}{bd^2 f_c''}}$$

$$f_s = \frac{M}{A_s z}. \qquad \text{(6 cont.)}$$

These equations can be written in the form well known in later years

$$\frac{M}{bd^2} = p f_s \left(1 - \frac{1}{2} p \frac{f_s}{f_c''}\right) \qquad (7)$$

in which b is the width of section, $p = \frac{A_s}{bd}$, f_s is generally the yield point, and the compressive strength in flexure, f_c'', has been given various values. Suenson put f_c'' equal to the cube strength, f_{cu}'.

b. L. J. Mensch, 1914[15]

The theory presented by Mensch covers tension as well as compression failures of rectangular beams with or without compression reinforcement. He criticized the building codes of that time and pointed out that the assumptions of the standard theory do not agree with the test results at high loads.

The expressions for ultimate moments were developed without the use of a compatibility equation, and no assumptions regarding ultimate strains, Bernoulli's hypothesis and absence of slip needed to be made. For the case of tension failure, Ritter's second degree parabola was assumed as stress-block (Fig. 8) and the computations made were very similar to those of Suenson.

In the case of compression failures (Fig. 8) Mensch assumed as a limiting condition that the neutral axis reached the centroid of the tension steel. Hence

$$\frac{M}{bd^2} = \frac{1}{2.4} f_c'.$$

Mensch realized that this limiting condition was too extreme, however, and he suggested for "balanced reinforcement"

$$\frac{M}{bd^2} = \frac{1}{2.6} f_c'. \qquad (8)$$

c. H. Kempton Dyson, 1922[18]

This theory, like that of Mensch, makes no use of a compatibility equation. Kempton Dyson assumed an elliptical stress-block as shown

in Fig. 8. In the case of tension failure, the difference from other theories is small. For compression failure

$$\frac{M}{bd^2} = \frac{1}{2.21} f_c''. \tag{9}$$

The effect of compression reinforcement was also discussed, and a design equation of the same form as Eq. (1) was recommended for centrically loaded columns.

d. F. Stüssi, 1932 [34]

This paper discusses rectangular beams with tension reinforcement only. Compression and tension failures were subjected to a mathematical analysis, and strain hardening as well as brittle fractures was mentioned in connection with very small reinforcement percentages. However, Stüssi's approach to the analysis of ultimate moments in such beams was so general that several later theories may be considered as refinements and improvements of his work. Hence, it is convenient to refer to these approaches as the Stüssi type of ultimate theory. The assumptions made are shown in Fig. 8. An arbitrary form of the concrete stress-block was assumed, which, for rectangular sections, may be characterized by the constants k_1 and k_2, the compressive strength in flexure, f_c'', and the ultimate strain in flexure, ϵ_u. These four quantities have been derived differently by the various authors who have contributed to ultimate theories of the Stüssi type. One or two of the following means have been used:

1. Tests of beams in bending
2. Tests of concrete in concentric compression
3. Studies of stress-strain relations of concrete in flexure

Stüssi used stress-strain relations derived from concentric compression of prisms to determine his constants. He found $k_1 = 0.70$ to 0.77, $k_2 = 0.39$ to 0.41 and $\epsilon_u = 2.0$ to 2.5 per mill. The compressive strength in flexure f_c'', was assumed equal to the prism strength, f_c'. It should be noted that Stüssi did not recognize that larger strains may be developed in bending than those corresponding to the ultimate load of a prism. Hence, his values for k_1, k_2 and ϵ_u are smaller than the values reported in later years.

With the assumptions shown in Fig. 8, and $f_c'' = f_c'$ the following equations were written

$$\text{Equilibrium of forces:} \quad A_s f_s = k_1 b c f_c' \tag{10a}$$

$$\text{Equilibrium of moments:} \quad M = k_1 b c f_c' (d - k_2 c). \tag{10b}$$

For tension failures, Stüssi further assumed the steel stress, f_s, to be at the yield level, f_{yp}. Hence the following equation for the ultimate moment was found

$$\frac{M}{bd^2} = pf_{yp}\left(1 - \frac{k_2}{k_1} p \frac{f_{yp}}{f_c'}\right). \tag{11}$$

For the ratio k_2/k_1, the value 0.55 was recommended as accurate enough for practical purposes.

For compression failures, Stüssi made the usual assumptions regarding linear distribution of strain, etc., and he used the following compatibility equation, Fig. 8

$$f_s = E_s\epsilon_s = E_s\epsilon_u \frac{d - c}{c}. \tag{12}$$

Solving Eqs. (12) and (10a) for the position of the neutral axis results in the expression

$$c/d = \sqrt{\frac{pm}{k_1} + \left(\frac{pm}{2k_1}\right)^2} - \frac{pm}{2k_1} \tag{13}$$

where $m = E_s\epsilon_u/f_c'$. By substituting Eq. (13) into Eq. (10b), an equation for the ultimate moment may be found.

Stüssi concluded his studies by showing that the standard theory leads to safety factors ranging from about 2.3 to 4.1.

e. C. Schreyer, 1933[37]

This theory of ultimate moments for reinforced concrete beams, which is of the Stüssi type, is based on stress-strain relations for concrete in compression obtained by tests of cubes, Fig. 8. A hyperbolic stress-strain relation was derived

$$\epsilon_c = \frac{0.63 \dfrac{f_c}{f_{cu}'}}{1.1 - \dfrac{f_c}{f_{cu}'}} \times 10^{-3}. \tag{14}$$

The ultimate strain, $\epsilon_u = 6.3$ per mill, was found to be independent of the concrete strength.

Schreyer's expressions for the ultimate moments, which are algebraically rather involved, were derived from the assumptions mentioned above by means of Eqs. (10) to (13).

f. S. Steuermann, 1933[38]

Steuermann's theory which was introduced in the Russian specifications, Mjassochladstroj, in 1932 is based on the assumptions shown in Fig. 8. In the case of tension failures, some tension was assumed to be taken by the concrete in beams and slabs, but not in T-beams. The tensile stress, f_{ct}, which was considered an equivalent stress rather than the tensile strength of the concrete, was generally assumed as $0.10f_{cu}'$.

For compression failures, a parabolic stress-block was assumed with the neutral axis at a depth $3d/4$. This stress-block was in turn converted into an equivalent triangular block, and the following formula for the ultimate moment resulted

$$\frac{M}{bd^2} = \frac{1}{3} f_{cu}'. \tag{15}$$

It should be noted that Mr. Steuermann's assumptions for tension failures are very similar to those made by J. Melan in 1896, Fig. 1.

g. G. v. Kazinczy, 1933[39]

Ultimate moments of rectangular beams failing in tension were derived on the basis of a rectangular stress-block, Fig. 8. The ultimate concrete stress, f_c'', was assumed equal to the prism strength, f_c', and the steel stress $f_s = f_{yp}$. Hence, Eq. (7) was derived in the form

$$\frac{M}{bd^2} = pf_{yp}\left(1 - \frac{1}{2} p \frac{f_{yp}}{f_c'}\right). \tag{16}$$

A major part of Kazinczy's paper was devoted to an analysis of test results regarding ten 2-span beams. Three of these beams were reinforced in accordance with the theory of elasticity, while five beams were under-reinforced and two were over-reinforced over the center support. It is believed that this paper initiated the study of the plastic theory of structures as applied to continuous reinforced concrete beams.

h. F. Gebauer, 1934[42]

Another theory for rectangular beams failing in tension, taking tensile stresses in the concrete into consideration, was developed by Gebauer with the assumptions shown in Fig. 8. The tensile stresses in the concrete were considered due to shrinkage of the concrete surrounding the steel.

i. O. Baumann, 1934[44]

This report is not a direct contribution to the inelastic flexural analysis of reinforced concrete, since the subject of Baumann's study

was the buckling of reinforced concrete columns subject to centric or eccentric loads. For the purpose of such a study, however, a relation between moments and rotations of reinforced concrete members in the range from zero to ultimate rotations was necessary. Hence, the assumptions shown in Fig. 8 were made.

The stress-strain relation of concrete in flexure was assumed to follow the virgin curves of centric compression, until the maximum stress, f_c'', was reached at a strain, ϵ_o. A parabola was found to be a satisfactory approximation for such virgin curves, and f_c'' was assumed equal to the prism strength, f_c'. However, Baumann found, through tests of eccentrically loaded prisms, that the ultimate strain in flexure, ϵ_u, was larger than the value ϵ_o corresponding to centric compression. For a concrete with about 3500 p.s.i. cylinder strength, he found $\epsilon_o = 1.8$ per mill and $\epsilon_u = 2.5$ to 3.3 per mill. This important observation had already been reported by Talbot in 1904-1906;[10, 11] but Baumann seems to have made an independent rediscovery.

Baumann's study of buckling was verified by tests of reinforced columns with two concrete qualities. The values of ϵ_o and ϵ_u were determined in auxiliary tests. No functional relationships between concrete strength and these strains were therefore developed.

j. E. Bittner, 1935[48, 53]

Bittner's inelastic theory is of the Stüssi type. He assumed a stress-block very similar to Baumann's, Fig. 8. It should be noted, however, that ϵ_o was assumed equal 1.5 per mill regardless of the concrete strength. Hence, ϵ_o is not related to the modulus of elasticity, E_c, as determined in compression tests. It was further assumed in the analysis of compression failures (Eqs. 10, 12 and 13) that $\epsilon_u = 3.0$, 5.0 and 7.0 per mill. No particular value of ϵ_u was recommended.

For tension failures, a rectangular stress-block with f_c' as the ultimate compressive stress was used, and Eq. (16) was developed.

k. A. Brandtzæg, 1935[51, 56, 57, 61]

These studies represent the first complete analysis of the ultimate capacity of rectangular sections with or without compression reinforcement subject to bending as well as bending combined with axial load.

The analysis of compression failures in beams is of the Stüssi type, based on the assumptions shown in Fig. 8. Brandtzæg improved and generalized on Baumann's stress-block by determining an empirical relation between the ultimate concrete strain in flexure, ϵ_u, and the compressive strength of concrete. Substituting $f_c' = 0.85 f_{cu}'$ and 1 p.s.i. = 0.07 kg per sq cm, this equation may be written as follows:

$$\epsilon_u = \left(6.88 - 0.77\frac{f_c'}{1000}\right) \times 10^{-3}. \qquad (17)$$

After determining the value of ϵ_o as a function of concrete strength and choosing the constant stress in the plastic range, f_c'', equal the prism strength, f_c', Brandtzæg introduced a "plasticity ratio" $\eta = \epsilon_u/\epsilon_o$, as a function of concrete strength. Equations (10), (12) and (13) were derived, introducing k_1 and k_2 as functions of the plasticity ratio, η. Equations (10a) and (10b) were also extended to include consideration of compression reinforcement and combined bending and axial load.

While this discussion of compression failures led to rather involved mathematical formulas, very simple expressions for tension failures were derived by extending Suenson's formula based on a rectangular stress-block, and Eq. (16) was derived for tension failures of beams.

For tension failures of rectangular sections subject to combined bending and axial load, Brandtzæg[51] developed an equation very similar to that used by the writer later in this paper, Eq. (39).

Brandtzæg verified his theory with tests of 20 beams, 13 eccentrically loaded columns and many auxiliary specimens. He further used this theory to develop a modified standard procedure which influenced the 1939 Norwegian Standard Specifications for design of reinforced concrete structures[73] to a considerable extent. In this modified standard theory, a fairly uniform factor of safety is achieved by introducing an allowable compressive stress for the concrete which is a function of the relative eccentricity of the load. Furthermore, the "modular ratio" for compression reinforcement is related to f_{yp}/f_c' while that for tension reinforcement is related to E_s/E_c.

l. F. v. Emperger, 1936[59]

Emperger, who was one of Europe's outstanding concrete engineers, initiated the thought-provoking discussions on ultimate theories in *Beton und Eisen* through his paper in October 1931[29] which was written just before his 70th birthday. In October 1936[59] he reviewed five years' discussions, and concluded that the ultimate analysis of reinforced concrete beams may be carried out with sufficient accuracy through the assumptions shown in Fig. 8. It should be noticed that the assumptions for tension failures, which do not satisfy statics, are very similar to Koenen's basic paper of 1886.[1]

m. R. Saliger, 1936[60, 66, 96, 99]

A thorough study of rectangular beams was presented in Saliger's original paper.[60] All five modes of failure mentioned in the introduction of Section 10 were considered.

The approach used in the development of ultimate moment equations was essentially the same as Stüssi's. The approximation was made, however, that $k_2 = \frac{1}{2}k_1$, which is equivalent to replacing the curved stress-block by a rectangular block with a depth $k_1 c$. Saliger further assumed $f_c'' = f_c'$ and developed Eq. (16). Thus, it was possible to determine k_1 by observing the position of the neutral axis in beam tests, without any specific assumptions regarding the stress-strain relation in flexure. Values from 0.90 to 0.94 were found.

In discussing compression failures of beams, Saliger emphasized that his tests had shown values of the ultimate strain in flexure, ϵ_u, from three to seven per mill. The following relation between ϵ_u and f_c' was suggested in his most recent paper[99]

$$\epsilon_u = 1.75 f_c' \times 10^{-6} \tag{18}$$

where f_c' is in p.s.i.

n. C. S. Whitney, 1937[63, 69, 74, 97]

This author is perhaps better known in this country than any other spokesman of ultimate theories for reinforced concrete. His theories for compression failures are not of the Stüssi type as no assumptions regarding ultimate strains, Bernoulli's hypothesis or the absence of slip were made.

Tension failures of beams were analyzed assuming a rectangular stress-block, Fig. 8, with $f_c'' = 0.85 f_c'$. Thereby the following formula was developed

$$\frac{M}{bd^2} = p f_{yp}\left(1 - \frac{1}{2} p \frac{f_{yp}}{0.85 f_c'}\right) \tag{19}$$

which is Eq. (7) with $f_s = f_y$ and $f_c'' = 0.85 f_c'$.

For the study of compression failures of beams no compatibility equation was used. A limiting value of a/d was assumed on the basis of values computed from test results. A value of $a/d = 0.537$ was found, which led to the following formula

$$\frac{M}{bd^2} = \frac{1}{3} f_c'. \tag{20}$$

This equation is very similar to Steuermann's Eq. (15) which was derived from entirely different assumptions. Beams with compression reinforcement were analyzed by adding the full yield stress of the compression reinforcement times its moment arm to the right side of Eq. (20).

On a semi-empirical basis the following equation for compression failures in combined bending and axial load was developed for rectangular sections

$$P = \frac{2A_s'f_{yp}}{\frac{2e}{d'} + 1} + \frac{btf_c'}{\frac{3te}{d^2} + 1.178}. \tag{21}$$

This equation reduces to the ultimate load for a centrically loaded column, Eq. (3), for $e = 0$ and to the ultimate moment for a beam when $e = \infty$. The equation is valid, however, only for rectangular sections with symmetrical reinforcement at the compression and tension faces.

For tension failures of such eccentrically loaded rectangular sections, Mr. Whitney developed equations very similar to those developed by Brandtzæg and the writer, Eq. (39), by assuming a rectangular stress-block in the concrete.

Finally, equations for rectangular and cylindrical columns with round cores were developed on a semi-empirical basis. These equations are discussed in Section 15.

o. USSR Specifications OST 90003, 1938[97, 109]

These Russian specifications were based on an ultimate design procedure. The stress-block in the concrete was assumed as a cubic parabola (Fig. 8). Thus the following equation was developed for tension failures of rectangular beams

$$\frac{M}{bd^2} = pf_{yp}\left(1 - \frac{pf_{yp}}{1.89f_c''}\right) \tag{22}$$

and for compression failures of beams

$$\frac{M}{bd^2} = 0.4f_c''. \tag{23}$$

In Eqs. (22) and (23), f_c'' is specified as a fraction of the ultimate strength of 8-in. cubes, varying from 0.8 to 1.0.

For axially loaded columns the following formula is used

$$P = f_cA_c + f_{yp}\,A_{st} \tag{24}$$

where $f_c = 4f_c''/5$.

Eccentrically loaded columns are analyzed on the basis of assumptions similar to those involved in Eqs. (22) and (23). Compression reinforcement is generally considered effective with the full yield-point stress.

p. K. C. Cox, 1941[75]

Mr. Cox reported tests of 110 rectangular beams. He developed equations for tension and compression failures with and without compression reinforcement based on a rectangular stress-block (Fig. 8), choosing $f_c'' = f_c'$. For tension failures Eq. (16) was developed. For compression failures he determined an empirical value for the critical reinforcement

$$p_{cr} = 0.47 \frac{f_c'}{f_{yp}} \tag{25}$$

which leads to

$$\frac{M}{bd^2} = \frac{1}{2.76} f_c'. \tag{26}$$

Thus, Mr. Cox's Eq. (26) is intermediate between Mensch's value of 1/2.6 and Whitney's 1/3.

q. V. P. Jensen, 1943[80, 81]

Jensen wrote one of the most complete studies of rectangular beams reinforced only in tension that have been published. His analysis, which is of the Stüssi type, was based on a trapezoidal stress-block in the concrete with a maximum stress $f_c'' = f_c'$ (Fig. 8). Contrary to Melan's assumptions,[58] however, the properties of Jensen's trapezoid were related to the cylinder strength

$$\epsilon_o = \frac{f_c'}{E_c} \tag{27a}$$

$$E_c = \frac{30{,}000{,}000}{5 + \dfrac{10{,}000}{f_c'}}. \tag{27b}$$

Furthermore

$$\epsilon_u (1 - \beta) = \epsilon_o \tag{27c}$$

in which the plasticity ratio, β, was defined by

$$\beta = \frac{1}{1 + \left(\dfrac{f_c'}{4000}\right)^2}. \tag{27d}$$

These assumptions led to the following ultimate moment

$$\frac{M}{bd^2} = pf_s \left(1 - \frac{1}{N} \frac{pf_s}{f_c'}\right) \tag{28}$$

where N is a function of β only.

Jensen then made the simplifying approximation that $N = 2$, which is the equivalent of using a rectangular stress-block with depth $k_1 c$ since Stüssi's constants k_1 and k_2 (Fig. 8) corresponding to $N = 2$ are related by $k_2 = \frac{1}{2}k_1$. Thus, Jensen's equation for tension failure was reduced to Eq. (16).

For compression failures, a compatibility equation was used, involving Eq. (27) and a trapezoidal stress-strain relation for the steel. Studies of the effects of strain hardening in the tension reinforcement were also made.

r. R. Chambaud, 1949[102, 108]

The flexure of beams with rectangular cross section and tension reinforcement only, was considered. The assumptions made were, however, of such a nature that the generalization of the theories involved is a matter of algebra only. In both his two papers dealing with ultimate theories for reinforced concrete beams, Chambaud developed theories of the Stüssi type, assuming a constant compressive ultimate strain for the concrete, $\epsilon_u = 3.6$ per mill. The correctness of this value was verified by tests.

Mr. Chambaud's first paper[102] presents a stress-block in the concrete very similar to those of Baumann, Brandtzæg and Bittner (Fig. 8). The initial modulus of elasticity, E_c, was determined from 5.5-in. cubes tested perpendicular to the direction of casting with cardboard pieces inserted between the bearing plates of the testing machine and the cubes. The maximum stress in flexure, f_c'', was assumed equal the compressive strength of the cubes mentioned above.

The second paper[108] presents a stress-block as indicated in Fig. 8, the modulus of elasticity, E_c, and the maximum concrete stress, f_c'', both being assumed as above.

s. Concluding Remarks

The ultimate moments derived in the theories discussed above differ relatively little in the case of tension failures of beams. The majority of the authors mentioned presented equations which may be derived from the following expression

$$\frac{M}{bd^2} = pf_{yp}\left(1 - \frac{k_2}{k_1} p \frac{f_{yp}}{f_c''}\right). \tag{29}$$

The ultimate compressive stress in flexure, f_c'', has been given values from $0.85 f_c'$ to $f_{cu}' = 1.18 f_c'$. The ratio k_2/k_1 has varied from 0.50, which corresponds to a rectangular stress distribution, to 0.67 for a triangular distribution. In practical cases, the ratio pf_{yp}/f_c'' is generally

of the order of 0.2. Hence, the extreme variation of Eq. (29) is from about 0.85 to 0.92 times pf_{yp}, or approximately eight percent. This variation is of the same order of magnitude as the experimental scatter in well-controlled laboratory tests. Hence, any reasonable equation such as Eq. (16) or (19), and even a fixed value of $7d/8$ for the internal moment arm, seem to be satisfactory for design purposes, when the member fails in tension and the percentage of reinforcement is small.

For compression failures, theories of the Stüssi type lead to Eq. (10) and (13). By proper choice of k_1, k_2 and ϵ_u, this system of equations will give accurate results, and the theory is further flexible enough to permit extension beyond the symmetrical bending of a rectangular section. It may also be noted that, in the standard theory, $k_1 = 0.5$ and the modular ratio n replaces m. Hence, Eq. (13) will reduce to the well-known expression

$$c/d = \sqrt{2pn + (pn)^2} - pn. \tag{30}$$

On the other hand, equations of the form

$$\frac{M}{bd^2} = \alpha f_c' \tag{31}$$

have great advantages in their simplicity. Values of α from 1/2.6 to 1/3 have been proposed.

All theories which include studies of compression reinforcement have proposed that such reinforcement should be considered effective with its full yield-point stress.

Some applications of ultimate theories to combined bending and axial load have been made, most of which are referred to in detail in Sections 14 and 15.

A number of authors not referred to above have made valuable contributions to the ultimate theories of reinforced concrete without claiming that their assumptions were new. This is especially so in recent years since every set of assumptions logically possible seems to have been tried in the past. These authors are referred to in the bibliography of this bulletin.

Numerous articles and several books have pointed out the shortcomings of the standard theory and a transition to ultimate load design has been recommended, at times emphatically. Safety factors to be used in such ultimate design have been subject to considerable discussion. The majority of authors seem to agree that, contrary to our present design methods, equal safety factors for steel and concrete should be used. It has often been recommended, however, that the various ultimate equa-

tions be entered with the minimum, not the average, concrete strength specified for a certain structure. It has also been repeatedly recommended that a smaller factor of safety be used for dead load than for live load.

11. Basic Assumptions in Writer's Flexural Analysis

A study of the many assumptions that have been made in the past as applied to the results of the tests reported herein showed that the approach used by Stüssi (Fig. 8) is satisfactory for the purpose of analyzing the behavior of reinforced concrete members subject to combined bending and axial load.

a. Distribution and Magnitude of Compressive Stresses in Concrete

The stress-strain relation of concrete subjected to concentric compression has been the subject of many tests and considerable discussion in the past. A great number of mathematical expressions for this relation have been developed, most of which consider the range from zero to the maximum stress only, since the final collapse of a compressive specimen generally was believed to take place very shortly after the maximum stress was reached. Such stress-strain relations were also applied to bending by assuming a linear distribution of strains in the compression zone of a beam. At the maximum load the extreme "fibers" in a beam were assumed to be subject to a maximum stress and a corresponding ultimate strain which were both similar to those determined from the simple compression test. Talbot[10, 11] recognized, however, that an ultimate strain can be developed in flexure which is greater than the strain corresponding to the maximum stress in concentric compression. Since most early investigators removed strain-measuring instruments before the ultimate load was reached in order to avoid damage, and since the researches in the first three decades of this century were concerned with conditions under working loads mainly, this important observation seems to have been little known until it was rediscovered by O. Baumann in 1934.[44]

It has later been shown that such sudden failures as have been observed in concentric compression often are properties of the testing machine rather than of the test specimen, and stress-strain relations for concrete in compression have been reported[59, 60, 92, 104] which have been obtained in such a manner that loads and strains could be observed beyond the maximum load. An example of such diagrams is given in Fig. 9. It is recognized that the application of such a stress-strain relation in a flexural analysis has been questioned.[113] A plain concrete specimen which has been strained beyond the ultimate load in concentric compression is generally badly cracked and the response to load is highly

sensitive to time. Furthermore, the application to bending of stress strain relations obtained in concentric compression rests on the assumption that the stress which occurs as a response to strain is independent of the space gradient of strain. This assumption is one of expediency only. Its justification has never been proved, since measurements of stresses rather than strains are difficult indeed.

It has been observed, however, that considerably larger strains may be developed in bending than in concentric compression before cracks appear on the concrete surface. The highly strained outer fibers seem to

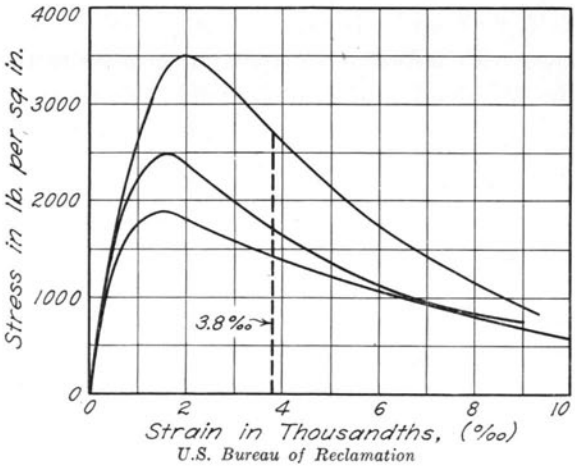

Fig. 9. Tests of 3- by 6-in. Cylinders

be able to yield and thus transfer stress to less strained fibers closer to the neutral axis and to compression steel. It is reasonable to assume, therefore, that the general characteristics of the diagrams in Fig. 9 are applicable to flexure. Hence the relation shown in Fig. 10 was adopted.

The maximum stress in flexure, f_c'', has generally been expressed in terms of the strength of cylinders, prisms or cubes tested in concentric compression. If such compressive specimens were cut from the actual structural elements, it is reasonable to expect that the relation between f_c'' and f_c' or f_{cu}' would be largely dependent on the effects of size and shape.[19, 45] However, auxiliary compression specimens are generally cast in separate forms, and it can therefore not be expected that the effects of degree of compaction during casting, curing conditions, and possible later drying conditions will be the same for the compression specimens as for the larger structural elements. It must also be recog-

nized that the quality of concrete in beams and columns cast from the same concrete mixture may differ, since beams generally are cast in a horizontal position while columns are cast vertically.

In later years it has been attempted to measure concrete strength in structural elements directly by means of indentation tests[101] or wave-velocity methods.[103] Since such methods are still in the experimental stage, however, the strength of 6- by 12-in. cylinders, f_c', has been adopted as a measure of concrete strength in the present tests. The maximum stress in flexure, f_c'', corresponding to the column specimens was chosen equal $0.85 f_c'$. This value was found as an average in numerous tests of vertically-cast concentrically loaded columns tested with flat ends.[43] Effects of size and shape of the columns as well as of the casting position is therefore included in the factor 0.85.

It is believed that the initial, curved part of the stress-strain diagram in Fig. 10 is fairly similar to the relation in direct compression. Since the important factors in a flexural analysis related to the stress-strain

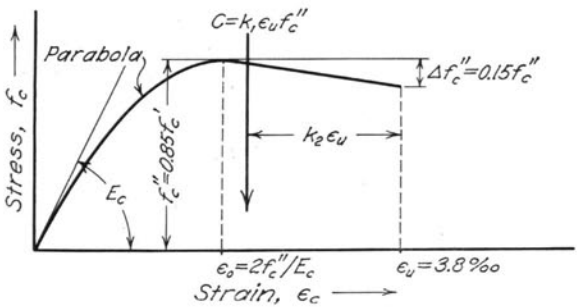

Fig. 10. Assumed Stress-Strain Diagram in Flexure

relation are k_1, k_2 and ϵ_u, small variations in the initial part of the stress-strain diagram are of minor importance. Auxiliary tests of 6- by 12-in. cylinders showed that Ritter's parabola is a good approximation when expressed in the following form

$$f_c = f_c'' \left[2 \frac{\epsilon}{\epsilon_o} - \left(\frac{\epsilon}{\epsilon_o} \right)^2 \right]. \tag{32}$$

With $\epsilon_o = 2f_c''/E_c$ this may be written as

$$f_c = \epsilon E_c \left(1 - \frac{\epsilon E_c}{4 f_c''} \right). \tag{33}$$

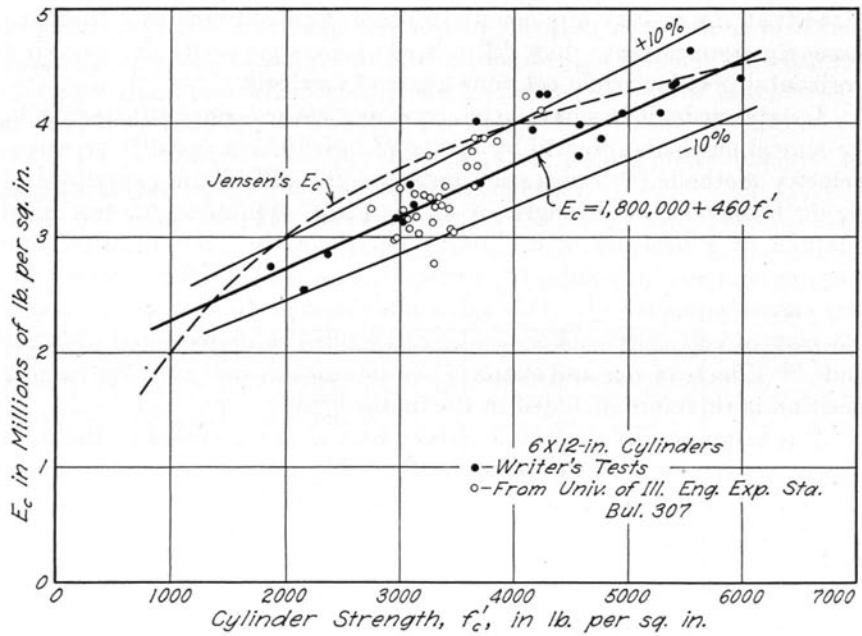

Fig. 11. Modulus of Elasticity of Concrete

The initial modulus of elasticity, E_c, was determined from cylinder tests, Fig. 11. A satisfactory agreement was found with Inge Lyse's equation

$$E_c = 1{,}800{,}000 + 460 f_c'. \tag{34}$$

It was decided, however, to use $f_c' = f_c''$ in Eq. (34) in order to determine the value of E_c corresponding to the column specimens. Hence, for a column with cylinder strength $f_c' = 4000$ p.s.i., f_c'' is 3400 p.s.i., and the modulus of elasticity, E_c, is $(1{,}800{,}000 + 460 \cdot 3400)$ p.s.i.

The ultimate strain, ϵ_u, was determined from tests of eccentrically loaded columns reported herein. Such strain measurements are, however, difficult to interpret. With one exception, all columns were cast and tested in the same vertical position, and it was observed that all columns failed in compression in the upper half. One column was turned upside down before testing, and only this column failed in the lower half. This weakness of the upper portion of vertically-cast columns, which the writer believes is due to a water gain with resulting lowered c/w ratio in the upper part and a better compaction in the lower part of the specimens, was also observed and discussed by Slater and Lyse.[25]

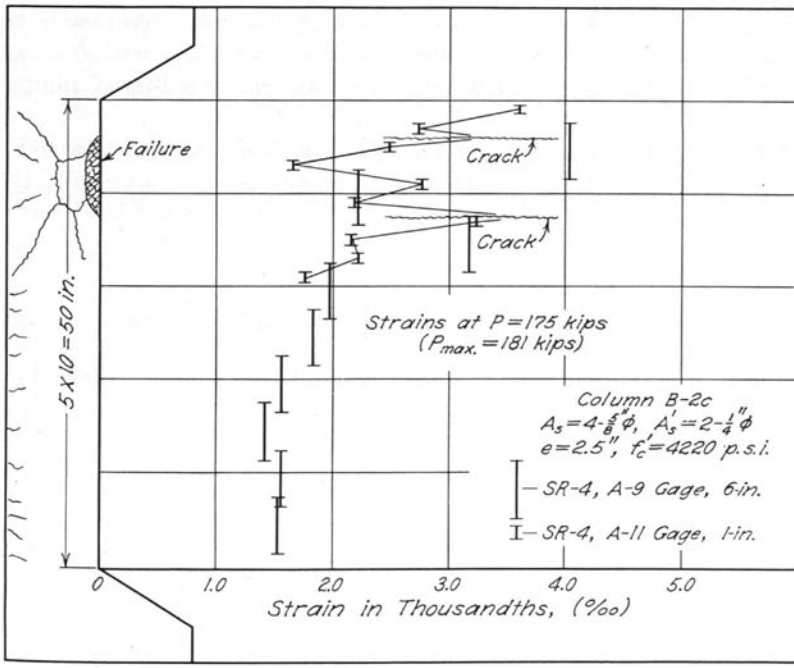

Fig. 12. Distribution of Strains over Height of Column

In order to throw some light on the distribution of strains along the length of the column shaft, an extra column specimen was prepared and tested with a large number of SR-4 gages attached to the compression face. The distribution of strains near the ultimate load is given in Fig. 12. It should be noticed that a general trend of increasing strains exists from the bottom towards the top of the column shaft. Near failure two major compression cracks extending horizontally across the compression face were developed as indicated in Fig. 12. As the final failure took place, the shaded area shown in the figure and marked "Failure" was extruded. Unfortunately, both major compression cracks occurred between two 1-in. gages. Nevertheless it appears that the strain at a given high load is not a well-defined quantity. At least three different quantities of strain may be considered: (1) The average strain over the entire length of the compression face, (2) A strain measured over a reasonably long gage length (6 in.) in the failure region, and (3) A local strain measured over a short gage length (1 in.) at a compression crack. These three quantities will increase in value in the order listed above, and it is believed that near failure No. 3 will be at least twice as large as No. 1.

It is felt, however, that No. 2 is the most reasonable value to be considered in a flexural analysis. Hence two SR-4, A-9 gages with 6-in. gage length were attached to the compression face of all columns, one near the center and one near the upper quarter point.

Strains measured in the failure region in this manner are shown in Fig. 13 for the columns C-1 to C-5. Similar curves were prepared for all other columns. It should be noted that while the ultimate load was observed in all cases, the last increment of strain could generally not be observed. Thus, the dotted lines in the last increment of all curves in

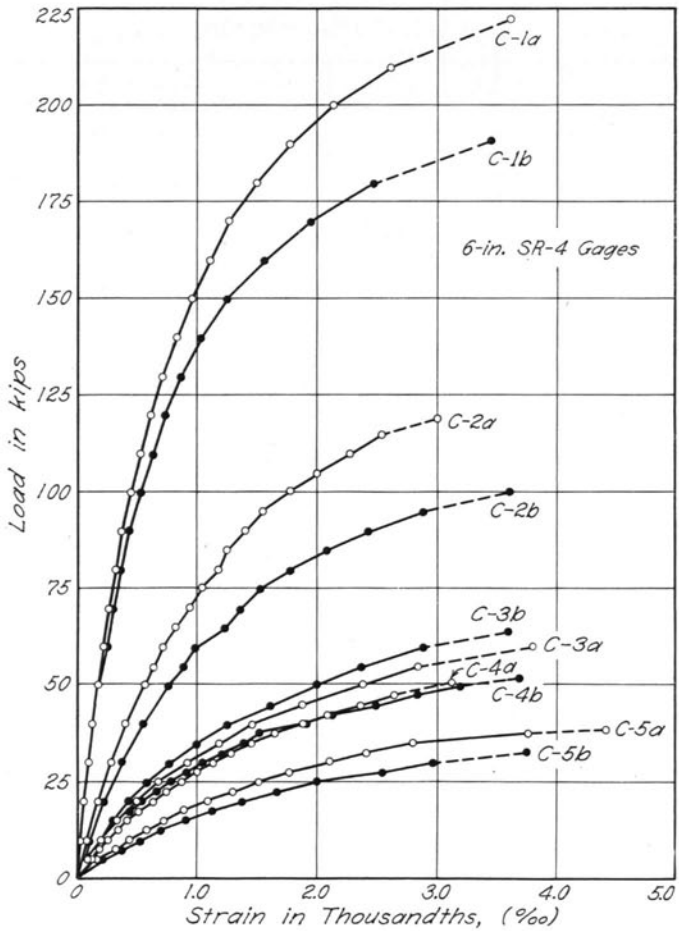

Fig. 13. Load-Strain Curves for Columns C-1 to C-5

Fig. 13 represent an extrapolation of strain to a known ultimate load. Ultimate strains obtained in this manner are presented in Fig. 14 for all square columns failing in compression before or shortly after the tension steel reached yielding.

The experimental findings in Fig. 14 are compared with relations between f_c' and ϵ_u given by previous investigators.

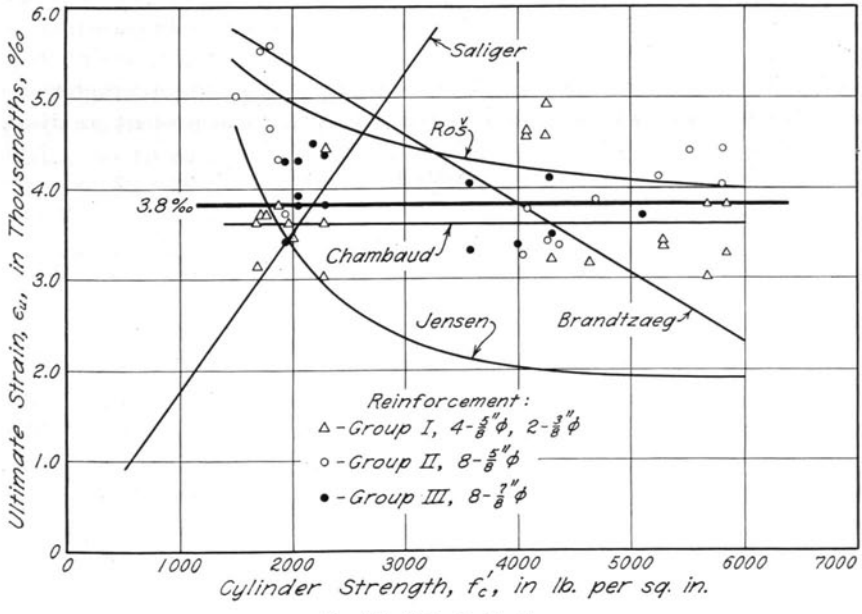

Fig. 14. Ultimate Strains

A. Brandtzæg[51, 56, 57, 61] developed the empirical Eq. (17). R. Saliger[60] reported values of ultimate strain from three to seven per mill and recommended Eq. (18).[99] V. P. Jensen[80, 81] assumed

$$\epsilon_u = \frac{f_c'}{(1 - \beta)\, E_c}$$

where the plasticity ratio, β, and the modulus of elasticity, E_c, were assumed as functions of f_c' (Eq. 27). M. Roš[78] gave the following equation for the ultimate strain

$$\epsilon_u = (3.5 + 2860/f_c')\, 10^{-3}. \qquad (35)$$

R. Chambaud reported some carefully made tests in 1949.[102, 108] In beam tests using electric strain gages, he found a constant value $\epsilon_u = 3.6$ per mill for cube strengths ranging from about 2000 to 7000 p.s.i.

It appears from Fig. 14 that the findings of these earlier investigators are very different. This is understandable, since the test values obtained probably are sensitive to time effects, the gage length used, and the location of the gage with respect to compression cracks.

A considerable scatter is also present in the test results presented in Fig. 14. Since the ultimate strength of reinforced concrete members is rather insensitive to variations in ϵ_u, however, a constant average value $\epsilon_u = 3.8$ per mill was considered satisfactory for the present analysis.

Table 6
Values of k_1 and k_2

	Writer's Theory Assumptions of Fig. 10			Jensen's Modified Theory $f_c'' = 0.85 f_c'$			Jensen's Original Theory $f_c'' = f_c'$		
f_c'	k_1	k_2	α	k_1	k_2	α	k_1	k_2	α
0	0.925	0.513	0.555	1.000	0.500	0.500	1.000	0.500	0.500
1000	0.873	0.481	0.551	0.978	0.490	0.501	0.970	0.485	0.501
2000	0.835	0.459	0.550	0.923	0.463	0.502	0.900	0.452	0.502
3000	0.808	0.444	0.550	0.856	0.431	0.503	0.820	0.417	0.508
4000	0.786	0.432	0.550	0.790	0.404	0.512	0.750	0.389	0.518
5000	0.770	0.423	0.550	0.735	0.383	0.521	0.695	0.370	0.531
6000	0.758	0.417	0.550	0.691	0.368	0.532	0.654	0.358	0.547

The descending part of the stress-strain diagram (Fig. 10) was assumed linear, and the value of $\Delta f_c'' = 0.15 f_c''$ was found to give the best agreement with the ultimate loads of columns. Thus the slope of the descending branch in Fig. 10 is intermediate between Chambaud's assumption (Fig. 8) and the results of compression tests (Fig. 9).

The constants k_1 and k_2 (Fig. 10) are presented in Table 6 as a function of the cylinder strength, f_c'. Values of the corresponding constants as determined from V. P. Jensen's assumptions are also entered in this table.

b. Tensile Stresses in Concrete

It is recognized that the concrete near the tensile reinforcement will, to a certain extent, relieve steel stresses between cracks.[60, 90] The writer also believes that concrete near the neutral axis develops some tensile stresses. It is felt, however, that such increases in ultimate flexural strength of reinforced concrete members as may be due to the concrete carrying longitudinal tension are generally small, and are further unreliable for practical purposes.

F. Gebauer[42] (Fig. 8) and others have pointed out that a precompression due to shrinkage of the surrounding concrete will exist in the

tensile reinforcement. Thus, an equivalent tension in the concrete should be considered. The strains which correspond to a precompression of this nature have generally been observed with reference or zero readings taken after the cement had set. In this manner, precompression stresses as large as 10,000 p.s.i. have been found. In the present tests, measurements of such compressive stresses in the reinforcement were made by means of electric SR-4 gages attached to the steel and embedded in the concrete. Reference readings could thereby be taken immediately after the concrete was placed and the steel strains could be followed throughout the period of setting, moist curing and final drying in the air of the laboratory. Variations in steel strains were found very similar to those reported by F. R. Beyer.[107] The total compressive stresses after 28 days, when the specimens were tested, varied from a few to about 500 p.s.i. only.

For these reasons it was assumed in the present analysis that no tensile stresses exist in the concrete.

c. Bernoulli's Hypothesis

The hypothesis of linear distributions of strains in bending has sometimes been questioned when applied to combined bending and axial load. The numerous strain measurements made in these tests provide some evidence on this question.

Figures 15a, b and c and 16a, b and c show typical distributions of strains across a section near the failure region. Some representative examples of compression and tension failures as well as those near balanced sections are given. Some deviation from linearity must be expected due to inaccuracies in individual strain measurements and to small errors in location of gage lines. It is evident from the figures, however, that a reasonable agreement exists between strains measured in the reinforcement and on the concrete surface. Furthermore, the departures from linearity appear to be inconsistent, indicating accidental or local rather than systematic variations. Hence it is assumed that Bernoulli's hypothesis is valid.

d. Absence of Slip

Bond was of minor importance in these tests since theoretically no shear existed in the prismatic part of the columns in which failure took place. Even so, local bond stresses and local slips must exist near tension cracks. Such slips were believed to be small, however, since a modern type of deformed bar was used as longitudinal reinforcement. It is reasonable to assume, therefore, that no general slip exists between concrete and reinforcing steel.

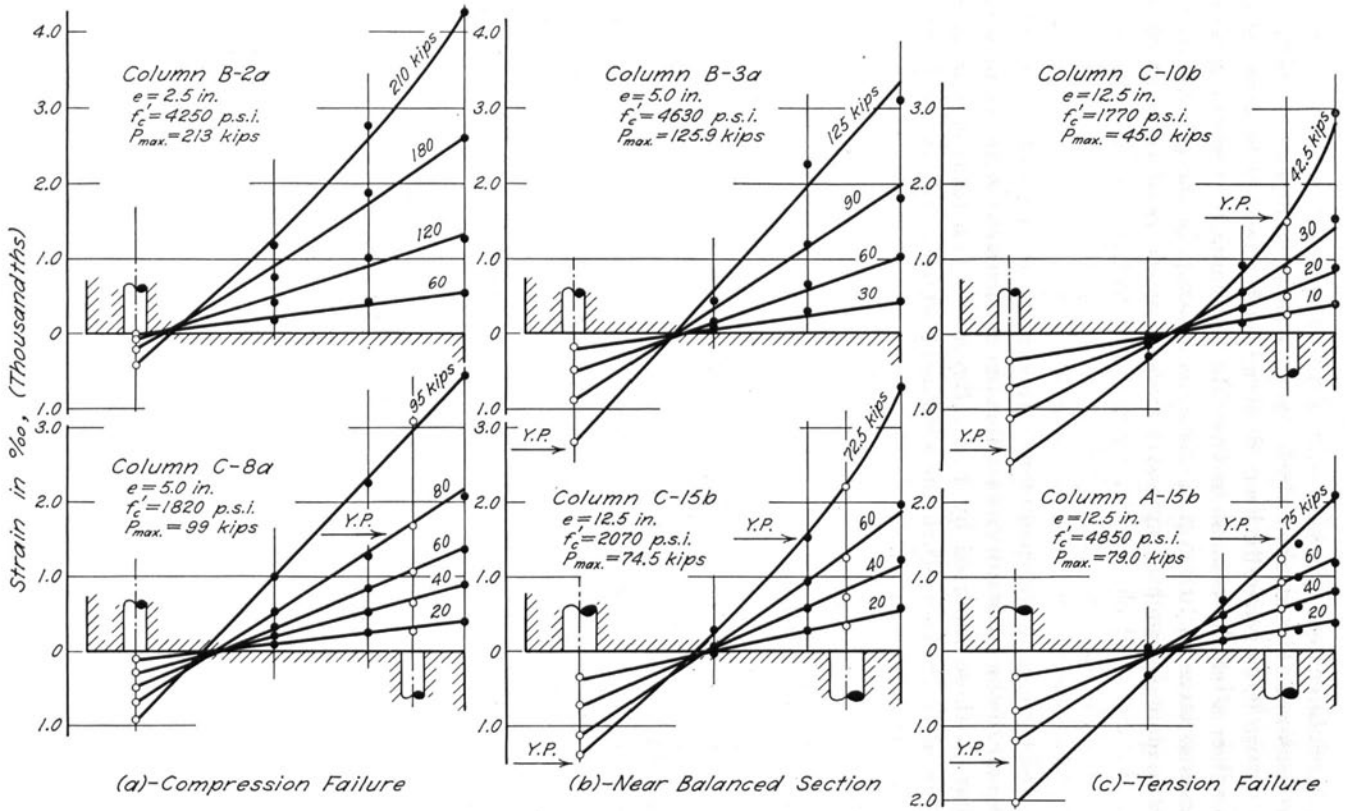

Fig. 15. Strain Distribution across Section, Tied Columns

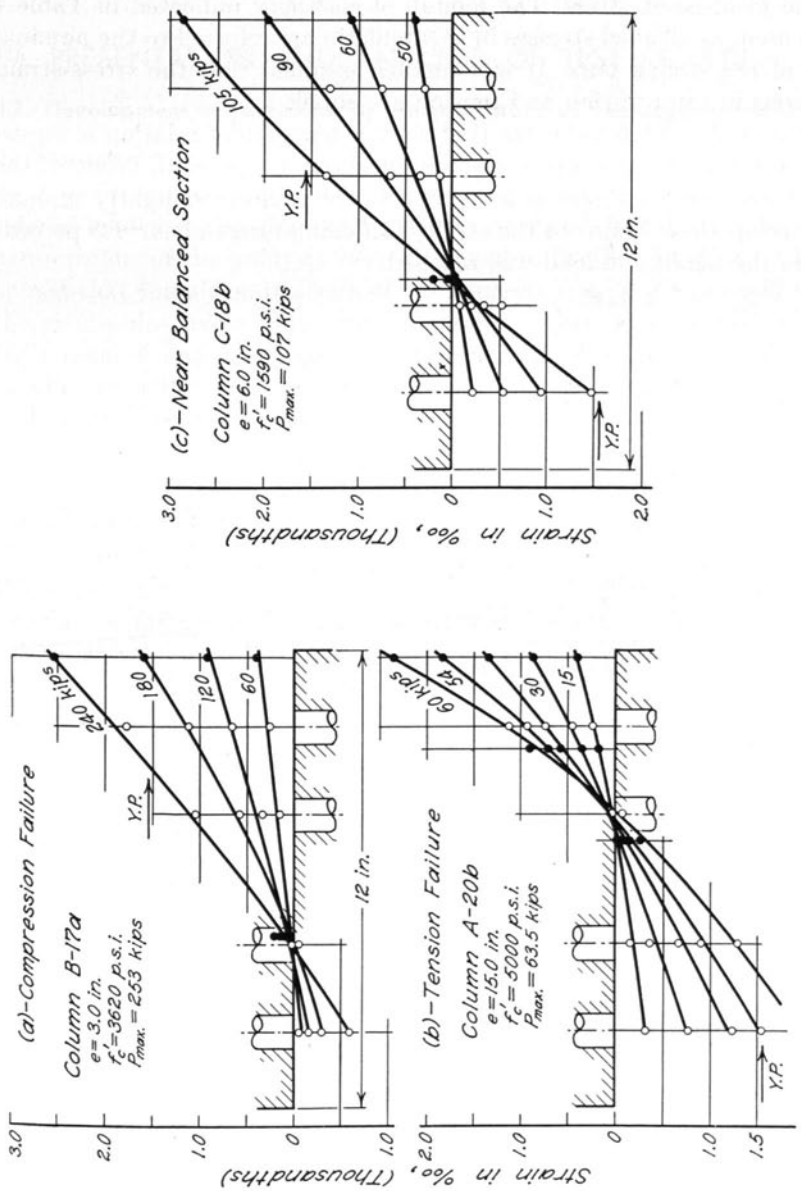

Fig. 16. Strain Distribution across Section, Spiral Columns

e. Stress-Strain Relation for Reinforcing Steel

This relation was assumed as the usual trapezoid with a yield level at the yield-point stress. The moduli of elasticity indicated in Table 4 were used, as all steel stresses in this bulletin are referred to the nominal area of reinforcing bars. It was further assumed that the stress-strain relations in compression and tension are equal.

Figure 3a and b indicates that such a trapezoidal relation is an excellent approximation up to a strain of about 1.5 percent. None of the specimens reported herein appeared to be reinforced lightly enough to develop steel strains in the strain hardening range above 1.5 percent before the maximum load was reached.

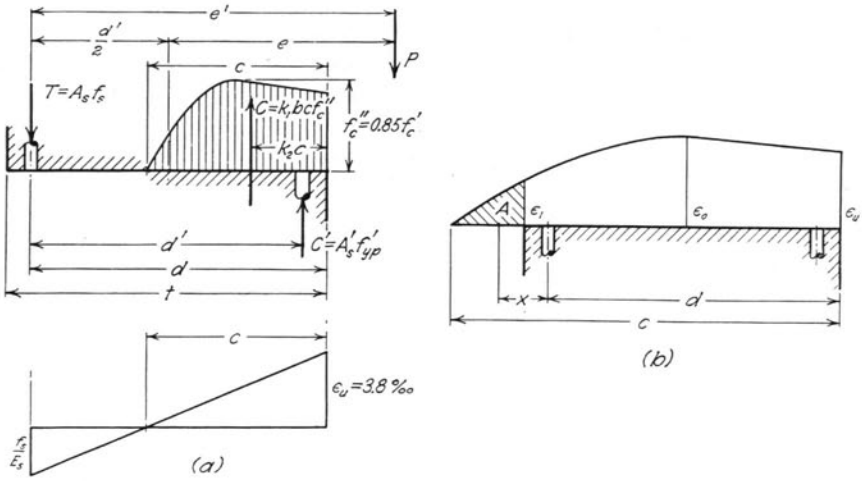

Fig. 17. Flexural Analysis of Rectangular Columns

IV. PRESENTATION AND ANALYSIS OF TEST RESULTS

12. Development of Equations for Ultimate Loads of Rectangular Sections

a. Tension Failures

A rectangular section with reinforcement at opposite faces is considered loaded in the plane of symmetry as shown in Fig. 17. The basic assumptions of the analysis were discussed in Section 10. Since it is assumed that the ultimate strain of the concrete is $\epsilon_u = 3.8$ per mill while the yield-point strain of the steel generally is about one to two per mill, both tension and compression reinforcement may be assumed to be strained over the yield point at failure. Using the notation of Fig. 17a, and taking moments about the tension steel

$$Pe' = k_1 f_c'' bc\,(d - k_2 c) + A_s' d' f_{yp}'. \tag{36}$$

Equilibrium of forces gives

$$P = k_1 f_c'' bc + A_s' f_{yp}' - A_s f_s. \tag{37}$$

For tension failure $f_s = f_{yp}$, and solving for c/d, we obtain with $\alpha = k_2/k_1 = 0.55$ (Table 6)

$$k_1 \frac{c}{d} = \frac{1}{2\alpha}\left\{-\left(\frac{e'}{d} - 1\right) + \sqrt{\left(\frac{e'}{d} - 1\right)^2 + 4\alpha\left[p'\frac{f_{yp}'}{f_c''}\frac{d'}{d} + \frac{e'}{d}\left(p\frac{f_{yp}}{f_c''} - p'\frac{f_{yp}'}{f_c''}\right)\right]}\right\} \tag{38}$$

in which $p' = \dfrac{A_s'}{bd}$, $p = \dfrac{A_s}{bd}$ and $f_c'' = 0.85 f_c'$. Substituting Eq. (38) in Eq. (37) gives

$$P = f_c'' bd\left\{p'\frac{f_{yp}'}{f_c''} - p\frac{f_{yp}}{f_c''} + \frac{1}{2\alpha}\left[-\left(\frac{e'}{d} - 1\right) + \sqrt{\left(\frac{e'}{d} - 1\right)^2 + 4\alpha\left[p'\frac{f_{yp}'}{f_c''}\frac{d'}{d} + \frac{e'}{d}\left(p\frac{f_{yp}}{f_c''} - p'\frac{f_{yp}'}{f_c''}\right)\right]}\right]\right\}. \tag{39}$$

Brandtzæg, Saliger, Whitney, Jensen and others have assumed $\alpha = \frac{1}{2}$ which corresponds to an equivalent rectangular stress-block. When this value, $\alpha = \frac{1}{2}$, is substituted in Eq. (39) the resulting expression for the ultimate load is very similar to those developed by A. Brandtzæg and C. S. Whitney.

Equation (39) may be simplified for symmetrical reinforcement, when $pf_{yp} = p'f_{yp}'$,

$$P = \frac{f_c''bd}{2\alpha}\left[-\left(\frac{e'}{d} - 1\right) + \sqrt{\left(\frac{e'}{d} - 1\right)^2 + 4\alpha p\frac{f_{yp}}{f_c''}\frac{d'}{d}}\right]. \quad (40)$$

When there is no compression reinforcement, $p' = 0$ and the ultimate load is

$$P = f_c''bd\left\{-p\frac{f_{yp}}{f_c''} + \frac{1}{2\alpha}\left[-\left(\frac{e'}{d} - 1\right) + \sqrt{\left(\frac{e'}{d} - 1\right)^2 + 4\alpha p\frac{f_{yp}}{f_c''}\frac{e'}{d}}\right]\right\}. \quad (41)$$

When e'/d is large (>1.5), the two equations above do not give satisfactory slide-rule accuracy. This can be improved by multiplying and dividing by $\left[+\left(\frac{e'}{d} - 1\right) + \sqrt{\ldots\ldots}\right]$. Furthermore, putting $\alpha = \frac{1}{2}$ results in an error less than one percent if e' is large. For symmetrical reinforcement,

$$P = \frac{2A_sf_{yp}d'}{(e' - d) + \sqrt{(e' - d)^2 + 2A_s\frac{f_{yp}}{f_c''}\frac{d'}{b}}} \quad (42)$$

and when there is no compression steel

$$P = A_sf_{yp}\frac{(e' + d) - \sqrt{(e' - d)^2 + 2A_s\frac{f_{yp}}{f_c''}\frac{e'}{b}}}{(e' - d) + \sqrt{(e' - d)^2 + 2A_s\frac{f_{yp}}{f_c''}\frac{e'}{b}}}. \quad (43)$$

In addition when $e' = \infty$ (pure bending), Eq. (42) becomes $M = A_sf_{yp}d'$, while Eq. (43) reduces to Eq. (16).

For large percentages of compression steel ($p' > 2$ percent) and relatively small eccentricities, the error involved in neglecting a sub-

traction of the concrete area displaced by the compression steel may be four to six percent on the unsafe side. This error may be corrected by considering an effective yield point, $f_{yp}' - f_c''$. For symmetrical reinforcement this leads to

$$P = f_c'' bd \left\{ -p + \frac{1}{2\alpha}\left[-\left(\frac{e'}{d} - 1\right) + \sqrt{\left(\frac{e'}{d} - 1\right)^2 + 4\alpha p\left(\frac{f_{yp}}{f_c''}\frac{d'}{d} + \frac{e' - d'}{d}\right)}\right]\right\}. \quad (44)$$

b. Compression Failures

The stress in the tension steel at failure, being less than the yield point, must be determined by geometrical considerations. Referring to Fig. 17, we obtain the compatibility equation

$$f_s = \epsilon_u E_s \frac{d - c}{c} \leqq f_{yp}. \quad (45)$$

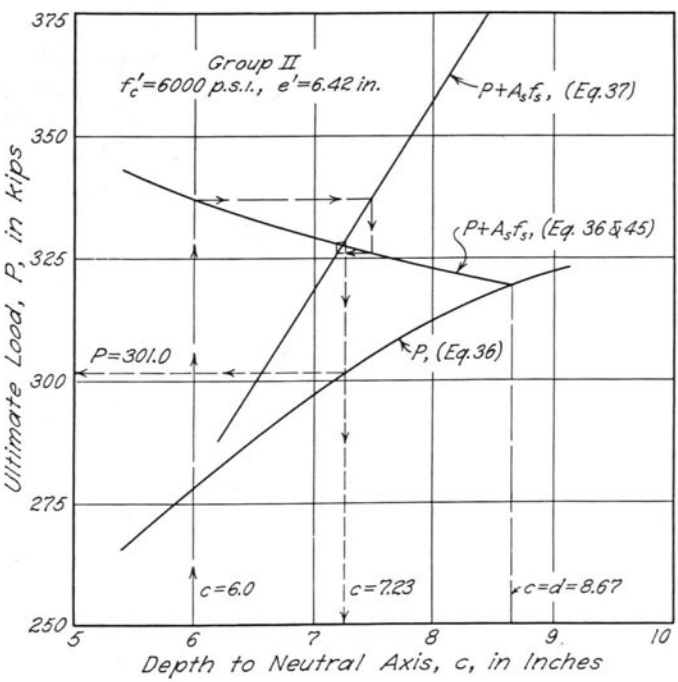

Fig. 18. Approximation Procedure

For compression failures, the error that is involved in neglecting a subtraction in Eqs. (36) and (37) for the concrete displaced by the compression reinforcement may be of the order of 4–6 percent on the unsafe side. This error may be corrected by considering the effective yield point of the compression steel as $f_{yp}' - f_c''$ in Eqs. (36) and (37).

Solving Eqs. (36), (37) and (45) for c and P yields a cubic equation in c, the solution of which is very time-consuming. Therefore a procedure involving successive approximations was developed for the purpose of the present analysis.

With known section dimensions, material constants and eccentricity e', the problem is to find c and P. The approximation procedure is illustrated in Fig. 18 for a column of Group II with $f_c' = 6000$ p.s.i. and $e' = 6.42$ in. An estimated value of c is substituted in Eqs. (36) and (45). The resulting values of P and f_s are introduced in Eq. (37) and a new value of c results. This new c is carried back to Eqs. (36) and (45), etc. Solving Eq. (37) for c involves a linear equation only. The computations of this example are tabulated below:

For Group II: $A_s = A_s' = 1.24$ sq in., $d = 8.67$ in., $d' = 7.34$ in., $b = 10$ in.
If $f_c' = 6000$ p.s.i., $f_c'' = 5100$ p.s.i., $k_1 = 0.758$, $k_2 = 0.417$
Corrected $f_s' = 43.6 - 5.1 = 38.5$ ksi; $\epsilon_u E_s = 3.8 \cdot 28.0 = 106.4$ ksi
Eccentricity $e' = 2.75 + 3.67 = 6.42$ in.

	$c =$	6.0	7.46	7.19	7.23	in.
	$k_1 f_c'' bc =$	232.0	288.4	278.0	279.5	kips
Eq. (36)	$k_1 f_c'' bc(d - k_2 c) =$	1431.4	1603.5	1576.3	1582.0	kips-in.
	$A_s' f_s' d' =$	350.4	350.4	350.4	350.4	kips-in.
	$Pe' =$	1781.8	1953.9	1926.7	1932.4	kips-in.
	$P =$	277.5	304.3	300.1	301.0	kips
Eq. (45)	$f_s =$	47.3	17.3	21.9	21.2	ksi
	$A_s(f_s' - f_s) =$	−10.9	26.3	20.6	21.5	kips
Eq. (37)	$P - A_s(f_s' - f_s) =$	288.4	278.0	279.5	279.5	kips
	$c =$	7.46	7.19	7.23	7.23	in.

Solution: $P = 301.0$ kips, $c = 7.23$ in.

By differentiation it may be found that this procedure will converge if

$$k_1 f_c'' \left(1 + \frac{d - 2k_2 c}{e'}\right) - p\epsilon_u E_s \left(\frac{d}{c}\right)^2 > 0 \qquad (46)$$

which is generally the case.

If the left side of Eq. (46) is near or equal to zero, oscillations will take place. In this case the average of the original and the new c should be used in the next approximation cycle.

Finally, if the left side of Eq. (46) is negative, which may occur for large values of p and e' with small values of f_c'', divergence will take

place. The above procedure should then be modified as follows: Eqs. (36) and (45) are entered with a value $c=c_1$, and $c=c_2$ results from Eq. (37). Then a value $c_1+\gamma(c_2-c_1)$, where γ is a fraction, should be returned to Eqs. (36) and (45). Convergence will result if a suitable value of γ is chosen by trial.

If the eccentricity, e, is very small, the neutral axis will fall outside the section, Fig. 17b. The equilibrium equations must then be modified to

$$Pe'=k_1f_c''bc(d-k_2c)+A_s'd'f_{yp}'+Abx \tag{36a}$$

$$P=k_1f_c''bc+A_s'f_{yp}'-A_sf_s-Ab. \tag{37a}$$

Equation (45) is still valid; and the quantities A and x may be found by geometrical considerations. Hence, the approximation procedure outlined above may still be used.

c. Balanced Sections

A given section is considered balanced when it is loaded with such an eccentricity that the tension steel reaches its yield point and the concrete reaches its ultimate strain at the same load. When, for a given eccentricity and concrete section, both limiting conditions are reached at the same load, the reinforcement is referred to as being balanced. The limiting condition between tension and compression failures, which is defined as a balanced failure, may be referred to in terms of the ratio $k=c/d$. For the balanced condition, this ratio is

$$k_b=\frac{c_b}{d}=\frac{\epsilon_u}{\epsilon_u+f_{yp}/E_s}. \tag{47}$$

A tension failure will result if $0<k<k_b$, and compression failure will take place if $k_b<k\leqq\infty$. The various balanced quantities, P_b,e_b, p_b and p_b' may then be computed from Eqs. (36) and (37), if the concrete section is given. Any two of the four quantities may be chosen, and the remaining two may be computed.

13. Test Results of Rectangular Sections, Groups I, II and III

a. General Behavior and Modes of Failure of Specimens

Two modes of failure prevailed in the tests reported herein: compression failures and tension failures. Only a few columns had such a combination of variables that the mode of failure was close enough to balanced conditions to be difficult to observe. The observed modes of failure of the individual test columns are listed in Tables 7, 8 and 9. The agreement with predicted modes of failure is discussed in Section 13b.

The general behavior of the test columns may, perhaps, best be studied in the light of the assumptions made in Section 11. For the given sections and eccentricities (including deflections) the theoretical strains in concrete and steel may be computed from the smallest loads throughout the loading range to failure. This may be achieved by assuming a range of values for the concrete strain ϵ_c at the compression face and computing the corresponding values of k_1 and k_2 in accordance with Fig. 10. For example when $\epsilon_c = \epsilon_o$, $k_1 = 2/3$ and $k_2 = 3/8$. When $\epsilon_c < \epsilon_o$, it may be found by integration of Eq. (32) that

$$k_1 = \frac{\epsilon_c}{\epsilon_o}\left(1 - \frac{\epsilon_c}{3\epsilon_o}\right) \qquad k_2 = \frac{4 - \frac{\epsilon_c}{\epsilon_o}}{12\left(1 - \frac{\epsilon_c}{3\epsilon_o}\right)}. \tag{48}$$

For $\epsilon_o < \epsilon_c < \epsilon_u$, the constants k_1 and k_2 may be found by geometrical considerations. Then the position of the neutral axis and the load corresponding to the given section and eccentricity with the successive chosen values of ϵ_c may be computed by an approximation procedure very similar to that presented in Section 12b.

In the following discussion, the observed and predicted behavior of eight typical specimens is presented.

Columns A-7b, C-8a and B-13a (Figs. 19, 20 and 21) are typical examples of compression failures. Observed strains in the tension and compression reinforcement are presented as an average of three SR-4, A-11 gages. The strains on the compression face of the columns are generally given as measured by an SR-4, A-9 gage at and a short distance away from the failure region. Center deflections of the prismatic part of the column between the brackets are given as the center reading of the deflection bridge minus the average of the readings at the top and bottom of the column shaft (Fig. 7). The theoretical deflections were found as: $\delta = \epsilon_c L^2/8c$, where $L = 50$ in. The observed values of the position of the neutral axis were obtained as indicated in Fig. 15.

It appears that Column A-7b (Fig. 19) deformed continuously under increasing load with a slight movement of the neutral axis towards the compression face until the yield point of the compression reinforcement was reached. Then a discontinuity occurred in all theoretical curves presented in the figure as the compression steel continued to deform without any increase in stress, and thus the concrete alone was carrying all further increase in internal compressive force.

Columns C-8a and B-13a (Figs. 20 and 21) behaved in a very similar manner. The neutral axis did, however, move slightly towards the tension face of these columns before the compression steel reached yielding.

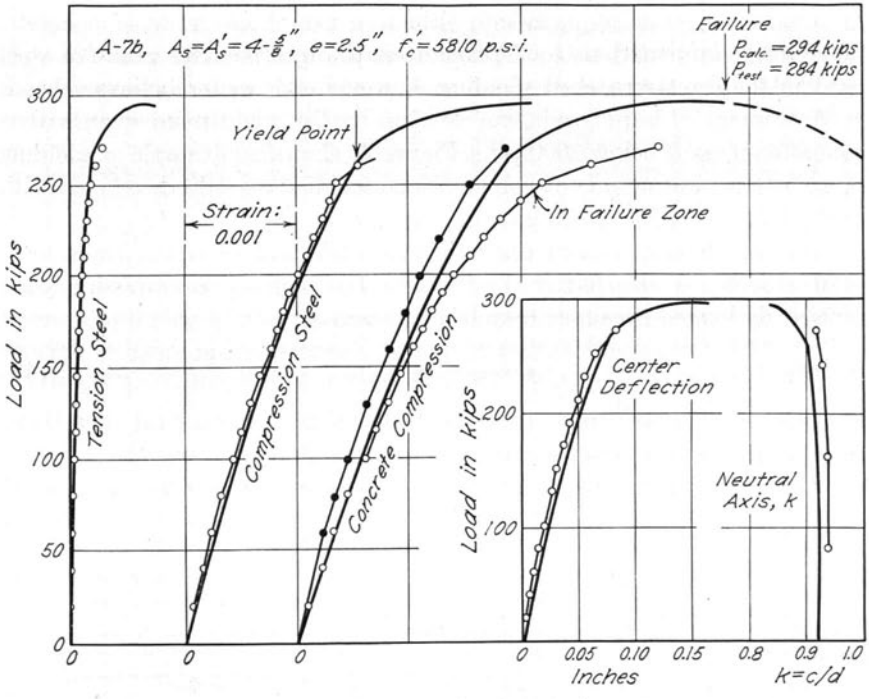

Fig. 19. Behavior of Column A-7b

The mode of failure for all three columns mentioned above was a typical compression failure. The final failure was caused by crushing of the concrete at the compression face of the specimens after the compression steel reached yielding, while the tension steel did not reach yielding.

It should be noted that strains increased very rapidly with load when the compression steel was yielding. Throughout these tests this phenomenon was found to be more pronounced, the larger the contribution of the compression reinforcement to the total internal compressive force. This rapid increase of strains reflects important properties of eccentrically loaded members. It is apparent that such a member is in a semi-neutral state of equilibrium when failure takes place. The concrete is in a plastic state in which the rate of loading and the duration of loads become factors of considerable importance.

The presence of such a semi-neutral equilibrium has been observed in the past and it has been stated that the concrete fails in compression *because* the compression steel yields. Thus it has been claimed that a high strength steel cannot be used effectively as a compression reinforcement

in eccentrically loaded members without a very high grade of concrete. Since large deformations took place after the intermediate grade of steel used in these tests reached yielding, however, the writer believes that a reinforcement of hard grade can develop its full yield point even with a concrete strength below 2000 p.s.i. Figure 20 shows an example of yielding in an intermediate grade of compression steel being easily developed with a concrete strength of 1820 p.s.i.

Volume changes of concrete due to centric and eccentric loads have been studied in the past.[20, 21, 22, 35, 51] The volume compression of a centrically loaded specimen may be expressed as

$$\epsilon_v = \epsilon_1 - 2\epsilon_2 \tag{49}$$

where ϵ_1 and ϵ_2 are the strains in longitudinal and lateral directions, respectively. For a small element at the compression face of an eccentrically loaded member, however, a strain gradient is present and the

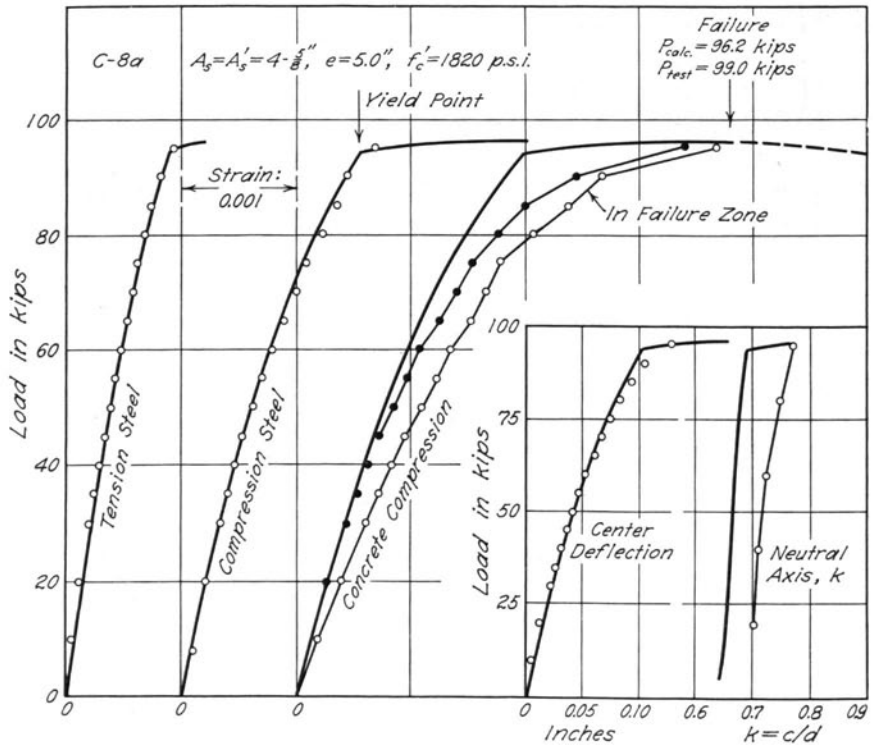

Fig. 20. Behavior of Column C-8a

strains in the two lateral directions are probably not equal. Nevertheless, Eq. (49) may be used as an approximation, ϵ_2 being the lateral strain at the compression face. Numerous tests have shown that the volume of concrete specimens decreases under increasing uni-axial compression, whether a strain gradient is present or not, until a stress of 80 to 90 percent of the ultimate is reached. Then the volume starts increasing at an increasing rate, so that a volume expansion is present at failure. The load at which the derivative of volume strain with respect to load is zero has been referred to as the *critical load*. It is believed that progressive internal splitting of the concrete is initiated at the critical load. Such a concept is basic in Brandtzæg's theory of failure for concrete.[20]

In the present tests of columns with a prismatic shaft 50 in. long it was found that the lateral strains had to be measured in the region of local compression failure if the volume strains were to be significant. One lateral gage only was used for each specimen, and this gage could generally not be placed in the expected failure region, since the longitudinal gages were already placed in this position. Therefore, the information gained regarding lateral and volume strains was of qualitative value

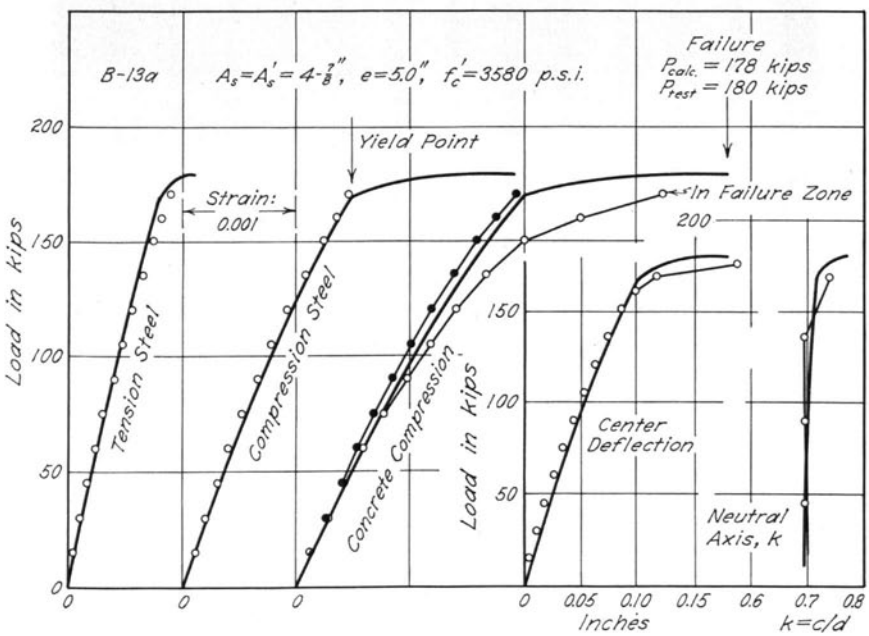

Fig. 21. Behavior of Column B-13a

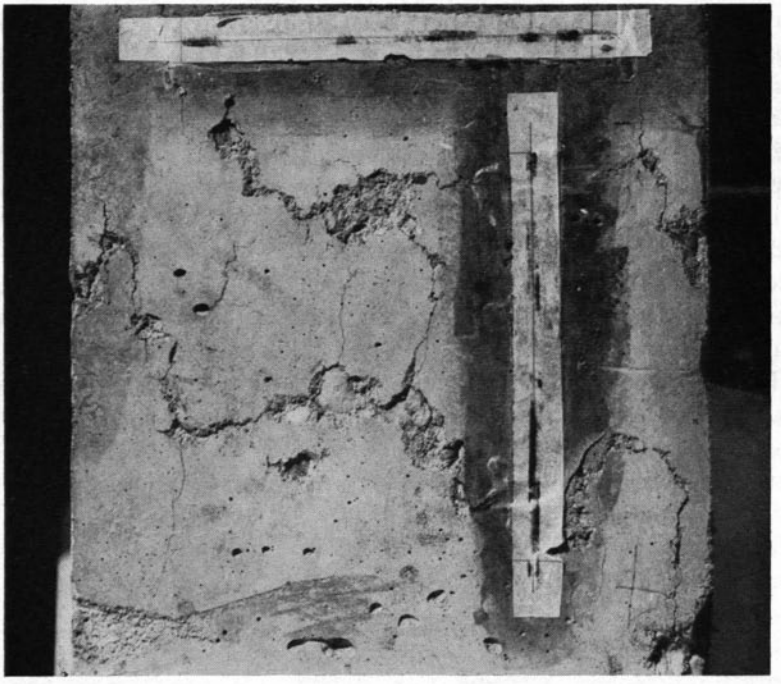

Fig. 22. Detail of Compression Failure

only. Critical loads ranged from about 80 to 95 percent of the ultimate loads, the percentage generally being higher the greater the force in the compression steel with respect to the total internal compressive force.

The presence of a disintegration of the concrete was also visible on the surface of the specimen shortly before failure. First, vertical tension cracks appeared on the compression face of the columns as shown in Fig. 22. At a slightly higher load compression cracks with a general horizontal trend formed as shown in Fig. 22, and the layer of concrete over the steel spalled off at a slightly higher load. Immediately after such spalling, the compression reinforcement buckled between ties, as shown in Fig. 23, and the load capacity of the members thereby dropped to a fraction of the ultimate load.

It may be noted, therefore, that the compression mode of failure of eccentrically loaded tied columns was found to be very similar to the failure of such columns subjected to concentric compression. After failure

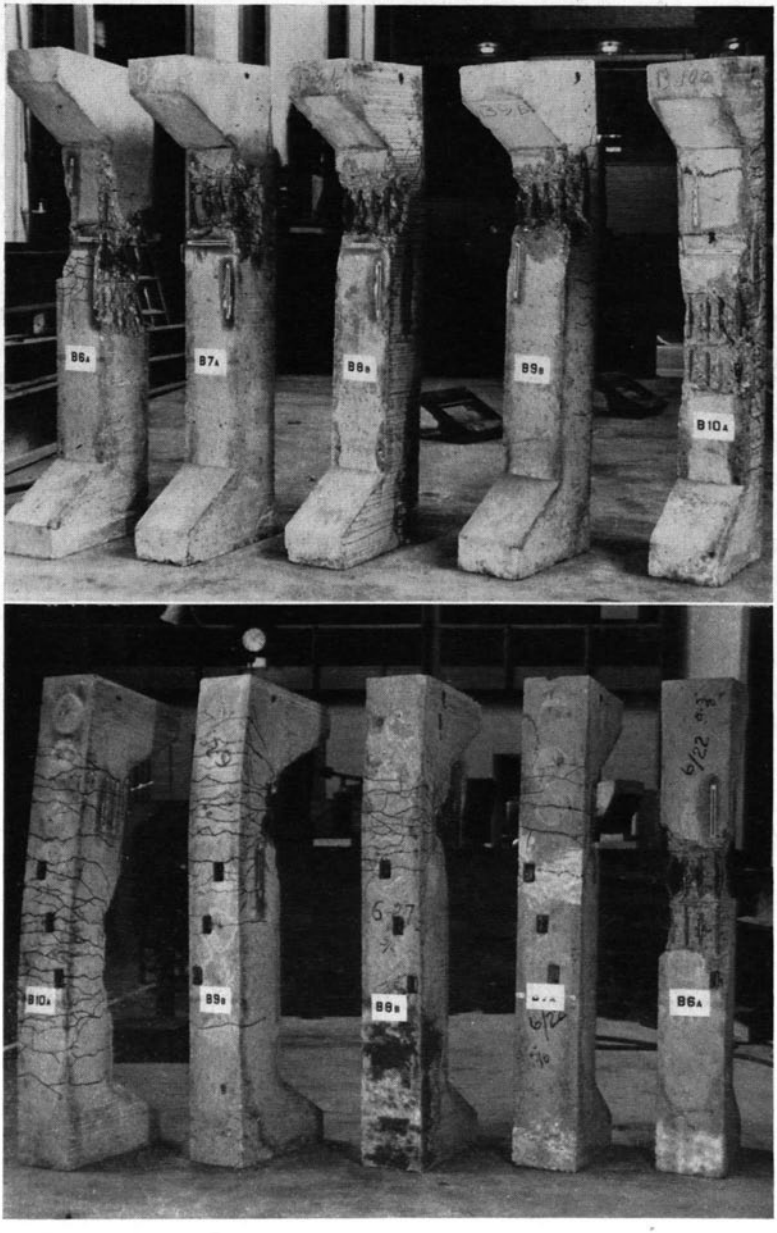

Fig. 23. Columns B-6 to B-10 after Failure

had been initiated by crushing and spalling of the concrete at the compression edge, the load fell off very quickly if further deformations were applied to the column.

The behavior of the columns which were loaded at mid-depth of the section, $e = 0$, was found to be very dependent on the arrangement of the reinforcement. In Group I an unsymmetrical reinforcement was used. The plastic centroid of such a section may be defined as the point at which the resultant of internal uniform stresses, computed with $f_s = f_{yp}$ and $f_c = 0.85\ f_c'$, cuts the section. If the load is applied exactly at this plastic centroid, the column is truly centrically loaded. For unsymmetrical reinforcement, the plastic centroid is not at mid-depth of the section, but closer to the geometric centroid of the reinforcement. Hence, it is reasonable that the behavior of Columns No. 1 was found to be very similar to the compression failures already discussed, since these columns actually were eccentrically loaded.

Columns No. 6 and 11 were symmetrically reinforced and therefore concentrically loaded for $e = 0$. The behavior of these columns is discussed in Section 16.

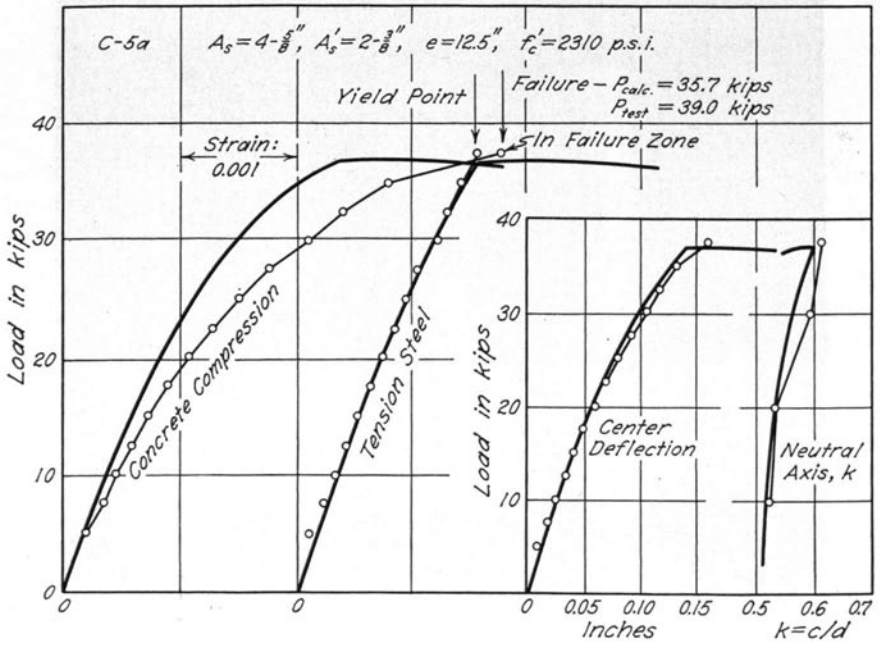

Fig. 24. Behavior of Column C-5a

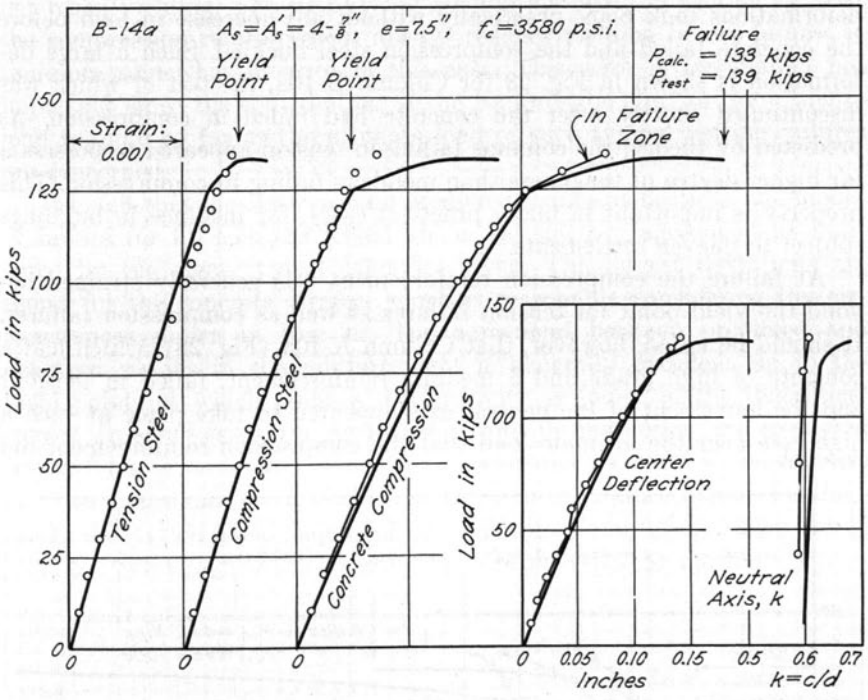

Fig. 25. Behavior of Column B-14a

Column C-5a (Fig. 24) is an example of a column with an almost balanced section. The tension steel, however, theoretically reached yielding and caused some movement of the neutral axis towards the compression edge before the concrete reached its ultimate compressive strain.

Column B-14a (Fig. 25) gives an almost perfect balanced condition. As loading proceeded, the first discontinuity was caused by yielding of the compression steel. Yielding in the tension reinforcement followed, and failure of the concrete in compression took place after a small increase in deformation, but practically no increase in load.

Columns A-5a, A-15a and A-10a (Figs. 26, 27 and 28) are typical examples of tension failures. The specimens behaved much like those failing in compression until the tension steel reached yielding. Then, however, a neutral equilibrium even more pronounced than that for compression failures was established, and it was practically impossible to set the columns to rest under an applied load so that readings of strains and deflections could be made. It was nevertheless noted that very large

deformations took place practically without any increase in load before the concrete failed and the compression steel buckled. Such a large deformation is shown in Fig. 23 for Column B-10a, the test of which was discontinued shortly after the concrete had failed in compression. As predicted by theory, the columns failing in tension appeared to possess a far higher degree of toughness than members failing in compression. This property is important in many practical cases, for instance in buildings subject to uneven settlements.

At failure the compression reinforcement was generally strained beyond the yield point for tension failures as well as compression failures. It should be noted, however, that Column A-10a (Fig. 28), which had a concrete of high grade and a medium reinforcement, failed in tension; and the movement of the neutral axis appeared to take place at such a high rate near the ultimate load that the compression reinforcement did

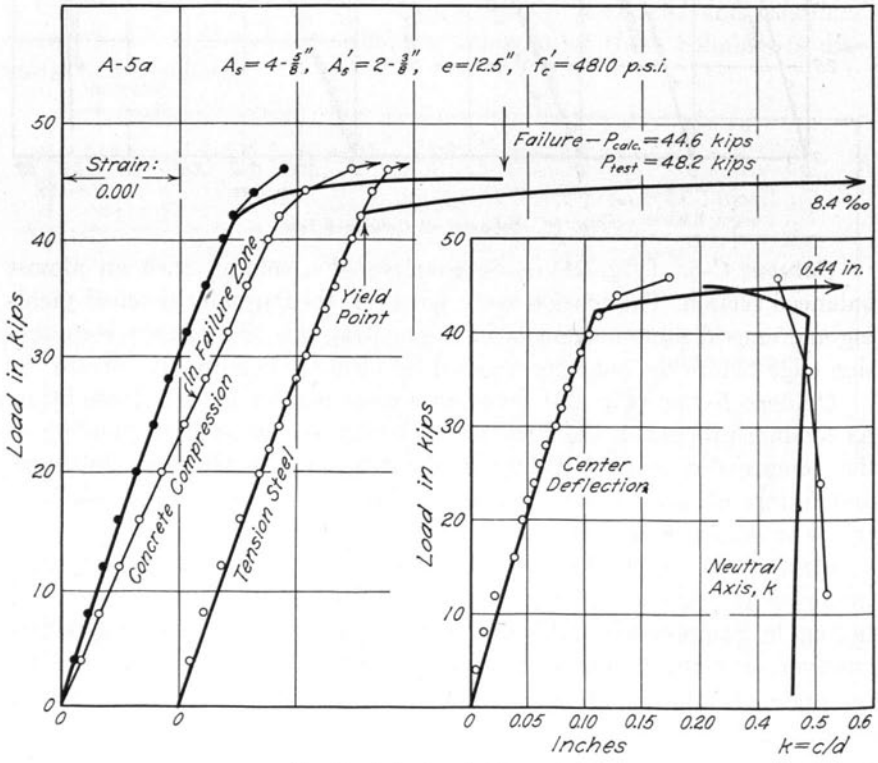

Fig. 26. Behavior of Column A-5a

not reach yielding. The simplifying assumption made in Section 11, that the compression reinforcement always reaches yielding before failure, is therefore somewhat in error in this case. This error is fortunately not important since the contribution of the compression steel to the ultimate load is small as far as the ultimate load of such typical tension failures are concerned.

It is felt that the observed and predicted strains, deflections and modes of failure for all columns tested are in satisfactory agreement as indicated by the eight typical examples given. The largest deviations are found for the concrete strains, which is reasonable considering the circumstances shown in Fig. 12. The agreement between predicted and observed strains in the reinforcement is generally excellent up to the yield point, at which point a discontinuity is found in the theoretical curves. In some cases, the measured strains do not follow the predicted break. This is reasonable, since these measured strains are the average of three gages and not a local observation in the failure region. Furthermore, the actual yield points of the individual reinforcing bars varied from the average property assumed in the theoretical analysis.

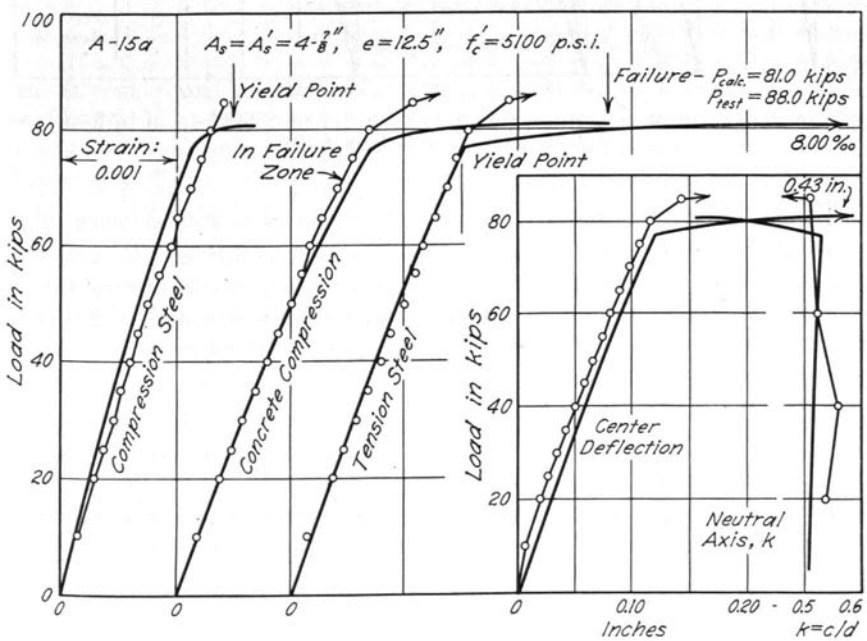

Fig. 27. Behavior of Column A-15a

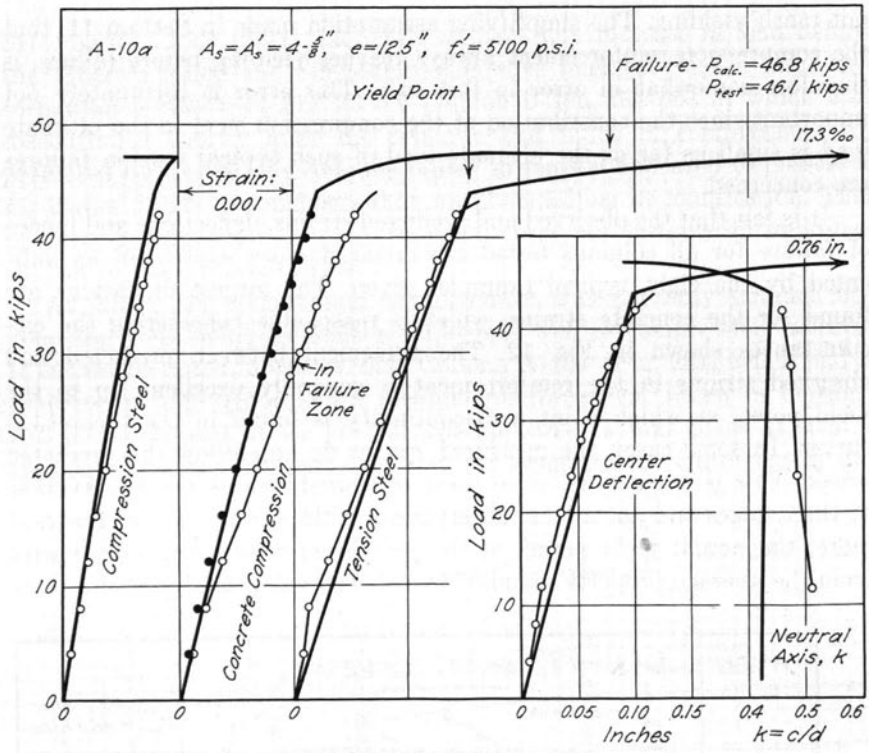

Fig. 28. Behavior of Column A-10a

The observed and predicted behavior of the test columns may also be compared by studies of steel stresses and the position of the neutral axis at failure. An example of such studies as applied to Group III is presented in Figs. 29 and 30. The observed steel stresses in Fig. 29 were obtained by multiplying the observed strains by E_s. The theoretical values were obtained by the writer's theory. It is felt that an agreement of general nature exists between them. The relatively low measured steel stresses for $e = 2.73$ may be interpreted as fairly good evidence of tensile stresses in the concrete.

The observed positions of the neutral axis presented in Fig. 30 were derived from graphs similar to those given in Fig. 15. As the theoretical positions of the neutral axis are referred to the ultimate loads, while the observed values refer to the last strain readings which were made at 90 to 95 percent of the ultimate, the direction of travel of the neutral axis is indicated as observed in the tests. Two columns with $e = 12.90$ in.,

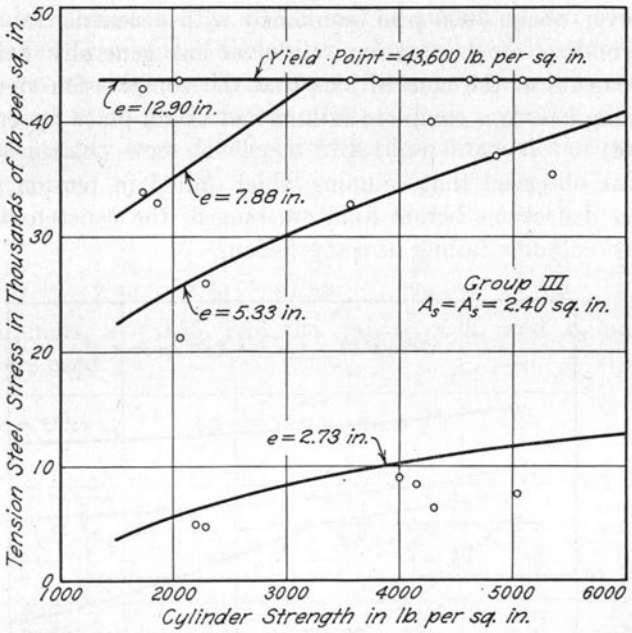

Fig. 29. Tension Steel Stresses at Failure

A-15a and b, are not plotted in the figure because no strain readings were made close enough to the ultimate to give significant information regarding the position of the neutral axis at failure. A general agreement between observed and predicted behavior is present in Fig. 30.

Hence it is believed that the behavior of tied reinforced concrete members subject to combined bending and axial load is rather well represented through the assumptions made in Section 11.

The behavior of eccentrically loaded tied columns as observed in these tests may be re-emphasized as follows:

1. The final failure of all columns was caused by crushing of the concrete at an ultimate strain of about 3.8 per mill. After such crushing had taken place, the compression reinforcement buckled between ties, and the load capacity of the columns thereby suddenly dropped to a very low value.

2. For moderate eccentricities it was found that the intermediate grade compression steel used always reached the yield point before failure of the concrete took place, even though the concrete strength varied from about 1500 to 5500 p.s.i. This was also the case for eccentricities as large as $1.25t$ if the concrete strength was low. For concrete

strengths over about 3000 p.s.i. combined with eccentricities over $1.0t$, however, yielding of the tension reinforcement generally caused such rapid movements of the neutral axis that the compression steel did not reach yielding before a complete failure had taken place by crushing of the concrete.

3. It was observed that columns which failed in tension developed much larger deflections before final crushing of the concrete took place than did the columns failing in compression.

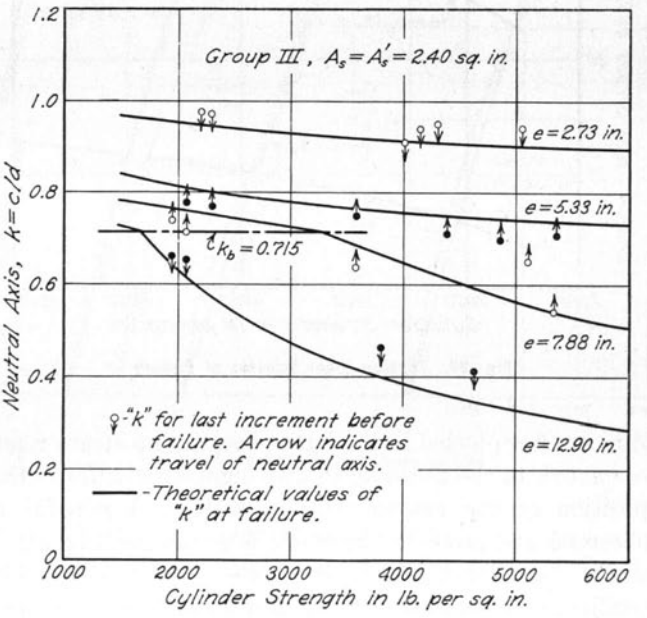

Fig. 30. Neutral Axis at Failure

4. Preceding the final failure of the concrete all columns were in a semi-neutral equilibrium with the applied load. This semi-neutral state of equilibrium was characterized by considerable increases in deformation for very small additions of load. Such relatively rapid increases in deformation with load were initiated by yielding either of the tension or the compression reinforcement, depending on the mode of failure.

b. Ultimate Loads

The essential information regarding the ultimate load capacities of the test columns is given in Tables 7, 8 and 9. The measured ultimate

loads are also plotted in Figs. 31, 32 and 33 and compared with ultimate loads predicted by means of the writer's, Jensen's and Whitney's theories. The latter two theories are discussed in Sections 14a and b, respectively.

Theoretical relations between ultimate load, cylinder strength and applied eccentricity were developed with these properties of the sections:

Group No.	$b=t$ in.	A_s in.^{2}	A_s' in.^{2}	f_{yp} p.s.i.	E_s p.s.i.$\times 10^6$	f_{yp}' p.s.i.	d in.	d' in.
I	10	1.24	0.22	43 600	28	60 000	8.67	7.47
II	10	1.24	1.24	43 600	28	43 600	8.67	7.34
III	10	2.40	2.40	43 600	29	43 600	8.50	7.00

For all columns, $\alpha = 0.55$, and the values of k_1 and k_2 presented in Table 6 were used.

Table 7
Results of Tests, Group I

Col. No.	Cyl. Str. f_c' p.s.i.	Eccentricity		Ultimate Column Loads			Ult. Strain ϵ_u ‰	Mode of Failure†
		e in.	Δe in.	P_{test} kips	P_{calc} kips	$\frac{P_{test}}{P_{calc}}$		
A-1a	5280	0	0.12	388	430	0.90	3.40	C
b	5660	0.37	0.14	441*	460	0.96	3.80	C
B-1a	4250	0	0.12	343	348	0.99	4.90	C
b	4070	0	0.12	352	334	1.05	4.56	C
C-1a	2270	0	0.13	222	199	1.11	3.60	C
b	2020	0	0.13	191	179	1.07	3.44	C
	Av Cols. 1		0.13			1.01		
A-2a	5280	2.5	0.22	239	232.5	1.03	3.34	C
b	5830	2.5	0.28	253	253.5	1.00	3.26	C
B-2a	4250	2.5	0.27	213	192.5	1.11	4.56	C
b	4070	2.5	0.24	190	186.0	1.02	4.60	C
C-2a	2270	2.5	0.27	118.5	114.0	1.04	3.00	C
b	1970	2.5	0.27	100.0	101.0	0.99	3.60	C
	Av Cols. 2		0.26			1.03		
A-3a	5660	5.0	0.32	133.5	147.0	0.91	3.00	T
b	5830	5.0	0.28	140.0	149.5	0.94	3.82	T
B-3a	4630	5.0	0.41	125.9	130.0	0.97	3.16	CT
b	4290	5.0	0.37	116.0	124.0	0.94	3.20	CT
C-3a	1880	5.0	0.28	60.5	67.0	0.90	3.80	C
b	1690	5.0	0.33	64.0	61.6	1.06	3.60	C
	Av Cols. 3		0.33			0.95		
A-4a	4810	7.5	0.45	84.5	83.3	1.01	....	T
b	5600	7.5	0.35	81.0	88.5	0.92	....	T
B-4a	3800	7.5	0.48	80.0	75.6	1.06	....	T
b	4290	7.5	0.52	81.0	79.5	1.02	....	T
C-4a	1690	7.5	0.32	50.5	47.5	1.06	3.12	C
b	1730	7.5	0.31	52.0	48.1	1.08	3.68	C
	Av Cols. 4		0.40			1.03		
A-5a	4810	12.5	0.40	48.2	44.6	1.08	....	T
b	5600	12.5	0.40	42.8	46.2	0.93	....	T
B-5a	4290	12.5	0.42	46.1	43.3	1.06	....	T
b	4590	12.5	0.45	45.5	44.1	1.03	....	T
C-5a	2310	12.5	0.34	39.0	35.7	1.09	4.40	CT
b	1770	12.5	0.34	32.8	32.0	1.02	3.68	CT
	Av Cols. 5		0.39			1.04		
	Av Group I					1.012		

* Error in eccentricity. P corrected from 401 to 441 kips.
† C, CT and T indicate compression, near balanced, and tension failure, respectively.

In the following discussion of ultimate loads the interest is aimed at the properties of a column section, not at the properties of a column with a certain length. Hence, the eccentricities used in predicting ultimate loads are the initially applied eccentricities plus the deflections at failure measured at mid-depth with respect to the knife edges. Such deflections, Δe, are entered in Tables 7, 8 and 9. It may be noted that the indicated values of Δe for tension failures probably are too small since they refer to the beginning of the state of semi-neutral equilibrium preceding failure. Fortunately, the columns which failed in tension had a large initial eccentricity, so that errors in Δe are relatively insignificant.

Theoretical curves based on Eqs. (37) and (47) are shown in Figs. 31 to 33 representing the predicted balanced conditions of failure. All combinations of cylinder strength and eccentricity giving ultimate loads

Table 8
Results of Tests, Group II

Col. No.	Cyl. Str. f_c' p.s.i.	Eccentricity		Ultimate Column Loads			Ult. Strain ϵ_u %	Mode of Failure†
		e in.	Δe in.	P_{test} kips	P_{calc} kips	$\frac{P_{test}}{P_{calc}}$		
A-6a	5240	0	....	414	.....	....	....	Be
b	5520	0	....	480	.....	....	....	Be
B-6a	4080	0	0.07	456	412	1.10	....	C
b	4040	0	0.06	420	409	1.03	....	C
C-6a	2020	0	0.10	225	253	0.89	....	C
b	1520	0	0.18	202	209	0.97	....	C
	Av Cols. 6					1.00		
A-7a	5240	3.25	0.19	274*	273	1.00	4.12	C
b	5810	2.5	0.26	284	294	0.97	4.40	C
B-7a	4080	2.5	0.25	256	229	1.12	3.76	C
b	4040	2.5	0.24	248	227	1.09	3.24	C
C-7a	1970	2.5	0.28	141	146	0.97	3.72	C
b	1520	2.5	0.27	126.8	127	1.00	5.00	C
	Av Cols. 7		0.25			1.03		
A-8a	5520	5.0	0.34	162	166.0	0.98	4.40	T
b	5810	5.0	0.40	152	169.6	0.90	4.02	T
B-8a	4700	5.0	0.35	156	154.0	1.01	3.86	CT
b	4260	5.0	0.32	146	147.8	0.99	3.40	CT
C-8a	1820	5.0	0.32	99	96.2	1.03	4.64	C
b	1820	5.0	0.39	99	96.2	1.03	5.56	C
	Av Cols. 8		0.35			0.99		
A-9a	5100	7.5	0.37	89.0	95.6	0.93	....	T
b	5170	7.5	0.39	91.2	95.8	0.95	....	T
B-9a	4700	7.5	0.35	94.0	94.0	1.00	....	T
b	4370	7.5	0.32	89.5	92.3	0.97	3.36	T
C-9a	1880	7.5	0.38	73.0	72.6	1.01	4.32	CT
b	1730	7.5	0.35	65.5	70.6	0.93	5.52	CT
	Av Cols. 9		0.36			0.97		
A-10a	5100	12.5	0.28	46.1	46.8	0.98	....	T
b	5170	12.5	0.25	44.0	46.9	0.94	....	T
B-10a	4260	12.5	0.28	43.5	46.3	0.94	....	T
b	4370	12.5	0.29	44.0	46.4	0.95	....	T
C-10a	2300	12.5	0.35	44.5	43.2	1.02	....	T
b	1770	12.5	0.38	45.0	41.7	1.08	....	T
	Av Cols. 10		0.31			0.99		
	Av Group II					0.992		

* Error in eccentricity. P corrected from 229 to 274 kips.
† Be, C, CT and T indicate bearing, compression, near balanced and tension failure, respectively.

above or below these lines are predicted to result in compression and tension failures, respectively. The mode of failure of the various test specimens was observed through measurements of strains and visual inspection of the formation of cracks. Compression failures were characterized by the formation of irregular compression cracks on the compression face (Fig. 22) before the strains in the tension reinforcement reached the yield strain. Tension failures, on the other hand, were characterized by yielding in the tension reinforcement followed by large deformations and considerable movement of the neutral axis before crushing of the concrete took place. In intermediate cases, that is under near balanced conditions, the mode of failure was difficult to observe since the last strain readings generally were made shortly before the ultimate load, and readings after the ultimate load are insignificant.

Table 9
Results of Tests, Group III

Col. No.	Cyl. Str. f_c' p.s.i.	Eccentricity		Ultimate Column Loads			Ult. Strain ϵ_u ‰	Mode of Failure*
		e in.	Δe in.	P_{test} kips	P_{calc} kips	$\frac{P_{test}}{P_{calc}}$		
A-11a	4150	0	....	460	.....	....	....	Be
b	5050	0	....	440	.....	....	....	Be
B-11a	3870	0	0.08	500	494	1.01	....	C
b	4010	0	0.10	485	501	0.97	....	C
C-11a	2200	0	....	275	.....	....	....	Be
b	2070	0	0.00	353	366	0.97	....	C
	Av Cols. 11					0.98		
A-12a†	4150	2.5	0.20	315	286	1.10	....	C
b†	5050	2.5	0.22	325	321	1.01	....	C
B-12a	4300	2.5	0.22	303	292	1.04	3.48	C
b	4010	2.5	0.26	284	281	1.01	3.36	C
C-12a	2300	2.5	0.26	252	214	1.18	3.82	C
b	2200	2.5	0.22	230	210	1.10	4.48	C
	Av Cols. 12		0.23			1.07		
A-13a†	5350	5.0	0.36	220	219.5	1.00	....	C
b†	4850	5.0	0.34	210	208.0	1.01	....	C
B-13a	3580	5.0	0.35	180	178.0	1.01	4.04	C
b	4290	5.0	0.34	206	195.0	1.06	4.12	C
C-13a	2300	5.0	0.33	151	146.5	1.03	4.36	C
b	2070	5.0	0.28	137	140.5	0.98	3.80	C
	Av Cols. 13		0.33			1.02		
A-14a†	5350	7.5	0.37	142	150.0	0.95	....	T
b	5100	7.5	0.43	153	148.0	1.03	3.70	T
B-14a	3580	7.5	0.39	138.8	133.0	1.04	3.30	CT
b	4590	7.5	....	110	.....	....	....	Bond
C-14a	1950	7.5	0.34	115.5	105.5	1.09	4.30	C
b	2070	7.5	0.37	104.0	108.0	0.96	3.92	C
	Av Cols. 14		0.38			1.01		
A-15a	5100	12.5	0.42	88.0	81.0	1.09	....	T
b	4850	12.5	0.35	79.0	80.4	0.98	....	T
B-15a	3800	12.5	0.41	74.0	78.0	0.95	....	T
b	4630	12.5	0.42	84.5	80.0	1.06	....	T
C-15a	1950	12.5	0.39	72.5	72.1	1.01	3.40	C
b	2070	12.5	0.41	74.5	72.6	1.03	4.28	CT
	Av Cols. 15		0.40			1.02		
	Av Group III					1.026		

* Be, C, CT and T indicate bearing, compression, near balanced and tension failure, respectively.
† Strains were measured at midheight only. Hence, the ultimate strains are not significant.

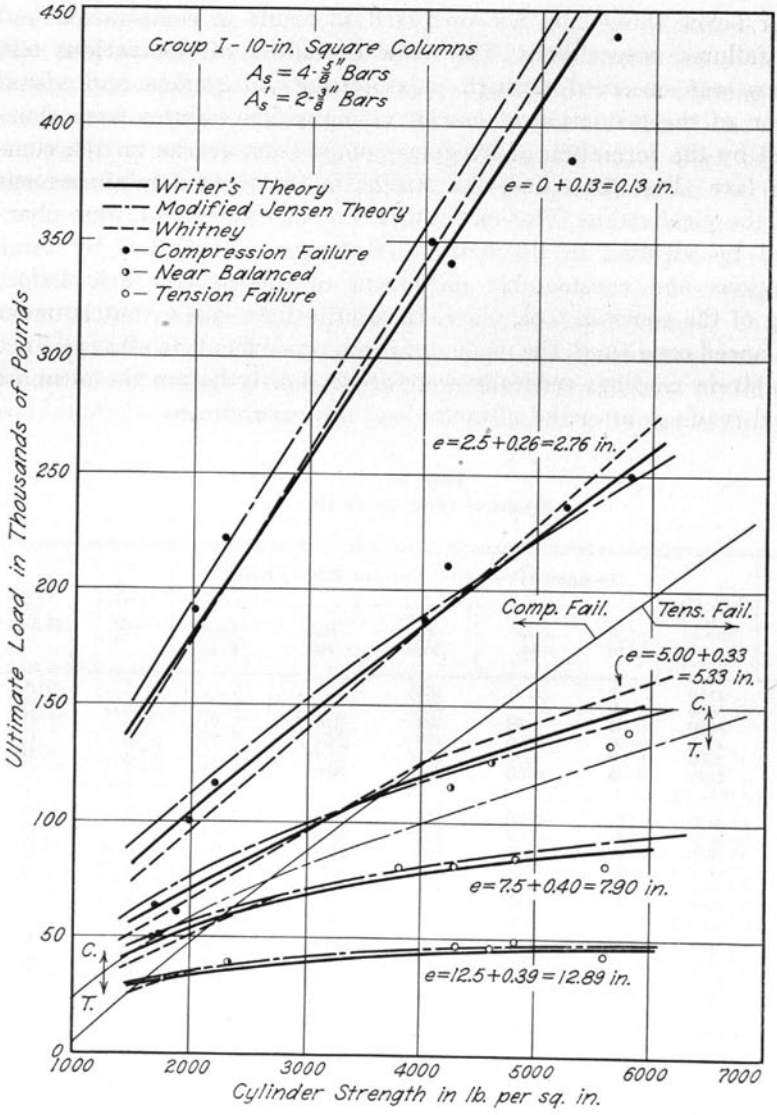

Fig. 31. Ultimate Loads, Group I

Such observed modes of failures are listed in Tables 7, 8 and 9. When compared with the predicted modes in Figs. 31 to 33, it appears that all failures observed as compression and tension failures were predicted correctly; and failures observed as near balanced correspond to ultimate loads near the theoretical dividing curve. Only one test specimen, Column B-14a (Figs. 25 and 33) fell very close to a theoretical balanced condition. Nevertheless, it is felt that the agreement between observed and predicted modes of failure is very satisfactory.

The ultimate loads corresponding to the various eccentricities in each group were computed by means of the equations developed in Section 11. The average values of Δe for each curve in Figs. 31 to 33 were used, and the curves were determined by establishing four to six points through which a continuous curve could be drawn. The predicted ultimate loads for the individual test columns, as presented in Tables 7 to 9, were determined graphically from the figures, which for such purposes were originally plotted to a much larger scale than presented herein. The theoretical equations used are referred to below:

Group I (Fig. 31) contains columns with a very light compression reinforcement. Hence, no correction of f_{yp}' was considered necessary. For $e = 0.13$ in., Eqs. (36a), (37a) and (45) were used. For $e = 2.76$ in., and for the compression failures of $e = 5.33$, 7.90 and 12.89 in., Eqs. (36), (37) and (45) were used. For all these compression failures, the mathematical solutions were obtained by means of successive approximations. For all tension failures, Eq. (39) was used.

Groups II and III (Figs. 32 and 33) contained sufficient compression reinforcement to warrant a correction of f_{yp}' to $f_{yp}' - f_c''$. Equations (36), (37) and (45) were used for all compression failures, and Eq. (44) was used for tension failures.

It may be seen from Figs. 31 to 33 and the ratios between test and calculated values of the ultimate loads in Tables 7 to 9, that the general agreement between observed and predicted ultimate loads is very satisfactory. It should be noted, however, that the slope of the descending branch of the assumed stress-strain relation in Fig. 10 was so chosen as to give such a general agreement. Hence, the average P_{test}/P_{calc} ratio for each group, 1.012, 0.992 and 1.026, may indicate a proper choice only. A reliable expression for the accuracy of the theory which has been advanced can only be obtained through statistical studies of the dispersion of the test results as compared to the various random errors in tests and analysis. Such a statistical study is presented in Section 17.

The influence of some variables on the ultimate load may be studied by means of Figs. 31 to 33. As may be expected, the ultimate load decreases for increasing eccentricity. The influence of concrete strength

varies with the mode of failure and the eccentricity. This influence is small for very large eccentricities, which generally cause tension failures. This is a reasonable result since the internal moment arm is large and the changes in moment arm due to changes in concrete strength are comparatively small. For small eccentricities, however, considerable variations in ultimate loads follow variations in concrete strength. For Group I (Fig. 31), which has a very small compression reinforcement, the effect of concrete strength on ultimate loads approaches proportionality.

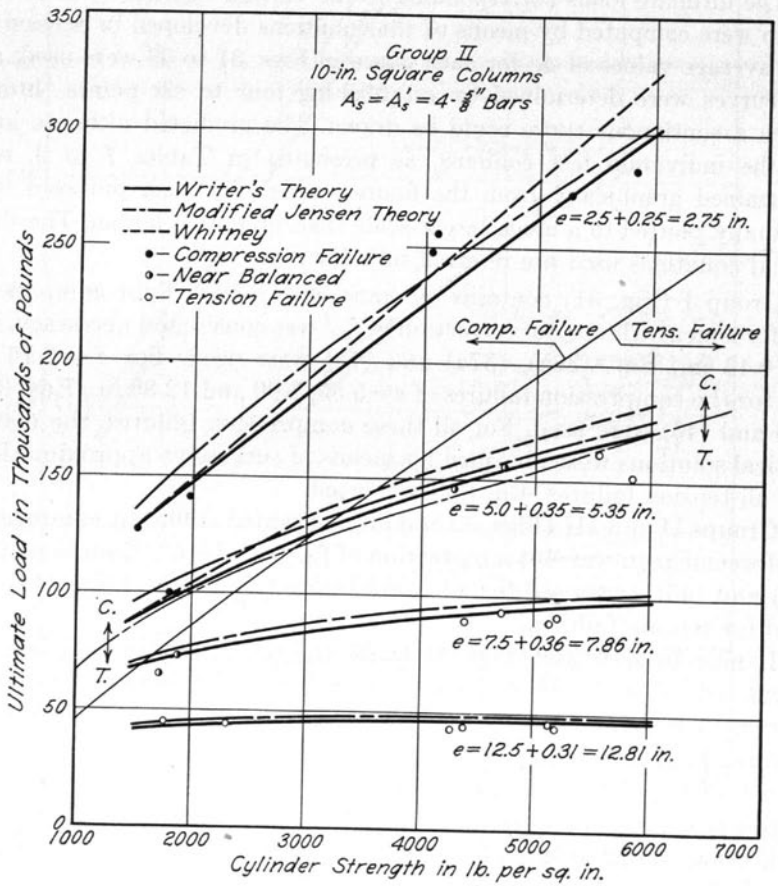

Fig. 32. Ultimate Loads, Group II

Some effects on ultimate loads of the amount and arrangement of reinforcement may be studied by comparing the three groups. First, the effects of amount of compression reinforcement, A_s', may be studied as the difference between Groups I and II. It appears that this effect is largely dependent on the mode of failure. The effect of a change in A_s' from 0.22 to 1.24 sq in. is considerable for compression failures, the

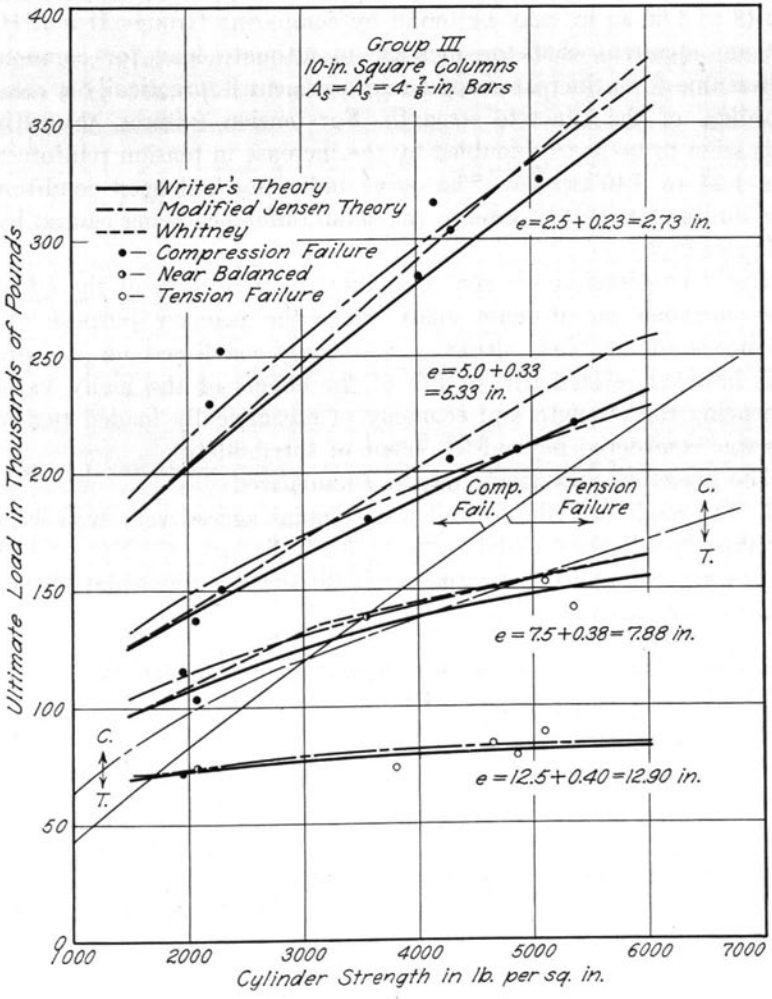

Fig. 33. Ultimate Loads, Group III

increase in ultimate load being nearly constant and not a function of concrete strength. For tension failures, however, especially for high concrete strengths, the effect of an increase in compression reinforcement is small. Such changes in compression reinforcement will not change the curvatures and slopes of the line corresponding to balanced conditions but displace this line in the direction of the load axis of the graphs.

The effects of changes in a symmetrical reinforcement from a total of 2.48 to 4.80 sq in. may be found by comparing Groups II and III. It is again apparent that the increase in ultimate load for compression failures due to an increased total reinforcement is practically a constant regardless of the concrete strength. For tension failures, the ultimate loads seem to be nearly doubled by the increase in tension reinforcement from 1.24 to 2.40 percent. The curve indicating balanced conditions is very similar for the two groups, the small difference being caused by the difference in d.

The discussions above give a qualitative indication of the effects of some variables on ultimate loads. Since the primary purpose of this bulletin is to establish ultimate load equations based on the present tests, however, systematic studies of the effects of the many variables influencing the strength and economy of eccentrically loaded tied members was considered beyond the scope of this bulletin.

The preceding statements can be summarized:

1. The mode of failure of all test columns agreed very well with the theoretical predictions based on the writer's theory.

2. A general agreement between the measured and calculated ultimate loads appears to exist.

14. Other Ultimate Theories for Rectangular Sections Subject to Combined Bending and Axial Load

a. Modification of Jensen's Theory

Jensen's studies of the ultimate strength of reinforced concrete members[80, 81] were strictly limited to beams with tension reinforcement only. Compression reinforcement in beams and the problem of combined bending and axial load were not considered.

A method for designing the necessary reinforcement in rectangular sections failing in tension under combined bending and axial load was developed by the Structural Bureau of the PCA[86] using Jensen's basic assumptions, Eqs. (27), in their original form. However, in place of Jensen's definition that a tension failure takes place when the ultimate strain, ϵ_u, is reached in the extreme concrete fiber, for design purposes failure was considered to occur when the tension steel first reaches the yield point. It was further assumed that the compression reinforcement,

for a balanced section, was effective with its full yield-point stress. A similar method for ultimate design of beams was also developed.

These studies of extensions of Jensen's theory were continued in the Committee on Masonry and Reinforced Concrete of the ASCE, especially valuable contributions being made by the late A. J. Boase, Chairman. The writer was fortunate to have access to some committee correspondence related to these matters, which is referred to here as Boase's method.

Case 1. Failure by Compression of Concrete; Part of the Section Is in Tension (Fig. 34a). With β given by Jensen's Eq. (27d), k_1 and k_2 may be expressed in terms of β

$$k_1 = \frac{1+\beta}{2} \qquad k_2 = \frac{1+\beta+\beta^2}{3\,(1+\beta)}. \tag{50}$$

The following equilibrium equations may then be written with the notation of Fig. 34a

$$P = f_c''bd\left[\frac{1+\beta}{2}k + p'\frac{f_s'}{f_c''} - p\frac{f_s}{f_c''}\right] \tag{51}$$

$$Pe' = f_c''bd^2\left[\frac{1+\beta}{2}k\left(1 - \frac{1+\beta+\beta^2}{1+\beta}\frac{k}{3}\right) + p'\frac{f_s'}{f_c''}\frac{d'}{d}\right]. \tag{52}$$

The steel stresses, f_s and f_s', may be determined by compatibility equations, assuming a linear distribution of strain,

$$f_s = E_s\epsilon_s = n\frac{f_c''}{1-\beta}\frac{1-k}{k} \tag{53}$$

$$f_s' = E_s\epsilon_s' = n\frac{f_c''}{1-\beta}\frac{d'/d + k - 1}{k} \tag{54}$$

in which n is given by Jensen's Eq. (27b) as $n = 5 + 10{,}000/f_c'$.

The position of the neutral axis, as expressed by the ratio k, is a parameter in Eqs. (51) to (54). The equations are valid within the following limits:

In Eq. (53), $f_s \leqq f_{yp}$, or

$$k \geqq \frac{1}{\dfrac{f_{yp}\,(1-\beta)}{nf_c''} + 1} = k_b. \tag{55}$$

If k is less than k_b, a tension failure takes place. For $k = k_b$, the section is balanced. In Eq. (54), $f_s' \leqq f_{yp}'$, hence

$$k \leqq \frac{1 - d'/d}{1 - \dfrac{1-\beta}{n}\dfrac{f_{yp}'}{f_c''}} = k_c. \tag{56}$$

When k is larger than k_c, f_s' is independent of k and equal to f_{yp}'. Finally the upper limit of k is given by

$$k \leqq t/d. \tag{57}$$

If k is larger than t/d, the neutral axis falls outside the section giving rise to Case 2.

Case 2. Failure by Compression of Concrete; Entire Section in Compression. From Fig. 34b are obtained the equations of equilibrium

$$P = f_c''bd\left[\frac{1+\beta}{2}k - \frac{f_c}{2f_c''}\left(k - \frac{t}{d}\right) + p'\frac{f_{yp}'}{f_c''} + p\frac{f_s}{f_c''}\right] \tag{58}$$

$$Pe' = f_c''bd^2\left[\frac{1+\beta}{2}k\left(1 - \frac{1+\beta+\beta^2}{1+\beta}\frac{k}{3}\right) - \frac{f_c}{2f_c''}\left(k - \frac{t}{d}\right)\left(k + 2\frac{t}{d} - 3\right) + p'\frac{f_s'}{f_c''}\frac{d'}{d}\right]. \tag{59}$$

For these conditions k is generally larger than k_c, and the stress in the compression steel is therefore assumed equal f_{yp}'. The stresses f_c and f_s, however, must be determined by means of a compatibility equation

$$f_c = f_c''\frac{k - t/d}{k(1-\beta)}. \tag{60}$$

The tension steel stress is given by Eq. (53) with reversed sign since the stress in this case is compressive.

Equations (58) and (59) are valid only if $k \geqq t/d$. From Eq. (53) we obtain another limit

$$k \leqq \frac{1}{1 - \dfrac{f_{yp}(1-\beta)}{nf_c''}}. \tag{61}$$

When k exceeds this value, f_s is independent of k and equal to f_{yp}.

The final limit is expressed by $f_c \leqq f_c''$, or

$$k \leqq \frac{t}{\beta d}. \tag{62}$$

When $k = t/\beta d$, the concrete section is subject to a uniform stress. For this value of k, Eq. (58) reduces to Eq. (3), and Eq. (59) combined with (58) gives a position of the force P at the plastic centroid of the section. The plastic centroid is the point at which the resultant of all internal forces cuts the section, the uniform stress in the concrete and steel being $0.85 f_c'$ and the yield point, respectively. For symmetrical reinforcement, the plastic centroid coincides with the geometric center of the section.

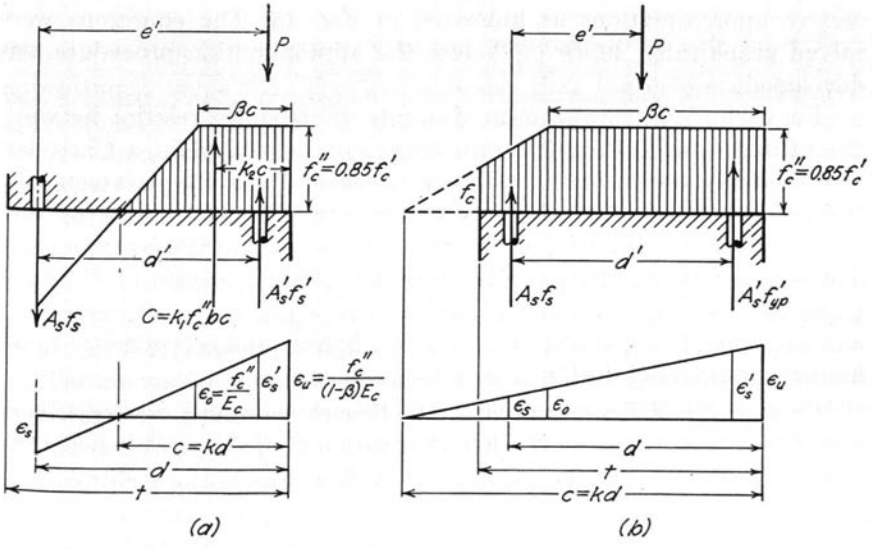

Fig. 34. Modification of Jensen's Theory

In Boase's method, equations very similar to Eqs. (50) to (62) were used. The ultimate stress in the concrete, f_c'', was assumed equal to 0.85 f_c', while Jensen's original theory for beams used $f_c'' = 1.0 f_c'$. Thus, it was recognized that the concrete in a column may be weaker than in a beam. Nevertheless, n and β were computed from Jensen's Eqs. (27b) and (27d) as a function of f_c'. This writer has chosen, however, to introduce $f_c'' = 0.85 f_c'$ in Eqs. (27b) and (27d), which is consistent with assuming an ultimate stress $0.85 f_c'$. Hence

$$n = 5 + 10{,}000/0.85 f_c' \tag{63}$$

$$\beta = \frac{1}{1 + \left[\dfrac{0.85 f_c'}{4000}\right]^2}. \tag{64}$$

Boase's method further used a compatibility equation (Eq. 54) for the determination of the stress in the compression reinforcement, f_s'. Since it appears that the ultimate strains predicted by Jensen's theory are too small (Fig. 14), the writer chose to consider the compression reinforcement effective with its full yield point, $f_s' = f_{yp}'$, regardless of the value of the ratio k.

The ultimate loads corresponding to the test specimens of the investigation reported herein could be computed by means of such successive approximations as indicated in Fig. 18. The equations were solved graphically, however, before the approximation procedure was developed.

For each of the three groups of square columns, the relation between the ultimate load, P, and eccentricity, e, was plotted in a Cartesian coordinate system with the cylinder strength, f_c', as the parameter for the family of curves. Such graphs were established by assuming successive values of k and f_c', which, when introduced in the compatibility and equilibrium equations, give the corresponding values of P and e. Once the relations between P and e were known, the ultimate load corresponding to a given section, concrete quality and eccentricity, could be determined graphically.

Case 3a. Yield Point of Member. In Boase's method a tension failure was considered to take place when the tension reinforcement reached the yield point. This condition is generally referred to as the yield point of the member. In this case, the horizontal part of the stress-block in Fig. 34a, is xc which is shorter than βc, since by definition of a tension failure the tension steel reaches yielding before the ultimate concrete strain is reached. Hence, since $f_s = f_{yp}$,

$$x = 1 - \frac{nf_c''}{f_{yp}} \frac{(1-k)}{k}. \tag{65}$$

Since n is given by Eq. (27b) and f_s' may be determined by Eq. (54), x may be entered in the equilibrium Eqs. (51) and (52) replacing the value β. A relation between P and e may be established by choosing successive values of k.

The upper limit for k in this case is the value k_b defined by Eq. (55). A lower limit for k is given by $x = 0$, or

$$k \geqq \frac{1}{\frac{f_{yp}}{nf_c''} + 1}. \tag{66}$$

When k is under this limit, a triangular distribution of stress with $k_1 = 1/2$ and $k_2 = 1/3$ will exist. Hence, the failure load may be expressed by Eq. (39) if $\alpha = 2/3$ is introduced.

Case 3b. Tension Failure. The writer chose to follow Jensen's original definition of tension failure which refers to a condition in which the ultimate concrete strain is reached while the tension reinforcement is yielding under a constant stress, f_{yp}.

In this case, the ultimate load may be found from Eq. (39) with $\alpha = k_2/k_1$, k_2 and k_1 being defined by Eq. (50)

$$\alpha = \frac{2\,(1+\beta+\beta^2)}{3\,(1+\beta)^2}. \tag{67}$$

This expression is Jensen's $1/N$ in Eq. (28), which he replaced by the approximate value 0.5. The writer found that the errors due to this approximation as applied to the test specimens in the present series are less than one percent. Hence, Eq. (39) with $\alpha = 0.5$ and $f_c'' = 0.85\,f_c'$ was used.

This modification of Jensen's theory is compared to the test results and the writer's theory in Figs. 31, 32 and 33.

The dividing curve between compression and tension failures was obtained by substituting $k = k_b$ from Eq. (55), $f_s = f_{yp}$, $f_s' = f_{yp}'$, and β from Eq. (64), into Eq. (51).

The curves for compression failures, which were referred to the total eccentricity at failure, were obtained by graphic solution of Eqs. (51) to (53) and (63) to (64). For $e = 0.13$ in Group I, Eqs. (58) to (60) were used. The stress in the compression steel was assumed at the yield point for all values of k and f_c'; $f_s' = f_{yp}'$. Such solutions were made in the early stages of the investigation, and no corrections for the concrete displaced by the compression steel were made.

The curves for tension failures were obtained by means of Eqs. (39) and (40) with $\alpha_1 = k_2/k_1 = 0.5$. In this case as well, no corrections of f_{yp}' were made.

Before this modification of Jensen's theory is compared with the writer's theory, it is convenient to list the major differences between the two:

1. From Fig. 14 it appears that Jensen assumed ultimate strains, which for f_c' = 3000–6000 p.s.i. were about half of the values found by the writer.
2. Table 6 shows that for the modified Jensen theory, k_1 is larger except for high concrete strengths, and k_2 is smaller except for low concrete strengths, than the values derived by the writer's theory.
3. There is some difference in the assumed relationship between f_c' and E_c, Fig. 11.

4. In the writer's theory, a correction was made for the concrete displaced by the compression reinforcement, $f_s' = f_{yp}' - f_c''$. No such correction was made in the other theory.
5. For tension failures, the writer used $\alpha = 0.55$, while $\alpha = 0.50$ was assumed in the modified Jensen theory.

Comparing the ultimate loads predicted by the two theories by means of Figs. 31 to 33, it is evident that the difference is small. The same general trend exists for both theories, which is reasonable since they both are of the Stüssi type.

The dividing curve between compression and tension failures is less inclined for the modified Jensen theory. This is primarily caused by the small values of ϵ_u; but the difference in k_1 has the same tilting effect. It appears that the writer's curve gives the best agreement with the observed modes of failure, but this is of minor importance since the Jensen theory is intended for prediction of ultimate loads, not for prediction of behavior.

The ultimate loads predicted by the modified Jensen theory are generally higher than those predicted by the writer's theory. One reason for this difference is that corrections for the concrete displaced by the compression steel were made in the writer's theory. Other reasons depend on the mode of failure of the columns for which predictions of ultimate loads are made.

In the case of compression failures, it is evident that higher values of k_1 and lower values of k_2 will tend to give higher ultimate loads. It is less obvious, however, that smaller values of ϵ_u will give higher ultimate loads. This may be seen from Eqs. (36), (37) and (45) by comparing the two theories with identical k_1 and k_2 but different ϵ_u. For a given position of the neutral axis, c, both theories will then give the same moment from Eq. (36). The ultimate load which may be combined with a given moment is evidently a one-valued quantity for a given section. In Eq. (45), however, the lower ϵ_u gives a lower f_s, which in turn causes a higher P in Eq. (37). The combined effects of these differences between the writer's and the modified Jensen theory give a general trend of higher loads for the latter theory.

In Group I, for $e = 5.33$ in., the difference in predicted ultimate loads is also influenced by the difference in predicted mode of failure.

The curves for tension failures were obtained from Eqs. (39) and (40). Hence, the difference in ultimate loads, which is smaller than the scatter in the test results, is due only to the difference in α, and to the correction $f_s' = f_{yp}' - f_c''$ made in the writer's theory.

It may be concluded that, within the scope of Groups I to III of the present tests, the differences between the writer's and the modified

Jensen theory are small as far as the accuracy of the prediction of ultimate loads is concerned.

b. Whitney's Theory[63, 69, 74, 97]

Contrary to the writer's theory and the modified Jensen's theory, the analysis developed by C. S. Whitney is not of the Stüssi type. Whitney's equation for the ultimate load of rectangular sections failing in compression under an axial load combined with bending (Eq. 21) was developed on a semi-empirical basis. This equation was developed from Eq. (20) by assuming that there is sufficient reinforcement to prevent tension failure, and by computing the compressive ultimate moment about the tension reinforcement. The expression for P was obtained as

$$P = \frac{2A_s'f_{yp}'}{\frac{2e}{d'}+1} + \frac{btf_c'}{\frac{3te}{d^2}+\frac{6dt-3t^2}{2d^2}}. \qquad (21a)$$

For small eccentricities, the neutral axis will be considerably further away from the compression face than the position corresponding to balanced conditions in a beam. Hence, the value $a/d=0.537$ which leads to Eq. (20), and thereby Eq. (20) itself, are not valid for small eccentricities. Therefore, Whitney adjusted Eq. (21a) by making P approach the proper value for a concentrically loaded column (Eq. 3) when e approaches zero. This procedure led to Eq. (21), which is outstanding in its mathematical simplicity. It should be noted, however, that this equation is developed with the assumption that the reinforcement is placed near the compression and tension faces, and that the equation reduces to Eq. (3) for $e=0$ only if $2A_s'=A_{st}$ or, in other words, if the reinforcement is symmetrical, $A_s'=A_s$. If these conditions are not strictly met, it nevertheless is believed that Eq. (21) will give a reasonably good approximation.

Equation (21) is compared to the test results and the two other theories in Figs. 31 to 33. Considering the simple form of the equation, the agreement with the test results is satisfactory. It seems probable, however, that Eq. (21) could be improved by adjusting the constants in the two terms containing e.

For tension failures, Whitney developed equations on a rational basis assuming a rectangular stress-block, that is $\alpha=0.50$. Thus, Eqs. (39) to (43) were developed with $\alpha=0.50$ and $f_c''=0.85\,f_c'$. Within the range of eccentricities and concrete strengths for which tension failures are predicted by the modified Jensen theory, Whitney's predictions will therefore coincide with the modified Jensen theory as discussed above.

In Group II (Fig. 32) for $e = 5.35$ in. and $f_c' = 6000$ p.s.i. both Whitney's and the writer's theory predict tension failure. There is some difference, however, in the value of the ultimate load, which is due only to the difference in α (0.50 and 0.55) and the correction for concrete displaced by the compression reinforcement, $f_s' = f_{yp}' - f_c''$. This difference in ultimate load may be estimated in this case from Eq. (40). Since $(e'/d-1)$ is small, P is nearly proportional to $\sqrt{f_{yp}/\alpha}$, which is $\sqrt{(43.6 - 5.1)/0.55} = 8.37$ and $\sqrt{43.6/0.50} = 9.33$ for the writer's and Whitney's theory, respectively. Hence, the writer's theory leads to about a ten percent lower value of the ultimate load. This percentage will decrease with increasing eccentricity.

It may be reemphasized that Whitney's Eq. (21) for compression failure of members subject to combined bending and axial load is reasonably accurate within the scope of the present tests.

15. Studies of Ultimate Loads of Cylindrical Columns, Group IV

This group of tests included 30 cylindrical columns, all having a core diameter of 10 in. and a shell thickness of 1 in. The shape and size of the specimens are shown in Fig. 4.

The longitudinal reinforcement of all specimens consisted of eight $\frac{7}{8}$-in. bars, the ratio of longitudinal reinforcement to the gross area being 0.0425. Three grades of concrete and five eccentricities were involved as outlined in Table 1.

The design of the drawn wire spirals indicated in Table 1 was based on the following equation from the ACI Building Code:[93]

$$p_{sp} = 0.45\left(\frac{A_c}{A_{\text{core}}} - 1\right)\frac{f_c'}{f_{sp}} \tag{68}$$

in which p_{sp} is the ratio of the volume of spiral reinforcement to the volume of the concrete core (out-to-out of spirals), and f_{sp} is the useful limit stress of spiral reinforcement, generally taken as 60,000 p.s.i.

Equation (68) has been derived from Eqs. (3) and (4) of Section 1, by equating the strength produced by the spiral reinforcement to the strength of the concrete shell. Strictly applied, this procedure leads to a coefficient of 0.425 in Eq. (68). Hence, the coefficient 0.45 as used should result in a spiral slightly more effective than the concrete shell, so that the characteristic behavior of spirally reinforced members may be recognized.

Since the actual useful limit of the spirals used, the stress corresponding to a strain of five per mill, probably was considerably more than

the 60,000 p.s.i. assumed, and since the concrete strengths varied somewhat from their designed values, the spirals did not conform strictly to the requirements of Eq. (68). Nevertheless, the spirals used are believed to represent designs resulting from the present ACI code fairly well.

The ultimate loads of such spirally reinforced cylindrical columns subject to eccentric loads may be studied on the basis of the same general assumptions which were made in Section 11. The spiral reinforcement is, however, a new variable needing consideration. It is recognized that spiral reinforcement contributes to the ultimate capacity of concentrically loaded members as indicated in Eq. (4). On the other hand, large deformations must take place and the concrete shell will generally spall off before lateral restraint of the concrete core is developed through the action of the spiral. In the case of eccentric loadings, such large deformations will generally increase the eccentricity considerably, and therefore in most cases the spiral is not able to replace the strength of the shell and later develop strength beyond the yield point of the member.

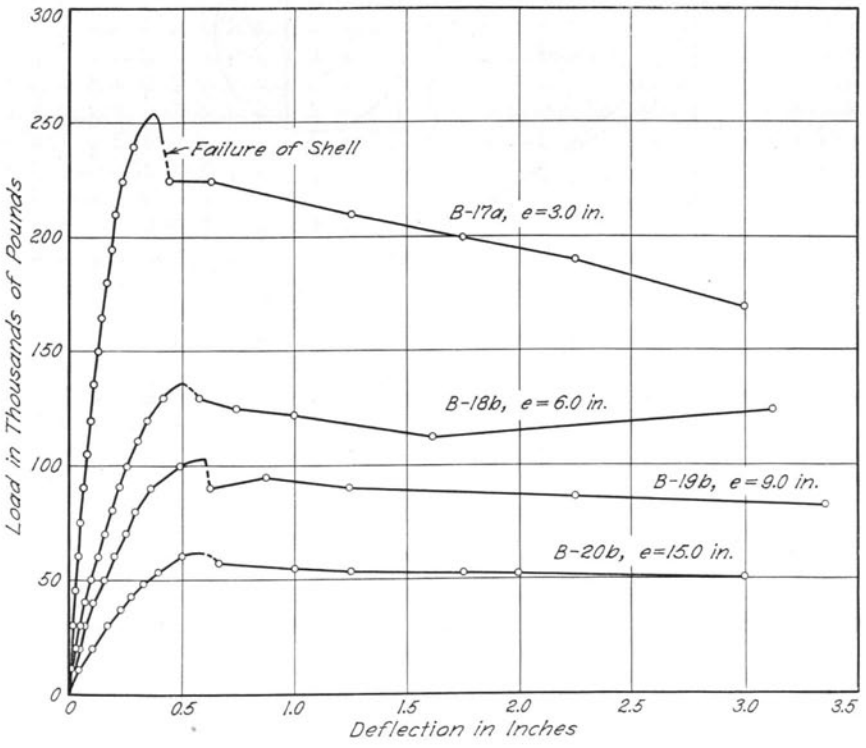

Fig. 35. Deflections of Spiral Columns

In the present tests, lateral deflections with respect to the knife edges of the loading device were observed before as well as after failure of the concrete shell. Some typical results of such measurements are shown in Fig. 35, which indicates an absence of the second maximum usually present in tests of concentrically loaded members. It is reasonable to expect, therefore, that the ultimate strength of eccentrically loaded columns with normal amounts of spiral reinforcement (Eq. 68) will coincide with the yield point of such members, which is independent of the amount of spiral reinforcement.

During the study of rectangular, tied columns (Fig. 17) it was found that the internal compressive force in the concrete may be expressed as $C = k_1 bcf_c''$, where k_1 is given in Table 6. An equivalent uniform stress distribution of intensity, f_c'', to a depth, $k_1 c$, gives the same force, C. The

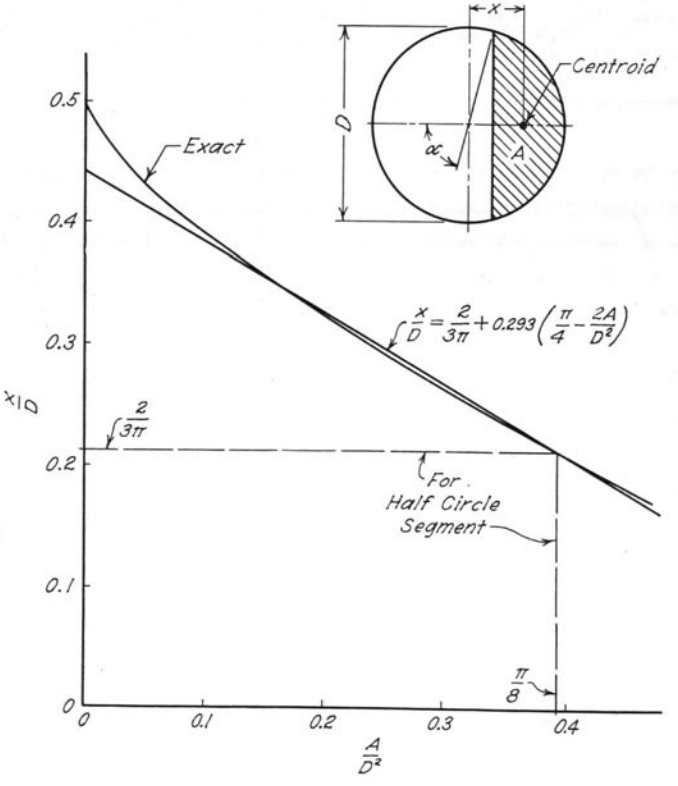

Fig. 36. Properties of a Circle Segment

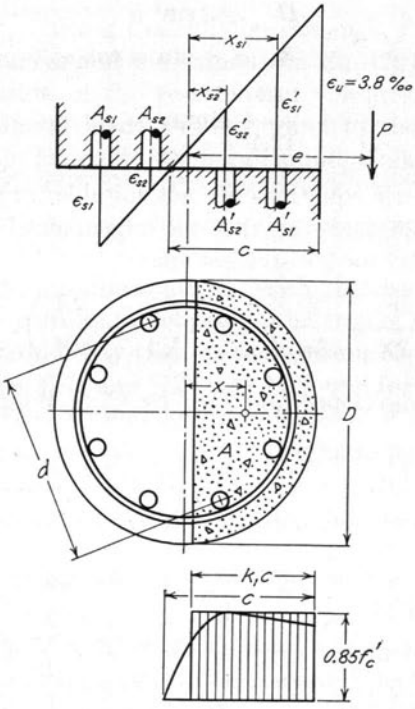

Fig. 37. Analysis of Circular Sections

centroid of such an equivalent distribution, however, will be found at a distance $\frac{1}{2}\ k_1c$ from the compression face, while the distance used in Fig. 17 and Table 6 is $k_2c = 0.55k_1c$.

In the case of cylindrical sections, an equivalent uniform stress distribution may be assumed over a segment with a rise k_1c. Strictly, the values of k_1 involved should be a function of the depth of the neutral axis, c, as well as the assumed stress distribution (Fig. 10). For the purpose of the present analysis, however, the values of k_1 corresponding to a rectangular section were used as an approximation. Furthermore, the resultant compressive force in the concrete was assumed acting at the centroid of the segment with a rise k_1c.

It is then convenient to study the properties of a segment. With reference to Fig. 36, the following expressions apply

Area: $$A = \frac{D^2}{4}(\alpha - \sin\alpha\cos\alpha)$$

Centroid: $$x = \frac{D}{3}\frac{\sin^3\alpha}{\alpha - \sin\alpha\cos\alpha}$$

Hence
$$\frac{x}{D} = \frac{D^2}{12A}\sin^3\alpha. \tag{69}$$

These trigonometric equations are not suitable for a flexural analysis. It is shown in Fig. 36, however, that the trigonometric equation for x/D may be approximated by the straight line

$$\frac{x}{D} = \frac{2}{3\pi} + 0.293\left(\frac{\pi}{4} - \frac{2A}{D^2}\right). \tag{70}$$

This equation was developed and used by C. S. Whitney.[74]

a. General Method of Analysis

The following method of analysis applies to tension as well as compression failures. With reference to Fig. 37, the following equations are available.

Equilibrium of forces: $$P = 0.85f_c'A + E_s\sum A_s\epsilon_s \tag{71}$$

Equilibrium of moments: $$Pe = 0.85f_c'Ax + E_s\sum A_s\epsilon_s x_s \tag{72}$$

Compatibility equations:
$$\begin{aligned}
\epsilon_{s1} &= \frac{\epsilon_u}{c}(D/2 + x_{s1} - c)\\
\epsilon_{s2} &= \frac{\epsilon_u}{c}(D/2 + x_{s2} - c)\\
\epsilon_{s1}' &= \frac{\epsilon_u}{c}(c - D/2 + x_{s1})\\
\epsilon_{s2}' &= \frac{\epsilon_u}{c}(c - D/2 + x_{s2}).
\end{aligned} \tag{73}$$

Upon substitution in Eqs. (71) and (72) we have, due to the assumed trapezoidal stress-strain relation for steel,

$$|\epsilon_s| \leqq \frac{f_{yp}}{E_s}. \tag{74}$$

The solution of the equations above is rather complicated since trigonometric expressions as well as a cubic equation in c are involved. Even the approximation procedure used for rectangular columns (Fig. 18) is rather time-consuming in the present case. Hence, Cartesian coordinate graphs were developed relating the ultimate load of the test columns, P,

to the eccentricity, e, using the cylinder strength, f_c', as the parameter for the family of curves and the value from Eq. (70) as an approximate value for the position of the resultant of compressive stresses in the concrete. The ultimate loads corresponding to the four eccentricities involved in Group IV could then be found from such graphs as a function of f_c'.

The curves relating P to e were found by assuming various values for the rise, k_1c, of the circular segment representing the concrete compression zone subject to a uniform stress. With the rise known, most engineering handbooks contain tables giving the area of the segment, A; the position of the centroid may then be found from Eq. (70). Accordingly, all quantities of Eqs. (71) and (72) may be found for a given section and given materials if k_1c is chosen, and the values of P and e corresponding to the chosen k_1c may be found. By varying f_c' as well as k_1c, the family of curves mentioned above may be established, and ultimate loads corresponding to given eccentricities may in turn be found graphically.

The results of such an analysis as applied to the eccentrically loaded columns in Group IV are shown in full lines in Fig. 38, which gives the ultimate load as a function of cylinder strength. It should be noted that the eccentricities used in the analysis are the total eccentricities at failure; i.e., the nominal values plus the measured deflections with respect to the knife edges of the loading device.

The curve shown in Fig. 38, which provides a division between tension and compression failures, was developed by studying the limiting conditions generally referred to as a balanced section. Such conditions exist if, at the ultimate load, the tension steel reaches yielding and the concrete reaches its ultimate strain simultaneously. Hence

$$c_b = \frac{\epsilon_u}{\epsilon_u + f_{yp}/E_s}\left(\frac{D}{2} + x_{s1}\right). \tag{75}$$

The values of P which correspond to this position of the neutral axis may then be found from Eqs. (70) and (71).

b. Test Results

The test results pertaining to failure of the specimens in Group IV are given in Table 10. The ultimate loads are also plotted in Fig. 38 as a function of cylinder strength with eccentricity as a parameter. Figure 39 shows a typical set of specimens after failure.

Four batches of concrete were used for casting every pair of columns, three cylinders 6 by 12 in. being made from each batch. Hence, the cylinder strengths entered in Table 10 each represent the average of 12 individual cylinders. The coefficient of variation, V, within each

such group of 12 cylinders has also been entered in the table. Using the general methods of statistical analysis, the coefficient of variation of the arithmetic mean of the 12 cylinders used should be near $V/\sqrt{12}$, or about $V/3$. Since the four batches of concrete were placed on top of each other in the forms rather than being thoroughly mixed, and since some segregation and bleeding took place during compaction, however, the principles of statistical analysis are not valid and the given values of V must be regarded as indications only.

Concentrically Loaded Specimens. Columns 16 were loaded with flat ends; i.e., the two 12-in. square steel blocks through which the specimens

Table 10
Results of Tests, Group IV

Col. No.	Cylinder Strength		Eccentricity*		Ultimate Column Loads†			2nd Max. Load kips	Ult. Strain ϵ_u ‰	Mode of Failure‡
	f_c' p.s.i.	V %	e in.	Δe in.	P_{test} kips	P_{calc} kips	$\frac{P_{test}}{P_{calc}}$			
A-16a	5150	4.2	0	....	760	704	1.08	760	....	C
b	4640	4.0	0	0.01	693	655	1.06	770	2.60	C
B-16a	2990	7.4	0	0.03	515	497	1.03	644	2.40	C
b	3310	16.1	0	0.01	514	527	0.98	655	2.60	C
C-16a	1590	10.3	0	0.03	371	362	1.02	447	2.60	C
b	1420	7.4	0	0.02	365	345	1.06	398	2.70	C
Av Cols. 16				0.02			1.04		2.58	
A-17a	5150	4.2	3.0	0.30	343	317	1.08		3.10	C
b	4640	4.0	3.0	0.29	283	298	0.95		3.10	C
B-17a	3620	9.0	3.0	0.34	253	258	0.98		3.20	C
b	3310	16.1	3.0	0.34	238	246	0.97		3.00	C
C-17a	1420	7.4	3.0	0.55	187	167	1.12		3.80	C
b	1600	10.3	3.0	0.50	179	175	1.02		4.04	C
Av Cols. 17				0.39			1.02		3.37	
A-18a	5020	6.1	6.0	0.44	162	172	0.94		2.60	T
b	5000	6.2	6.0	0.50	171	171	1.00		3.42	T
B-18a	3380	7.3	6.0	0.42	140	144	0.97		3.00	T
b	3580	6.4	6.0	0.47	136	147	0.93		3.00	T
C-18a	1680	10.4	6.0	0.80	127	113	1.12		4.60	CT
b	1590	10.3	6.0	0.60	107	111	0.96		3.20	CT
Av Cols. 18				0.54			0.99		3.30	
A-19a	5020	6.1	9.0	0.62	111.0	110.0	1.01		3.36	T
b	5310	7.1	9.0	0.62	114.3	112.0	1.02		3.40	T
B-19a	3380	7.3	9.0	0.54	98.5	97.5	1.01		3.56	T
b	3580	6.4	9.0	0.56	103.0	99.5	1.04		3.20	T
C-19a	1680	10.4	9.0	0.80	79.0	77.5	1.02		2.60	T
b	1630	8.9	9.0	0.80	79.0	77.0	1.03		5.00	T
Av Cols. 19				0.66			1.02		3.52	
A-20a	5310	7.1	15.0	0.68	67.7	62.0	1.09		3.28	T
b	5000	6.2	15.0	0.58	63.5	61.5	1.03		3.00	T
B-20a	2990	7.4	15.0	0.75	57.5	55.5	1.04		2.40	T
b	3620	9.0	15.0	0.60	62.0	57.0	1.09		2.84	T
C-20a	1630	8.9	15.0	0.60	47.0	50.5	0.93		3.20	T
b	1600	8.6	15.0	0.72	47.0	50.0	0.94		3.92	T
Av Cols. 20				0.66			1.02		3.11	
Av Group IV							1.018			

* The centrically loaded columns were loaded with flat ends, the remaining columns through knife-edges.
† The test values of ultimate loads were recorded at failure of the concrete shell. The centrically loaded columns did, however, generally develop a second and higher maximum load through the action of the spiral. The calculated ultimate loads were found using Eq. (3) for columns 16, Eq. (70) to (74) for columns 17 to 20.
‡ C, CT and T indicate compression, near balanced, and tension failure, respectively.

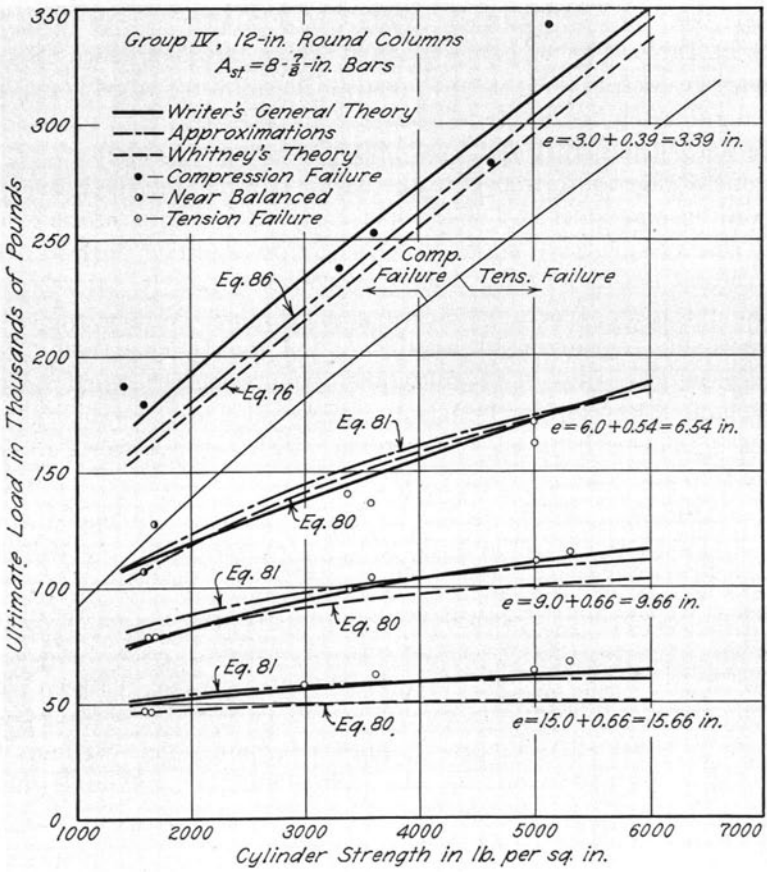

Fig. 38. Ultimate Loads, Group IV

were loaded were locked against all rotations after application of about 10 kips. Column A-16a was loaded with knife edges to 700 kips, at which load indications of failure in the knife edges were found. Hence, this column was unloaded and reloaded to failure with flat ends. The deflections at midheight of the columns with respect to the ends, Δe, corresponding to the yield point of the members, have been entered in Table 10. It appears that the values of Δe are small; further, since the specimens were restrained at the ends, they may be regarded as truly concentrically loaded.

The test values of ultimate loads for the concentrically loaded columns in Table 10 refer to the loads at which the shell failed. Hence, a comparison with Eq. (3) may be made. The resulting ratios between observed and computed ultimate loads average 1.04. Ultimate strains of the shells were of the order of 2.5 per mill, depending somewhat on the position of the gages with respect to the region in which the shell failed first, generally in the upper half of the specimens. After failure of the concrete shell, the specimens continued to deform, thus entering the spiral range. The second maximum load, which was reached shortly before fracture of the spiral, was generally somewhat higher than the yield point. This is reasonable considering the design of the spirals noted before. After fracture of the spiral, the longitudinal reinforcement buckled as shown for Column B-16b in Fig. 39. It may be concluded that the concentrically loaded specimens behaved in accordance with earlier reports by F. E. Richart[95] and others.

Eccentrically Loaded Specimens. These columns were loaded through knife edges as indicated in Figs. 6 and 7. Accordingly, the deflections at midheight of the specimens with respect to the knife edges, Δe, were included as part of the eccentricity during the calculation of ultimate loads.

The curve in Fig. 38 indicating the predicted division between tension and compression failures is in general agreement with the observed modes of failure. Thus, all Columns 17 failed in compression, Columns C-18 were near balanced conditions at failure, and the remaining columns failed in tension. It should be noted, however, that no columns of concrete qualities *B* or *A* were tested with such eccentricities that balanced conditions were to be expected.

Before failure of the concrete shell took place, the general behavior of these test columns with spiral reinforcement appeared to be very similar to the tied columns discussed in Section 13. This may be seen by studying Figs. 16a, b and c, which give strain measurements of typical specimens. Column B-17a (Fig. 16a) is a typical example of a compression failure. The stresses on the tension side of the section were small when the shell failed on the compression side as shown in Fig. 39. At least the outer layer of compression steel, however, did reach yielding before failure took place. For Column A-20b (Fig. 16b), which represents a typical tension failure, these conditions were reversed. At least one layer of tension steel was yielding when the shell failed, while the stresses in the inner layer of compression steel were very small. Column C-18b (Fig. 16c) represents a failure very near balanced conditions. The other layer of tension reinforcement reached yielding slightly before the concrete shell started spalling.

Fig. 39. Columns B-16 to B-20 after Failure

The spirally reinforced columns appeared to reach a stage of semi-neutral equilibrium very similar to that described for tied columns, before the shell failed. The ultimate strains of the shell (Table 10), however, appear to be somewhat smaller than the values found for tied square columns. Thus, the ultimate strain, ϵ_u, appears to be dependent on the

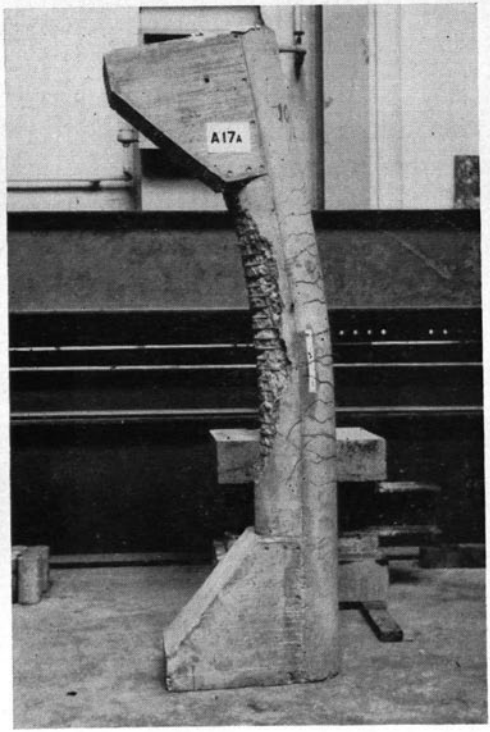

Fig. 40. Column A-17a after Failure

shape of the section. The difference is small, however, and since the constants k_1 and k_2 are rather insensitive to changes in ϵ_u, it is believed that the use of $\epsilon_u = 3.8$ per mill as determined for square columns will not cause important errors in the estimate of ultimate loads.

The behavior of tied columns at high loads was found to depend on the mode of failure. Members failing in tension were able to deform considerably after the tension steel reached yielding and before the concrete at the compression edge failed. For compression failures, such large deformations were not present. Regardless of whether the concrete in the compression zone failed before or after the tension steel reached

yielding, the compression reinforcement buckled between ties immediately after the concrete cover had spalled, and hence the load carrying capacity of the members was suddenly reduced very seriously. For all practical purposes the failure was complete.

The behavior of the spirally reinforced columns was different. When the concrete shell spalled off on the compression side, the spiral reinforcement prevented buckling of the compression reinforcement as well as failure of the concrete core. Hence, the failure was not complete: the specimens were still able to carry fairly high loads and deform very considerably, regardless of the amount of eccentricity. A typical example of such behavior is shown in Fig. 35, which represents four very similar specimens tested with different eccentricities. After failure of the concrete shell, large deflections were developed, and the eccentricity of the load thereby increased considerably. Hence, it is reasonable that no second maximum was found. It should be noted in Fig. 35, however, that Column B-17a, at a deflection of 3 in., had a total eccentricity of 6 in., and nevertheless carried a higher load than the maximum capacity of Column B-18b which was loaded with an initial eccentricity of 6 in. A similar comparison may be made for columns B-18b and B-19b. Hence, it appears that the section, due to the action of the spiral reinforcement, increased in strength after failure of the shell. The load carrying capacity of the member, however, was generally impaired by the large deflections present in the spiral range.

In the present tests, no attempts were made to measure strains in the spiral. If gages had been attached to the spiral before casting, the necessary waterproofing material would probably have upset the local conditions by introducing bending in the spiral. If core holes had been used to gain access to the spiral after casting, the shell area would have been badly reduced. In earlier tests of eccentrically loaded spiral columns without shells[95] it was found, however, that considerable stresses may develop in the spiral near the compression edge while the spiral stresses on the tension side of the section are very small.

It was further not found possible in the present tests to determine how far the eccentrically loaded specimens could be strained before fracture of the spiral. The great toughness of the members is, however, apparent from Fig. 40. This column, A-17a, which was loaded with a 3-in. initial eccentricity, lost its shell, with small stresses in the tension reinforcement, at a load of 343 kips. In the condition shown in Fig. 40, the deflection with respect to the knife edges was about 6 in., giving a total eccentricity of about 9 in.; nevertheless the column carried about 150 kips, which is about 40 percent more than the ultimate capacity of a similar column

loaded with an initial 9-in. eccentricity. After such large deformations, the capitals of this and similar specimens were so heavily inclined that it was feared the specimens might be ejected from the testing machine by the shock caused by the fracture of the spiral. For reasons of safety, the tests of all eccentrically loaded specimens were therefore discontinued before such fracture took place.

Considering the general behavior described above, it appears reasonable to recommend that the strength of eccentrically loaded spiral columns, when designed as structural members, should be referred to the yield point load at which the shell is lost. Such yield points as observed in the present tests have been compared with the general method of analysis as presented in Section 15a, in Table 10 and Fig. 38. It appears that the theoretical ultimate loads on the average are somewhat on the safe side. Since the control of the variables involved in the tests was limited as discussed in Section 17, however, the over-all average of 1.8 percent on the safe side is very satisfying.

c. Whitney's Method of Analysis

For rectangular sections, C. S. Whitney[74] developed a formula for ultimate loads in the case of compression failure, Eq. (21). However, he also adjusted this formula so that when e is zero, P will be $2\frac{1}{2}$ times the values given by the standard formula of the ACI code, Eq. (5).

The formulas for compression failures of square and circular sections with a circular arrangement of the longitudinal steel given by Whitney are both of the adjusted type mentioned above which reduce to $2\frac{1}{2}$ times, Eq. (5). It would not be proper to compare such equations to ultimate loads determined in tests. An equation for the ultimate load of cylindrical columns failing in compression was developed, therefore, from Eq. (21) with Whitney's assumptions.

In a column with diameter, D, the reinforcement is distributed around the circumference of a circle with diameter, d. Equation (21) can be adapted to this case by substituting for the value of d' the equivalent steel distance, $0.67d$. The effective depth of the concrete section, t, for a rectangular member should be replaced by the value $0.8D$. The following equation results

$$P = \frac{A_{st} f_{yp}}{\dfrac{3e}{d} + 1} + \frac{A_c f_c'}{\dfrac{9.6De}{(0.8D + 0.67d)^2} + 1.18} \tag{76}$$

in which A_{st} is the total steel area and A_c is the gross area of the section, $\pi D^2/4$.

The results of Eq. (76), which reduces to Eq. (3) when e is zero, is shown in Fig. 38 for $e=3.39$ in. It appears that the ultimate loads are somewhat conservative as compared to the test results and the more exact theory. If $0.75d$ rather than $0.67d$ is substituted for d', however, the following equation which practically coincides with the writer's theory in Fig. 36 is found

$$P = \frac{A_{st}f_{yp}}{\frac{2.67e}{d}+1} + \frac{A_c f_c'}{\frac{9.6De}{(0.8d+0.75d)^2}+1.18}. \qquad (77)$$

Whitney also developed an equation for the ultimate load of cylindrical columns failing in tension. However, $0.09D$ was added to the eccentricity, e, to allow for deflections. Since it has been chosen in the present study to refer measured ultimate loads to the actual eccentricities at failure, an equation for tension failures was developed without any addition to the eccentricity; but otherwise with the same assumptions as those used by Whitney.[74]

It was assumed that the total steel compression equals the total steel tension. This is an approximation only, since the sum of forces in the reinforcement will equal zero only if the neutral axis is at the center line of the section, which is generally not the case. Assuming an equivalent uniform stress-distribution as indicated in Fig. 37, this simplification, however, reduces Eq. (71) to

$$P = 0.85f_c'A. \qquad (71a)$$

It was further assumed that the centroid of the segment A may be determined by means of Eq. (70), that four tenths of the total steel area times the yield point is the effective force in the reinforcement on each side, and that the effective moment arm of the reinforcement is $0.75d$.

Then, equilibrium of moments about the effective centroid of the tension steel gives

$$P(e+0.375d) = 0.4A_{st}\,0.75df_{yp} + 0.85f_c'A(x+0.375d) \qquad (78)$$

or

$$Pe = 0.3A_{st}df_{yp} + P\left(0.442D - 0.586\frac{P}{0.85Df_c'}\right). \qquad (79)$$

For ultimate loads of cylindrical columns failing in tension this will reduce to

$$P = 0.85D^2f_c'\left[\sqrt{\left(\frac{0.85e}{D} - 0.377\right)^2 + \frac{p_{st}}{2.5}\frac{f_{yp}}{0.85f_c'}\frac{d}{D}} - \left(\frac{0.85e}{D} - 0.377\right)\right]. \quad (80)$$

The results of this equation are compared to the test results and the more accurate theory in Fig. 38. It appears that the equation is very conservative for the larger eccentricities if the concrete strength is over 3000 p.s.i. This result is reasonable because in these cases the neutral axis was not at the center line of the section as assumed, but closer to the compression edge.

An attempt was made to improve Eq. (80) by adjusting the constants involved. It was not found possible to achieve any excellent approximation for all values of eccentricities and concrete strengths within the range of tension failures by such means. An equation of the following form is plotted in Fig. 38

$$P = 0.85D^2f_c'\left[\sqrt{\left(\frac{0.85e}{D} - 0.325\right)^2 + \frac{p_{st}}{2}\frac{f_{yp}}{0.85f_c'}\frac{d}{D}} - \left(\frac{0.85e}{D} - 0.325\right)\right]. \quad (81)$$

This equation appears to be more satisfactory than Eq. (80) even though it is somewhat on the unsafe side for relatively small eccentricities. This adjusted Eq. (81) as well as Eq. (77) fits the results of the present tests. Their application beyond the scope of these tests (e.g., for lower reinforcement percentages) should be verified by comparison with the writer's more rational procedure, Section 15a, and preferably with further tests.

d. Summary

The present tests of spiral columns were limited to only one percentage of longitudinal reinforcement and an amount of spiral reinforcement designed after the present ACI code. With these limitations, the observed behavior of cylindrical spiral columns may be summarized as follows:

1. The concentrically loaded columns were found to behave as observed in numerous previous tests.[95] The yield points of these columns were found to be in good agreement with Eq. (3).

2. Two modes of failure prevailed in the tests of eccentrically loaded columns, compression failures and tension failures. These modes of failure, and the corresponding ultimate loads, were found to agree well with the predictions of the writer's theory. The ultimate loads predicted

by Whitney's equations appeared to be rather conservative. Within the scope of these tests, more accurate predictions were obtained by adjusting the constants in Whitney's equations.

3. The ultimate load of the eccentrically loaded columns was reached at failure of the concrete shell.

4. After such failure of the concrete shell, the eccentrically loaded columns developed extremely large deformations with relatively small corresponding decreases in load capacity. This evidence of great toughness was very pronounced, regardless of the amount of eccentricity and the mode of failure.

16. Interaction Diagrams

A general and simple procedure for the approximate prediction of ultimate loads of members failing in compression may be developed by means of interaction diagrams.

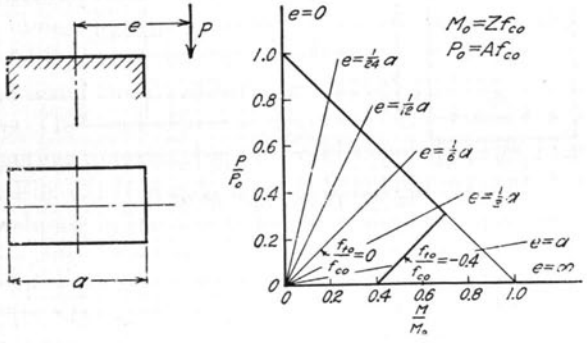

Fig. 41. Interaction Diagram for Ideal Material

The basic principle of such interaction diagrams is that the strength under one loading condition is affected by the presence of another superimposed loading condition. This principle has been made more general by dealing with ratios rather than actual loads and stresses.[85, 105]

As an example illustrating combined bending and axial load, a homogeneous and perfectly elastic material following Hooke's law is assumed loaded with an eccentric force (Fig. 41). Then

$$f_c = \frac{P}{A} + \frac{Pe}{Z}$$
$$f_t = \frac{P}{A} - \frac{Pe}{Z} \qquad (82)$$

in which f_c, f_t, A and Z are compressive stress, tensile stress, area and section modulus, respectively. Introducing

$$P_o = Af_{co}; \qquad M_o = Zf_{co} \tag{83}$$

gives at failure

$$\frac{P}{P_o} = 1 - \frac{M}{M_o}$$
$$\frac{P}{P_o} = \frac{f_{to}}{f_{co}} + \frac{M}{M_o} \tag{82a}$$

where f_{co} and f_{to} are compressive and tensile strength, respectively. An interaction diagram based on these two equations is drawn in Fig. 41.

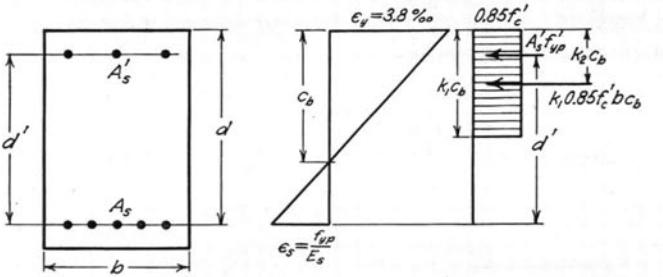

Fig. 42. Computation of M_o

For an isotropic material, $f_{co} = -f_{to}$, and the diagram is completed with one line only from $P/P_o = 1$ to $M/M_o = 1$. If the tensile strength is less than the compressive strength, however, a diagram consisting of two straight lines is obtained, as indicated in the figure for $f_{to}/f_{co} = -0.4$.

Combined bending and axial load in reinforced concrete members has been studied by similar methods by Thomas[68] and Whitney.[74] It has been claimed that Whitney's equation for compression failure of rectangular sections (Eq. 21) represents a straight line when plotted in a P versus Pe diagram.[74] The writer has found, however, that this is strictly the case only when

$$\frac{2}{d'} = \frac{3t}{1.178d^2} \text{ or } \frac{d'}{d} = 0.535.$$

It is nevertheless believed that a straight line in an interaction diagram may represent a satisfactory approximation for compression failures of any reinforced concrete section. In order to study the compression failure of the column tests reported herein with the aid of such

a hypothesis, P_o is defined by the ultimate load formula for a centrically loaded column, Eq. (3). The eccentricity, e, is measured from the plastic centroid of the transformed section computed with a plastic "modular ratio" $m = f_{yp}/0.85\, f_c'$. Since most columns are dimensioned in such a manner that they would fail in tension if subjected to bending without axial load, M_o is defined as the moment of all internal compressive forces about the centroid of the tension steel for a balanced section. Thus, the value of M_o for the section in Fig. 42 is computed from

$$c_b = \frac{\epsilon_u}{\epsilon_u + \epsilon_s} d = \frac{3.8‰}{3.8‰ + f_{yp}/E_s} d \tag{84}$$

and

$$M_o = A_s' f_{yp}' d' + k_1\, 0.85 f_c' b c_b\, (d - k_2 c_b) \tag{85}$$

where k_1 and k_2 are the constants given in Table 6. For cylindrical columns, M_o is computed in a similar manner with the aid of Fig. 37.

Sections of frames may at times be reinforced heavily enough to fail in compression under bending without axial load. In this case it is believed that M_o should be computed for the conditions at failure in bending with the aid of the usual two equilibrium equations and the one compatability equation, Eqs. (10) and (13).

An interaction diagram for all compression failures in these tests is presented in Fig. 43. It should be noted that the measured deflections at failure are included in the eccentricities in the same manner as in Figs. 31 to 33 and Fig. 38. The thin lines in the diagram represent a deviation of measured ultimate loads, P, equal to $\pm$ 10 percent from the theoretical interaction line. Thus it appears that the straight line is a good approximation considering that the scatter in Fig. 43 is caused not only by scatter of the test results but also by systematical errors introduced by referring two shapes of section, four types of reinforcement, and concrete strengths from about 1500 to 5500 p.s.i. to the *same* interaction line.

a. Columns with $e = 0$

The upper group of points in Fig. 43 represents columns loaded at the mid-depth of the section. Thus the results of Group I with a non-symmetrical arrangement of reinforcement are shown in the figure with an eccentricity equal to the distance between the mid-depth and the plastic centroid plus the deflection at failure.

Groups II and III were symmetrically reinforced and thus loaded through knife edges at the centroid. In the past, it has been observed that such columns generally show a strength about 10 to 15 percent lower[74, 95] than similar columns loaded with flat ends. The writer believes that this reduction in strength is due to the fact that very few

concentrically loaded columns with hinged ends have been truly concentrically loaded. Small initial eccentricities due to errors in centering the columns in the testing machine as well as inhomogeneities of the concrete in the lateral direction will generally cause deflections and thereby eccentricities which are large enough, when the plastic stage of loading is reached, to explain the reduction in strength mentioned above. The columns of Groups II and III were loaded through knife edges ½-in. thick as indicated in Fig. 7. Due to the unknown position of the force within this ½-in. width and errors in centering the columns, the results of the concentrically loaded columns in Groups II and III were plotted in Fig. 43 with an eccentricity of ¼-in. plus the measured deflection at failure. It should be noted that, for concentrically loaded columns with knife-edge loading, a centering error in any direction will cause reductions in strength. For eccentrically loaded columns with hinged ends, however, an error in centering will cause increases or reductions in strength depending on the direction of the error. Furthermore, the ultimate loads of concentrically loaded members are far more sensitive to such centering errors than eccentrically loaded columns.

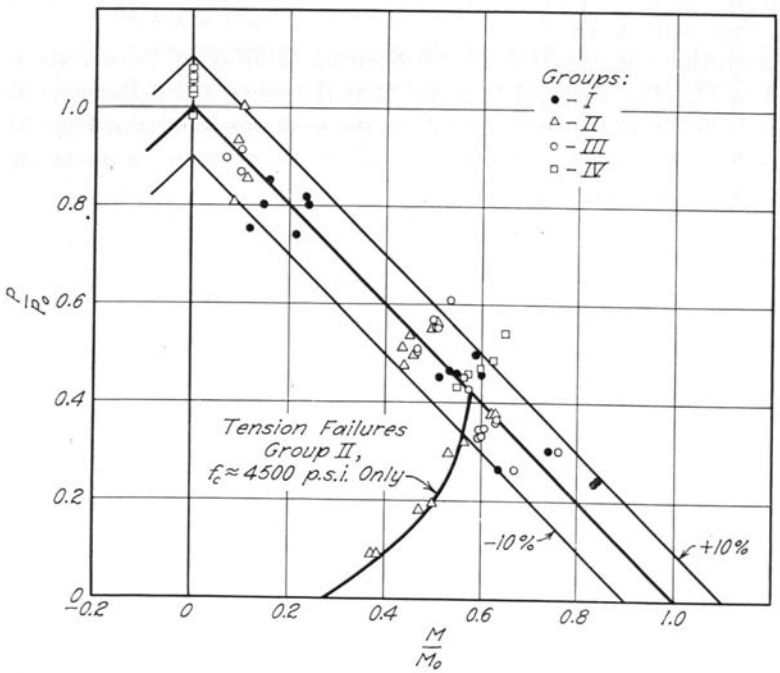

Fig. 43. Interaction Diagram, All Compression Failures of Columns

Hence, the writer believes there exists no reason to question the validity of the test results of eccentrically loaded columns with hinged ends on the basis that similar concentrically loaded columns show a reduction in strength, as compared to columns with flat ends.

The concentrically loaded cylindrical columns of Group IV were loaded with flat ends since their capacities at times were over the estimated safe load on the knife edges. Thus, these columns are shown in Fig. 43 as truly centrically loaded members.

b. Eccentrically Loaded Columns, $e > 0$

With the aid of the interaction diagram discussed herein, the ultimate capacity of an eccentrically loaded column may be expressed as

$$P = \frac{P_o}{1 + \frac{P_o}{M_o} e}. \tag{86}$$

This equation is very similar to Richart's equation[95]

$$P = \frac{P_o}{1 + C \frac{a}{k^2} e} \tag{87}$$

in which C is a constant, a is the distance from the centroid to the extreme edge of the section, and k is the radius of gyration of the section.

These two equations coincide if

$$C = \frac{P_o}{M_o} \frac{k^2}{a}. \tag{88}$$

Studying rectangular columns with $d' = 0.8t$, $f_c' = 2000$, 4000 and 6000 p.s.i., and a symmetrical reinforcement of 1.0, 2.0, 3.0 and 4.0 percent, it was found that C varied from 0.53 to 0.61. This result is in agreement with the experimental findings of Fig. 10 in Bulletin 368.[95]

The equations for ultimate loads of eccentrically loaded members failing in tension (Eqs. 39 and 81) can be introduced in the interaction diagram (Fig. 43) in a similar manner as the second straight line for an ideal material (Fig. 41). An example is indicated in Fig. 43 for Group II with cylinder strengths near 4500 p.s.i.

Such complete interaction diagrams with a compression as well as a tension branch are believed to be most helpful in studying the effect of various variables on the ultimate capacity of eccentricity loaded members.

The concepts of interaction curves also lead to very simple expressions for the ultimate loads, Eq. (86). Nevertheless, it appears from Fig. 43 that the accuracy of Eq. (86) generally will be within $\pm$ 10 percent. Hence, this equation should be suitable for practical purposes, at least for preliminary design of sections in monolithic structures.

17. Errors in Tests and Analysis, Variation of P_{test}/P_{calc}

The tests and the analysis reported herein are both subject to errors. The components of variation in the tests were not perfectly controlled, and the assumptions on which the analysis is based may not be strictly correct.

The ratio between measured and calculated values of ultimate loads as presented in Tables 7 to 10 derived by the writer's theory is believed to be a convenient means of studying such errors with the aim of establishing some evidence regarding the reliability of the theoretical analysis. There are a number of possible sources of error.

Of a total number of 120 column specimens, six failed locally in such a manner that the observed ultimate loads were entirely irrelevant to the problem of combined bending and axial load. For instance, Column B-14b failed in tension and bond through the top bracket since, by an error, the bracket reinforcement was not properly welded to the longitudinal bars. These six local failures were caused by obvious errors and the results, being entirely irrelevant, were discarded. The results of the remaining 114 tests are believed to be significant, but are nevertheless subject to various errors indicated in the following discussion.

1. All test pieces were manufactured in the laboratory, and the strength of 6- by 12-in. cylinders was used as a measure of concrete quality in the column specimens. From each batch of concrete three cylinders were made, the average strength of which is believed to represent the true strength of the batch with a coefficient of variation of about two to three percent. However, three to four batches were used in casting every pair of columns, and these batches were stacked on top of each other rather than being thoroughly mixed. Hence, the significance of the average strength of all cylinders cast with a pair of columns as well as the corresponding variance is questionable. The strength of a column may possibly be more closely related to the batch with lowest quality or to the batch located near the failure region of the member. Since no better measure of concrete strength seems to be available at the present time, an over-all average f_c' was nevertheless used as a measure of the quality of concrete used in casting the columns. The coefficient of variation of this average f_c', $V_{mean} = V/\sqrt{n-1}$, from Table 10 was probably of the order of one to four percent.

The concrete strength developed in the columns, however, was not solely dependent on the quality of concrete as expressed by the over-all average f_c'. Even though both columns and cylinders were compacted by vibration, a longer period of vibration was generally necessary for the columns than for the cylinders. Furthermore, the casting of the columns was at times influenced by such irregularities as leaky forms and delays between batches. Finally, the height of the columns was of the order of 6 to 7 ft as compared to the 12-in. height of the cylinders. Hence, it is reasonable that a differential in strength, due to different degrees of compaction, was present in the columns as indicated by the fact that all columns failed in the upper half, and the intensity of this differential may have varied from one pair of columns to another.

Four lots of aggregates and two lots of cement were used during the manufacture of specimens. Even though these lots were very similar, the relation between column and cylinder strength may have been influenced by these step-wise changes of materials.

Columns and cylinders were cured in 100 percent moisture for seven days. This period of curing was relatively well controlled. Before testing, however, columns and cylinders were stored in the air of the laboratory for 21 days. The tests were made over a period of about a year. Hence, the temperature and relative humidity varied quite considerably, probably from 70 to 95 deg F and 30 to 95 percent. These changes may have influenced the relation between cylinder and column strength.

It may be noted that the errors resulting from using the over-all average f_c' discussed above will influence the measured ultimate loads of columns failing in compression almost to the extent of proportionality. Columns failing in tension, however, are relatively unaffected by changes in f_c'.

2. The concrete dimensions of the column sections were found to vary up to $\pm$ 0.1 in., which corresponds to a variation of ultimate loads of the order of one to two percent.

3. The yield points of the longitudinal reinforcement, which was received in one shipment, were determined by means of eight to ten samples for each size of bar. It appears from Table 4 that deviations from the average yield points of the order of five to eight percent was present. Unfortunately the number of tension tests is entirely insufficient to establish statistical trends. The ultimate loads of columns failing in tension are almost proportional to the yield point of the tension reinforcement; such columns will therefore be strongly influenced by variations in such yield points. The ultimate loads of columns failing in compression, however, will be independent of the yield point in the tension steel and will be relatively little affected by variations in the quality of compression steel.

4. The positions of the reinforcing bars in the sections probably varied up to $\pm \frac{3}{8}$ in. from the nominal values. This error is not important for compression failures. For tension failures, however, the variations of the internal moment arm of the tension steel, and consequently variations of ultimate loads, may have been of the order of four to six percent.

The errors discussed above under (1) to (4) were related to the manufacture of the specimens; another group of errors was introduced through the testing procedure used.

5. The columns were leveled in the testing machine by means of a plumb line. Hence, no columns were placed in the machine in a strictly perpendicular position, and irregularities in the method of loading may have been present.

6. For reasons of safety and stability, the spherically seated block in the movable head of the testing machine had to be locked by wedges before the jacks which served as a temporary support were removed (Fig. 7). Therefore, the bending of the specimens under load did not take place strictly in a plane of symmetry as was intended and assumed in the analysis. Some evidence of such errors was found, as observed strains at times were consistently larger on one side of the column than on the opposite side.

7. The columns were placed in the testing machine with the desired eccentricity of load by means of a plumb line and an inch rule. At least twice during the tests, errors resulted from the use of a rule with $\frac{1}{10}$-ft divisions or with the end broken off. Two such cases, Columns A-1b and A-7a, were found by check measurements. The actual eccentricities were recorded and the measured ultimate loads were corrected to the nominal eccentricities.

Because the knife edges were $\frac{1}{2}$ in. thick and because small errors normally accompany the use of plumb lines and inch rules, the eccentricities of the remaining columns probably deviated up to $\frac{1}{4}$ in. from the nominal values. The effect of such errors is relatively small for large eccentricities. However, the influence on the ultimate loads of columns with small eccentricities may have been of the order of three to five percent.

8. The total time used in testing the columns to failure varied about from 45 to 75 min. The level of load at which the last readings were made varied about from 90 to 98 percent of the ultimate load. Finally, the rate of applying load increments was not strictly controlled. Hence, it is possible that uncontrolled time factors may have influenced the ultimate loads.

9. The three testing machines used for the tests of reinforcement, cylinders and columns, respectively, have been calibrated in the past.

There is every reason to believe that the machines are all sensitive and accurate enough to indicate actual loads with an error of less than one percent within the loading ranges used.

The final group of sources of error are related to the theoretical analysis of ultimate loads.

10. Some of the basic assumptions in the analysis, which were discussed in Section 11, may be in error. It was assumed, for instance, that the maximum concrete stress in the columns subject to eccentric loads, f_c'', equals $0.85 f_c'$. This constant 0.85 may be systematically too high or too low. The ratio f_c''/f_c' may even not be a constant, but a function of f_c' and/or the space-gradient of strain. It was further assumed that no tensile stresses exist in the concrete and that strains vary linearly across the section, both of which assumptions are not strictly true.

11. Variables which were not considered in the basic assumptions of the analysis may be significant. For instance, the spacing of ties in the square columns was 8 in. for $\frac{3}{8}$-in., $\frac{5}{8}$-in. and $\frac{7}{8}$-in. compression steel. It is possible that the spacing of ties in terms of bar diameters is a significant variable.

12. The ultimate loads were computed by means of a slide rule, and some graphical solutions were made. The calculations are therefore believed to be accurate only to about 0.5 percent.

13. Even if the manufacture of specimens, tests, and theoretical analysis were perfect, concrete is a heterogeneous material, all properties of which are subject to variations from statistical mean values.

The ratios between measured and computed loads may then be studied in the light of these possible sources of errors. The total population of 114 ratios was subjected to a statistical analysis, the results of which are given in Table 11.

The arithmetic mean of the total population is 1.012. This figure alone, however, cannot be used to indicate the reliability of the theoretical analysis, since the slope of the assumed stress-strain relation beyond the maximum stress in Fig. 10 was adjusted to fit the test results as well as possible. It is significant, however, that the standard deviation of the total population is 0.058 only. If the distribution is normal, this means that about 92 percent of the observed loads were within $\pm$ 10 percent of 1.01 times the predicted values, and 99 percent were within $\pm$ 15 percent. A standard deviation of this order of magnitude may easily have been caused by random errors from the sources (1), (3) and (13) alone.

It has not been proved, however, that the population *is* normal, and systematic trends may be present. For compression failures, Table 11 gives a mean, $\bar{x}_c$, of 1.027 with a standard deviation, σ_c, of 0.059. For

Table 11
Statistical Study of the Ratio P_{test}/P_{calc}

Variable		Arithmetic Mean	Standard Deviation	Number
Group	I	1.012	0.062	30
	II	0.992	0.056	28
	III	1.026	0.053	26
	IV	1.018	0.052	30
Concrete	A	0.993	0.057	36
	B	1.016	0.049	39
	C	1.024	0.063	39
Eccentricity	0	1.013	0.060	19
	$\frac{1}{4}t$	1.038	0.059	24
	$\frac{1}{2}t$	0.986	0.053	24
	$\frac{3}{4}t$	1.006	0.047	23
	$1\frac{1}{4}t$	1.015	0.057	24
Mode of Failure*	C	1.027	0.059	58
	T	0.996	0.052	56
All Columns		1.012	0.058	114

* Mode of failure as predicted by writer's theory—C: compression failure; T: tension failure.

tension failures, these statistics are $\bar{x}_T = 0.996$ and $\sigma_T = 0.052$, respectively. In order to determine whether the difference in means, $\bar{d} = 0.031$, is statistically significant, it is assumed that the distribution within the two groups is normal. The "t test" of significance,

$$t = \bar{d}/\sigma_{\bar{d}} \tag{89}$$

where $\sigma_{\bar{d}}$ is the standard deviation of $\bar{d}$, may then be used. Since both groups are larger than 30, the variance of $\bar{d}$ may be expressed as

$$(\sigma_{\bar{d}})^2 = \frac{\sum(x_c - \bar{x}_c)^2 + \sum(x_T - \bar{x}_T)^2}{n_c n_T} = \frac{\sigma_c^2}{n_T} + \frac{\sigma_T^2}{n_c} \tag{90}$$

in which $n_c = 58$ and $n_T = 56$. With these figures, $\sigma_{\bar{d}} = 0.010$ and $t = 3.1$. Hence, a statistical probability of 516 to 1 exists that the difference, $\bar{d}$, is significant and not due to chance. This may indicate that the value of $f_c'' = 0.85 f_c'$ is chosen too low, since such a systematic error in the analysis would increase the load ratio for compression failures without any significant influence on tension failures.

In a similar manner it may be shown that the difference in means between eccentricities of $\frac{1}{4}t$ and $\frac{1}{2}t$ is significant with a probability of 727 to 1. This may be interpreted as evidence of tension stresses in the concrete since negligible cracking occurred with eccentricities of $\frac{1}{4}t$ even though part of the section was stressed in tension. The increasing trend of means for the three qualities of concrete is statistically insignificant, and no definite trend appears to be present for the four groups.

A trend of the variation of load ratios with time is possible since temperature, humidity, and aggregates varied with time. In addition different laboratory assistants worked on the project and it is possible that the skill with which the tests were made improved with time.

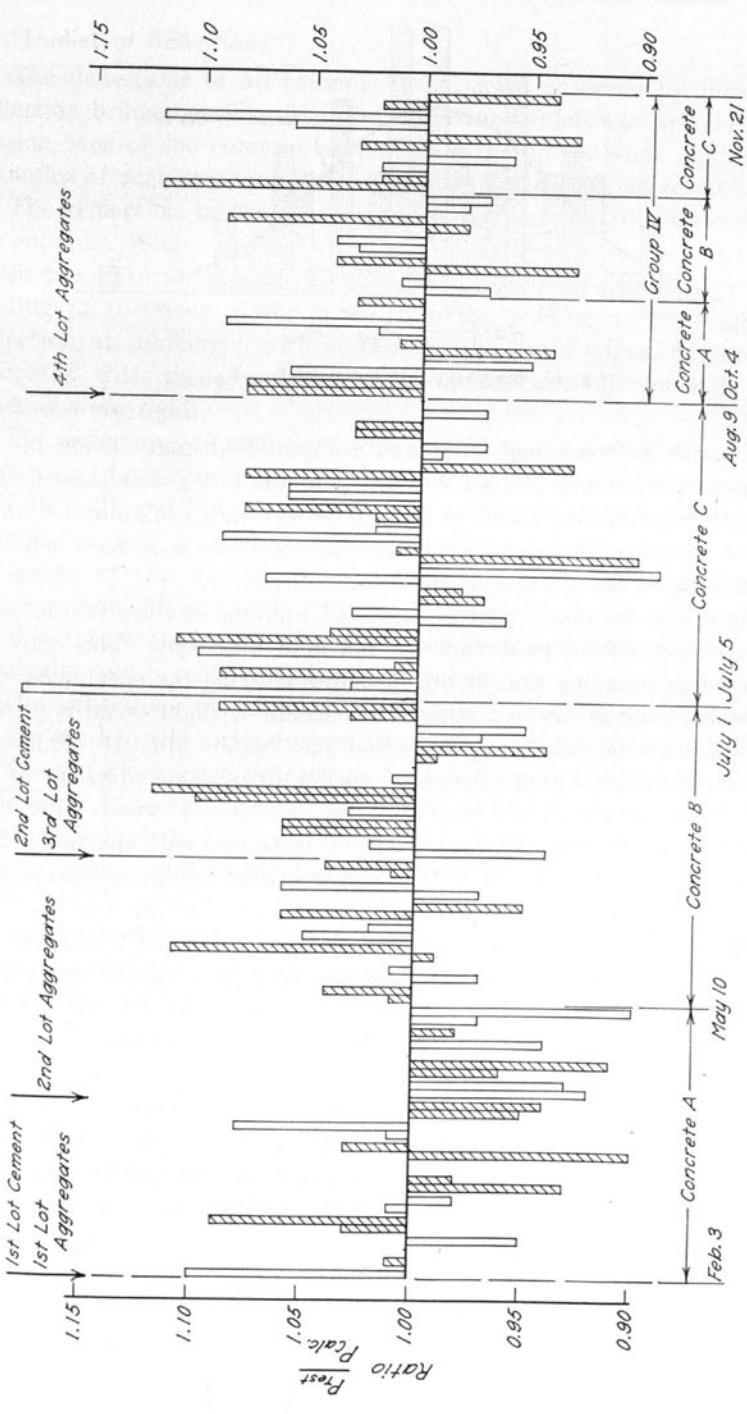

Fig. 44. Variations of P_{test}/P_{calc} with Time

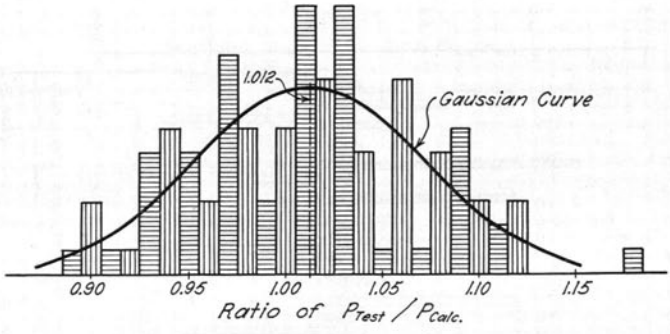

Fig. 45. Frequency Distribution of P_{test}/P_{calc}

The ratios between measured and computed ultimate loads for all columns were therefore plotted in Fig. 44 in the order that the columns were cast. Neighboring blank or shaded blocks indicate columns which were cast as pairs. There are six blocks without such a related neighbor corresponding to the six discarded tests.

It may first be noted that 35 pairs of columns deviate in the same direction while 19 pairs deviate in opposite directions. This may be interpreted as meaning that errors in manufacturing the specimens were more serious than errors in testing. Furthermore a slight trend is present indicating low test values in the period just before May 10. This may have been the effect either of a rainy spring, or of some property of the second lot of aggregates. Otherwise, no systematic trend with time appears to exist. Hence, the improvements in testing skill did not reduce the scatter of the test results, though many time saving methods were developed as the tests proceeded.

Finally Fig. 45 shows the frequency distribution of the load ratios for all 114 columns. The class interval of one percent is rather small compared to the population, and a "saw-tooth" variation results. Nevertheless it appears that the results fall fairly close to the Gaussian curve of a normal distribution.

Within the scope of the tests reported herein it may be concluded that the predicted ultimate loads are, on the average, one percent on the safe side. The test results appear to be distributed at random, since, for all *practical* purposes, no systematic trends of variation were found. The standard deviation of the ratio between measured and computed ultimate loads was 0.058. Hence, 99 percent of the results of tests similar to those reported herein may be expected to fall between 1.16 and 0.86 times the values predicted by a flexural analysis based on the assumptions made in Section 11.

18. Studies of Deflections

The deflections of all columns tested were observed by means of a deflection bridge carrying five dial indicators which was attached to the tension face of the columns as indicated in Fig. 7. Some characteristic examples of such measurements are presented in Figs. 46 to 49.

The deflection bridge was extended beyond the prismatic shaft of the columns. Hence, the deflection at midheight with respect to the ends of the prismatic shaft could be obtained by subtracting the average dial reading at the ends of the shaft from the reading at midheight. The deflection at midheight with respect to the knife edges, however, was computed with the assumption that the brackets at the ends of the columns were rigid.

The deflections at midheight with respect to the ends of the prismatic shaft were discussed in Section 13a for the typical columns shown in Figs. 19 to 21 and Figs. 24 to 28. It was shown that such deflections may be predicted with a satisfactory accuracy throughout the range of loading by means of the writer's theory. This is important, since a relation between moment and curvature is a necessary basic assumption in possible future studies of effects of L/d on the ultimate loads of concentrically and eccentrically loaded members.

The deflections at midheight with respect to the knife edges were extrapolated to the ultimate load in order to estimate the actual eccentricities at failure. Such deflections, Δe, are given in Tables 7 to 10.

In Figs. 46 to 49 it may be noted that at high loads the deflections of the upper half of the columns are relatively larger than for the lower half. This is another indication of a strength differential of the concrete due to the method of casting, the fact that all columns failed in the upper half being another indication. It may finally be noted in Figs. 46 to 49 that the deflection curve of the prismatic shafts of the columns is approximately a sine wave.

All equations for ultimate loads of eccentrically loaded members discussed in this report have been referred to the actual eccentricity at failure. Hence, some consideration must be devoted to deflections if these equations are applied to the design of structural members. The effects of such deflections may be considered by several means:

1. The increased eccentricity may be accounted for in the safety factor. This simple approach may be justified because the decreases in ultimate load in monolithic structures due to deflections probably are less than ten percent in the most common cases. Moments in a building with flat slab floors, for instance, are often known with less accuracy than ten percent.

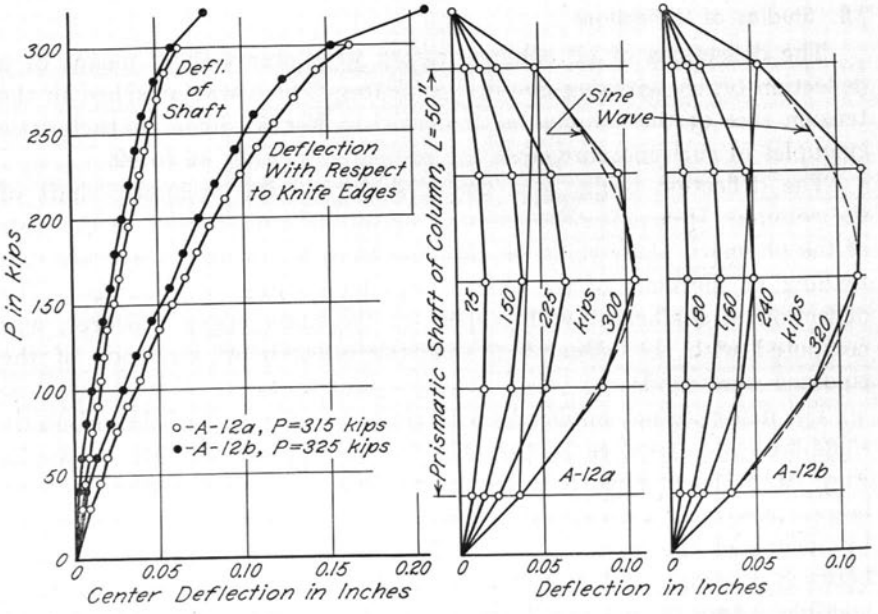

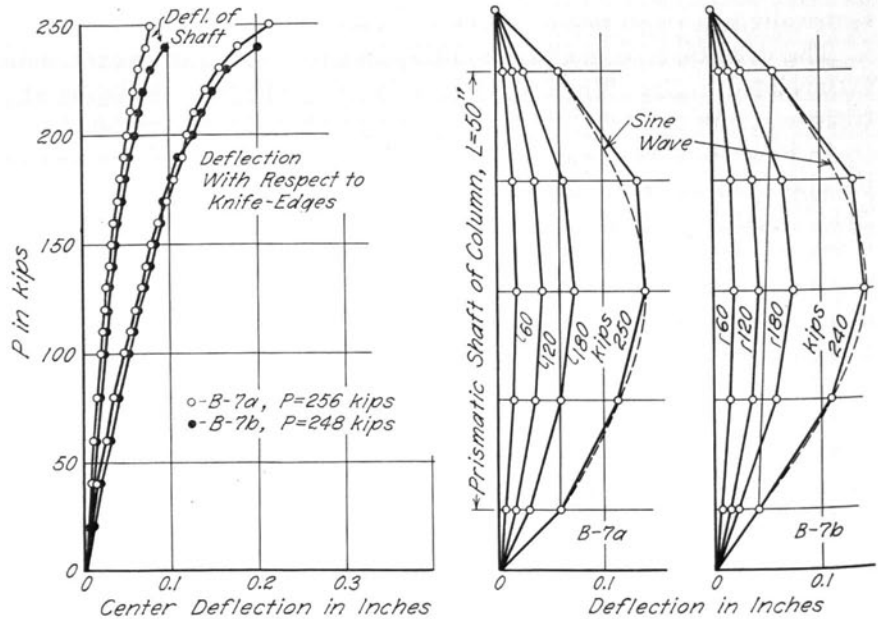

Above: Fig. 46. Deflections, Columns A-12
Below: Fig. 47. Deflections, Columns B-7

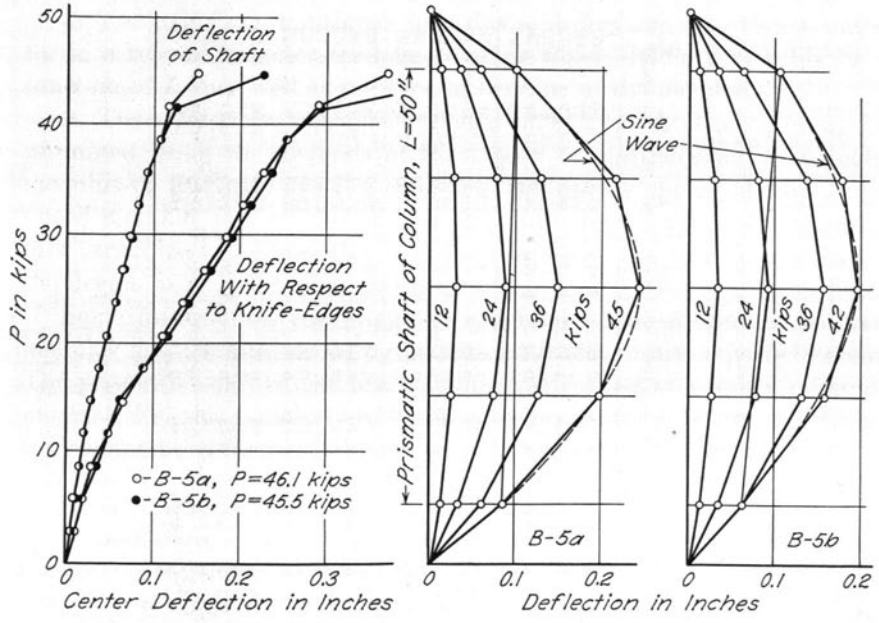

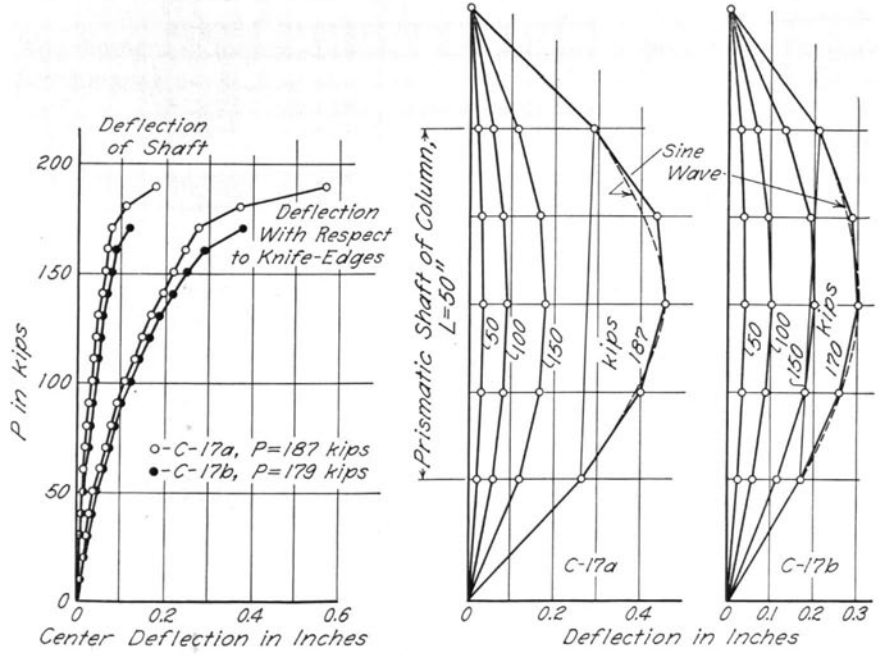

Above: Fig. 48. Deflections, Columns B-5
Below: Fig. 49. Deflections, Columns C-17

Table 12
Reduced Moduli of Elasticity

Eccentricity	Group I				Group II				Group III				Group IV			
	Col. No.	f_c' p.s.i.	E_{cc} p.s.i. $\times 10^6$	E_{ct}	Col. No.	f_c' p.s.i.	E_{cc} p.s.i. $\times 10^5$	E_{ct}	Col. No.	f_c' p.s.i.	E_{cc} p.s.i. $\times 10^6$	E_{ct}	Col. No.	f_c' p.s.i.	E_{cc} p.s.i. $\times 10^6$	E_{ct}
	A-2a	5280	2.52	1.80	A-7a	5240	2.97	1.76	A-12a	4150	4.76	2.60	A-17a	5150	3.40	2.07
	b	5830	2.81	2.09	b	5810	3.32	2.11	b	5050	4.01	1.97	b	4640	3.37	2.04
$\frac{1}{4}t$	B-2a	4250	2.01	1.29	B-7a	4080	3.16	1.96	B-12a	4300	3.88	1.72	B-17a	3620	2.72	1.39
	b	4070	2.15	1.43	b	4040	2.60	1.40	b	4010	3.28	1.12	b	3310	2.84	1.51
	C-2a	2270	1.06	0.34	C-7a	1970	1.54	0.34	C-12a	2300	3.07	0.91	C-17a	1420	1.69	0.36
	b	1970	1.09	0.37	b	1520	1.42	0.22	b	2200	2.96	0.80	b	1600	1.53	0.20
	A-3a	5660	1.87	1.15	A-8a	5520	2.56	1.36	A-13a	5350	3.36	1.20	A-18a	5020	2.29	0.96
	b	5830	2.02	1.30	b	5810	2.24	1.05	b	4850	2.71	0.55	b	5000	2.50	1.17
$\frac{1}{2}t$	B-3a	4630	1.78	1.06	B-8a	4700	2.46	1.26	B-13a	3580	2.88	0.72	B-18a	3380	2.47	1.04
	b	4290	1.59	0.87	b	4260	2.23	1.03	b	4290	3.30	1.14	b	3580	2.14	0.75
	C-3a	1880	1.20	0.48	C-8a	1820	1.44	0.24	C-13a	2300	2.69	0.53	C-18a	1680	1.72	0.39
	b	1690	0.95	0.23	b	1820	1.30	0.10	b	2070	2.63	0.47	b	1590	1.54	0.21
	A-4a	4810	1.79	1.07	A-9a	5100	1.84	0.64	A-14a	5350	3.26	1.11	A-19a	5020	1.96	0.63
	b	5600	1.70	0.99	b	5170	1.78	0.58	b	5100	3.20	1.04	b	5310	2.02	0.69
$\frac{3}{4}t$	B-4a	3800	1.73	1.01	B-9a	4700	2.04	0.84	B-14a	3580	2.65	0.49	B-19a	3380	1.98	0.65
	b	4290	1.54	0.82	b	4370	2.22	1.02	b	4590	....	....	b	3580	2.12	0.79
	C-4a	1690	1.14	0.42	C-9a	1880	1.48	0.28	C-14a	1950	2.76	0.60	C-19a	1680	1.66	0.33
	b	1730	1.08	0.37	b	1730	1.33	0.13	b	2070	2.48	0.32	b	1630	1.56	0.23
	A-5a	4810	1.68	0.96	A-10a	5100	2.10	0.90	A-15a	5100	2.88	0.72	A-20a	5310	2.06	0.72
	b	5600	1.39	0.67	b	5170	2.30	1.10	b	4850	3.24	1.08	b	5000	1.96	0.63
$1\frac{1}{4}t$	B-5a	4290	1.44	0.72	B-10a	4260	2.05	0.85	B-15a	3800	2.88	0.72	B-20a	2990	1.74	0.41
	b	4590	1.61	0.89	b	4370	1.56	0.36	b	4630	3.12	0.96	b	3620	2.10	0.77
	C-5a	2310	1.30	0.58	C-10a	2300	1.46	0.26	C-15a	1950	2.29	0.13	C-20a	1630	1.87	0.54
	b	1770	1.12	0.40	b	1770	1.48	0.28	b	2070	2.50	0.34	b	1600	1.78	0.45

2. The reduction in ultimate load due to deflections may be accounted for in a reduction factor for long columns which should preferably be a function of L/d as well as the type of bending of the member.

3. The deflections near the ultimate capacity of a structure may be estimated using the methods of the theory of elasticity and a reduced modulus of elasticity for the concrete. The proper choice of such a reduced modulus is a matter of opinion, since the actual secant modulus in a structure will generally vary from section to section depending on the degree of strain in the various sections.

Some information regarding the minimum value of such a reduced modulus may be established by means of the test results reported herein. The prismatic shaft of the test columns was subject to a fairly constant moment, Pe, and a deflection, δ, was developed over a length, L. Hence, the common elastic theory gives

$$\delta = \frac{M}{EI} \frac{L^2}{8}$$

or

$$EI = \frac{L^2 M}{8\delta}. \tag{91}$$

The moment of inertia of reinforced concrete members may be assumed for the concrete section alone as

$$EI = E_{cc} I_c \tag{92}$$

or for the transformed section as

$$EI = E_{ct} I_c + \mathrm{E}_s \mathrm{I}_s. \tag{93}$$

In Table 12 are presented for all eccentrically loaded test columns values of E_{cc} and E_{ct} as derived from Eq. (91) and Eq. (92) or (93) with the observed values of M and δ corresponding to the last readings before failure; i.e., at 90 to 95 percent of the ultimate load. It appears that both E_{cc} and E_{ct} are functions of f_c'. However, the moduli, as presented in Table 12, also vary with the eccentricity and the amount of reinforcement. It should also be noted that some scatter is caused by the fact that the moduli are not referred to exactly the same percentage of the ultimate load. The average values of E_{cc} were 2.56, 2.33 and 1.72 for concrete A, B and C, respectively. The corresponding values of E_{ct} were 1.21, 1.00 and 0.37.

The writer believes that the most rational consideration of reductions in ultimate loads due to deflections may be obtained through such reduction factors as were mentioned under (2) above.

V. CONCLUSION

19. General Summary of Investigation

It was the object of the investigation reported herein to throw new light on the behavior of reinforced concrete members subject to combined bending and axial load.

A total of 120 eccentrically loaded column specimens were manufactured and tested to failure in short-time tests, the total time between the first and last increment of load being about an hour. The test columns were divided into four groups, each containing 30 specimens. Groups I, II and III were 10-in. square tied columns with 1.46 to 4.8 percent reinforcement. Group IV was 12-in. cylindrical spiral columns with 4.25 percent reinforcement. Within each group, the concrete quality was varied from about 1500 to 5500 p.s.i., and the eccentricity of loading varied from 0 to 1¼ times the lateral dimension of the columns. The general behavior of the test columns was observed by measurements of load, strains and deflections.

A critical study of the basic assumptions in inelastic flexural theories for reinforced concrete was made. On the basis of such studies and of phenomena observed in the present tests, a general inelastic flexural theory was developed, by means of which the behavior of the test columns as well as the ultimate loads could be predicted. The theory developed by C. S. Whitney and a modification of V. P. Jensen's theory were also compared to the measured ultimate loads.

20. Behavior and Mode of Failure of Test Columns

a. General Phenomena

Since the investigation was confined to the combined stress problem, the specimens were purposely kept fairly short, so that the results would not be confused by the occurrence of buckling failures.

Two modes of failure prevailed in the tests, compression failures and tension failures. The compression failures were characterized by crushing of the concrete at the compression face while stresses in the tension reinforcement were less than the yield point. Tension failures, on the other hand, were characterized by yielding in the tension reinforcement followed by large deformations and considerable movements of the neutral axis before crushing of the concrete took place.

All columns were cast in a vertical position, and it was observed that all columns failed in the upper half. This phenomenon was interpreted as evidence of a variation in concrete strength from the bottom to the top of the columns due to a difference in degree of compaction during casting. Such a strength differential was also indicated by measured strains and deflections.

b. Tied Columns, Groups I, II and III

The concentrically loaded tied columns were loaded through knife edges. In agreement with the findings of earlier investigators, it was found that the ultimate loads were 10 to 15 percent lower than for similar columns tested with flat ends. This phenomenon is explained as being due to the fact that it is impossible practically to obtain a truly concentric application of load through knife edges.

The final failure of all eccentrically loaded tied columns was caused by a crushing of the concrete at an ultimate strain of about 3.8 per mill. After such crushing had taken place, the compression reinforcement buckled between ties, and the load capacity of the columns thereby dropped very considerably.

The intermediate grade compression reinforcement, in most cases, yielded before failure of the concrete took place.

Preceding the final failure of the concrete, all eccentrically loaded columns were in a semi-neutral equilibrium with the applied load. This state of equilibrium was characterized by considerable increases in deformation for very small additions of load.

It was observed that columns failing in tension developed much larger deflections before final crushing of the concrete took place than did the columns failing in compression.

A fairly linear distribution of strains across the section was found to exist from the smallest loads to failure.

c. Spiral Columns, Group IV

The concentrically loaded spiral columns were loaded with flat ends. The general behavior of these columns was in agreement with the findings of earlier investigators. A maximum load was reached at failure of the concrete shell. After considerable deformation, however, a second and generally higher maximum load was developed through the action of the spiral reinforcement.

The ultimate load of the eccentrically loaded columns, which were loaded through knife edges, was reached at failure of the concrete shell; no second maximum load was developed.

After failure of the shell, all eccentrically loaded spiral columns developed extremely large deflections without serious decreases in load capacity, since the spirals prevented buckling of the compression reinforcement and crushing of the concrete core. Regardless of the amount of eccentricity of load, the spiral columns appeared to possess great toughness.

21. Inelastic Flexural Theories

The writer's theory rests on such general assumptions that the behavior of the test columns may be predicted from the smallest loads to failure, including the mode of failure. The average ratio of measured to predicted ultimate loads for all test columns was 1.012, the standard deviation of the ratio being 0.058.

Whitney's theory and a modification of Jensen's theory also give satisfactory agreement with observed ultimate loads. However, behavior at low loads and mode of failure may not be predicted with accuracy by means of these theories.

The principles of interaction diagrams were used to develop a very simple and fairly accurate method of predicting ultimate loads of columns with small eccentricities.

APPENDIX: BIBLIOGRAPHY

1. 1886 Koenen, M., "Für die Berechnung der Stärke der Monierschen Cementplatten," Zentralblatt der Bauverwaltung, Vol. 6 No. 47, Nov. 1886, p. 462.

2. 1890 Neumann, P., "Ueber die Berechnung der Monier-Constructionen," Wochenschrift des Oesterr. Ing. und Arch. Vereines, Vol. 15 No. 22, May 1890, pp. 209-12.

3. 1894 Coignet, E. and Tédesco, N. de, "Du calcul des ouvrages en ciment avec ossature métallique," Mémoires de la société des ingénieurs civils de France, 1894 I, pp. 282-363.

4. 1895 Johnson, J. B., "Strength of Concrete and Steel in Combination," Engineering News and American Railway Journal, Vol. 33 No. 1, Jan. 1895, pp. 10-11.

5. 1896 Thullie, M. R. v., "Ueber die Berechnung der Biegespannungen in den Beton- und Monier-Constructionen," Zeitschrift des Oesterr. Ing. und Arch. Vereins, Vol. 48 No. 24, June 1896, pp. 365-69.

6. 1897 Thullie, M. R. v., "Ueber die Berechnung der Monierplatten," Zeitschrift des Oesterr. Ing. und Arch. Vereins, Vol. 49 No. 13, March 1897, pp. 193-97.

7. 1897 Emperger, F. v., "Zur Theorie der verstärkten Betonplatte," Zeitschrift des Oesterr. Ing. und Arch. Vereins, Vol. 49 No. 22, May 1897, pp. 351-55 and 364-67.

8. 1899 Ritter, W., "Die Bauweise Hennebique," Schweizerische Bauzeitung, Vol. 33 Nos. 5, 6 and 7, Feb. 1899, pp. 41-43, 49-52 and 59-61.

9. 1902 Ostenfeld, A., "Einige Folgerungen aus den Sanders'schen Belastungsversuchen," Beton und Eisen, Vol. 1 No. 5, Oct. 1902, pp. 19-22.

10. 1904 Talbot, A. N., "Tests of Reinforced Concrete Beams," University of Illinois Engineering Experiment Station Bulletin No. 1, Sept. 1904. 64 pp.

11. 1906 Talbot, A. N., "Tests of Reinforced Concrete Beams Series of 1905," University of Illinois Engineering Experiment Station Bulletin No. 4, April 1906. 84 pp.

12. 1908 Emperger, F. v., "Handbuch für Eisenbetonbau, Vol. 1: Entwicklungsgeschichte und Theorie des Eisenbetons," Wilhelm Ernst und Sohn Berlin, 1908.

13. 1912 Suenson, E., "Jærnprocentens Indflydelse paa Jærnbetonpladers Bæreevne," Ingenøiren, Copenhagen, Vol. 21 No. 72, Sept. 1921, p. 568.

14. 1912-1913 Bach, C. and Graf, O., "Versuche mit bewehrten und unbewehrten Betonkörpern, die durch zentrischen und exzentricshen Druck belastet wurden," Forschungsarbeiten auf dem Gebiete des Ingenieurwesens, Vols. 166-69, 1912-1913.

15. 1914 Mensch, L. J., "New-Old Theory of Reinforced Concrete Beams in Bending," ACI Journal, Vol. 2 No. 7, Dec. 1914, pp. 28-41.

15a. 1918 Wilson, W.M., Richart, F. E. and Weiss, C., "Analysis of Statically Indeterminate Structures by the Slope-Deflection Method," University of Illinois Engineering Experiment Station Bulletin No. 108, Nov. 1918. 214 pp.

16. 1920 Slater, W. A. and Zipprodt, R. R., "Compressive Strength of Concrete in Flexure," Proceedings ACI, Vol. 16, 1920, pp. 120-51.

17. 1921 McMillan, F. R., "A Study of Column Test Data," Proceedings ACI, Vol. 17, 1921, pp. 150-71.

18. 1922 Kempton Dyson, H., "What is the use of the Modular Ratio?" Concrete and Constructional Engineering, Vol. 17 Nos. 5, 6 and 7, London, May-July 1922, pp. 330-36, 408-15, 486-91.

19. 1925 Gonnerman, H. F., "Effect of Size and Shape of Test Specimens on Compressive Strength of Concrete," Proceedings ASTM, Vol. 25, 1925, pp. 237-50.

20. 1927 Brandtzæg, A., "Failure of a Material Composed of Non-Isotropic Elements," Det Kgl. Norske Videnskabers Selskabs Skrifter, No. 2, 1927. 68 pp.

21. 1928 Richart, F. E., Brandtzæg, A. and Brown, R. L., "Study of the Failure of Concrete Under Combined Compressive Stresses," University of Illinois Engineering Experiment Station Bulletin No. 185, Nov. 1928. 102 pp.

22. 1929 Richart, F. E., Brandtzæg, A. and Brown, R. L., "The Failure of Plain and Spirally Reinforced Concrete in Compression," University of Illinois, Engineering Experiment Station Bulletin No. 190, April 1929. 72 pp.

23. 1930 Slater, W. A., "Reinforced Concrete Column Investigation. Progress Report of Committee 105," ACI Journal, April 1930; Proceedings Vol. 26, pp. 601-15.

23a. 1930 Cross, H., "The Column Analogy," University of Illinois Engineering Experiment Station Bulletin No. 215, Oct. 1930. 75 pp.

24. 1930 Slater, W. A. and Lyse, I., "Compressive Strength in Flexure as Determined from Tests of Reinforced Beams," Proceedings ACI, Vol. 26, 1930, pp. 831-74.

25. 1931 Slater, W. A. and Lyse, I., "First Progress Report on Column Tests at Lehigh University," ACI Journal, Feb. 1931; Proceedings Vol. 27, pp. 677-730.

26. 1931 Richart, F. E. and Staehle, G. C., "Progress Report on Column Tests at the University of Illinois," ACI Journal, Feb. 1931; Proceedings Vol. 27, pp. 731-60.

27. 1931 Richart, F. E. and Staehle, G. C., "Second Progress Report on Column Tests at the University of Illinois," ACI Journal, March 1931; Proceedings Vol. 27, pp. 761-90.

28. 1931 Slater, W. A. and Lyse, I., "Second Progress Report on Column Tests Made at Lehigh University," ACI Journal, March 1931; Proceedings Vol. 27, pp. 791-835.

29. 1931 Emperger, F. v., "Der Beiwert $n=15$ und die zulässigen Biegungs-Spannungen," Beton und Eisen, Vol. 30 No. 19, Oct. 1931, pp. 340-46.

30. 1931 Slater, W. A. and Lyse, I., "Third Progress Report on Column Tests at Lehigh University," ACI Journal, Nov. 1931; Proceedings Vol. 28, pp. 159-66.

31. 1931 Richart, F. E. and Staehle, G. C., "Third Progress Report on Column Tests Made at the University of Illinois," ACI Journal, Nov. 1931; Proceedings Vol. 28, pp. 167-75.

32. 1932 Richart, F. E. and Staehle, G. C., "Fourth Progress Report on the Column Tests Made at the University of Illinois," ACI Journal Jan. 1932; Proceedings Vol. 28, pp. 279-315.

33. 1932 Lyse, I. and Kreidler, C. L., "Fourth Progress Report on Column Tests at Lehigh University," ACI Journal, Jan. 1932; Proceedings Vol. 28, pp. 317-46.

34. 1932 Stüssi, F., "Ueber die Sicherheit des einfach bewehrten Eisenbeton-Rechteckbalkens," Publications, International Association for Bridge and Structural Engineering, Vol. 1, Zürich, April 1932, pp. 487-95.

35. 1932 Brandtzæg, A., "Wirkungsweise umschnürter Betonkörper," Beton und Eisen, Vol. 31 No. 15, Aug. 1932, pp. 236-38.

35a. 1932 Cross, H. and Morgan, N. D., "Continuous Frames of Reinforced Concrete," John Wiley and Sons, 1932. 343 pp.

36. 1933 Richart, F. E., "Reinforced Concrete Column Investigation. Tentative Final Report of Committee 105," ACI Journal, Feb. 1933; Proceedings Vol. 29, pp. 275-84.

37. 1933 Schreyer, C.,"Elastizität und Festigkeit des Betons auf Grund von Würfelversuchen und relativen Spannungen," Beton und Eisen, Vol. 32 Nos. 3 and 4, Feb. 1933, pp. 42-49, 60.

38. 1933 Steuermann, S., "Das Wiederstandsmoment eines Eisenbetonquerschnittes," Beton und Eisen, Vol. 32 Nos. 4 and 5, Feb.-March 1933, pp. 61-66, 80-82.

39. 1933 Kazinczy, G. v., "Die Plastizität des Eisenbetons," Beton und Eisen, Vol. 32 No. 5, March 1933, pp. 74-80.

40. 1933 Lyse, I., "Fifth Report on Column Tests at Lehigh University," ACI Journal, June 1933; Proceedings Vol. 29, pp. 433-42.

41. 1933 Gebauer, F., "Neue Balkenversuche des österreichischen Eisenbetonauschusses. Vergleichsversuche mit St. 37, St. 55 und Isteg Stahl," Beton und Eisen, Vol. 32 No. 13, July 1933, pp. 204-07.

42. 1934 Gebauer, F., "Berechnung der Eisenbetonbalken unter Berücksichtigung der Schwindspannungen der Eisen," Beton und Eisen, Vol. 33 No. 9, May 1934, pp. 137-43.

43. 1934 Richart, F. E. and Brown, R. L., "An Investigation of Reinforced Concrete Columns," University of Illinois Engineering Experiment Station Bulletin No. 267, June 1934. 91 pp.

44. 1934 Baumann, O., "Die Knickung der Eisenbeton-Säulen," Eidg. Material-Prüfungsanstalt an der E. T. H. in Zürich, Bericht No. 89, Dec. 1934. 56 pp.

45. 1935 Blanks, R. F. and McNamara, C. C., "Mass Concrete Tests in Large Cylinders," ACI Journal, Jan.-Feb. 1935; Proceedings Vol. 31, pp. 280-303.

46. 1935 Steuermann, M., "Wirdschaftliche Bemessung von einseitig bewehrten Eisenbetonbalken," Beton und Eisen, Vol. 34 No. 3, Feb. 1935, pp. 50-51.

47. 1935 Steuermann, M., "Bemessung der aussermittig belasteten Eisenbetonquerschnitte," Der Bauingenieur, Vol. 16 Nos. 5 and 6, Feb. 1935, pp. 61-64.

48. 1935 Bittner, E., "Zur Klärung der n-Frage bei Eisenbetonbalken," Beton und Eisen, Vol. 34 No. 14, July 1935, pp. 226-28.

49. 1935 Coppée, R., "Considérations sur le calcul et le sécurité des pièces flèchies. Moments de rupture," Proceedings, International Association for Bridge and Structural Engineering, Vol. 3, Zürich, Sept. 1935, pp. 19-46.

50. 1935 Freudenthal, "Einfluss der Plastizität des Betons auf die Bemessung aussermittig gedrückter Eisenbetonquerschnitte," Beton und Eisen, Vol. 34 No. 21, Nov. 1935, pp. 335-38.

51. 1935 Brandtzæg, A., "Der Bruchspannungszustand und der Sicherheitsgrad von rechteckigen Eisenbetonquerschnitten unter Biegung oder aussermittigem Druck," Norges Tekniske Høiskole, Avhandlinger til 25-årsjubileet 1935, pp. 667-764.

52. 1936 Gebauer, F., "Das alte n-Verfahren und die neuen n-freien Berechnungsweisen des Eisenbetonbalkens," Beton und Eisen, Vol. 35 No. 2, Jan. 1936, pp. 29-39.

53. 1936 Bittner, E., "Die Berechnung der Eisenbetonbalken nach Zustand III," Beton und Eisen, Vol. 35 No. 9, May 1936, pp. 143-46.

54. 1936 Michielsen, H. F., "Zur Klärung der n-Frage bei Eisenbetonbalken," Beton und Eisen, Vol. 35 No. 9, May 1936, pp. 146-49.

55. 1936 Glanville, W. H. and Thomas, F. G., "The Redistribution of Moments in Reinforced Concrete Beams and Frames," Journal, Institution of Civil Engineers, Paper No. 5061, London, June 1936, pp. 291-329.

56. 1936 Brandtzæg, A., "Die Bruchspannungen und die zulässigen Randspannungen in rechteckigen Eisenbetonbalken," Beton und Eisen, Vol. 35 No. 13, July 1936, pp. 219-22.

57. 1936 Brandtzæg, A., "Zulässige Betondruckspannungen in rechteckigen Eisenbetonquerschnitten bei aussermittigem Druck," Final Report, Second Congress, International Association for Bridge and Structural Engineering, Berlin-Munich, Oct. 1936, pp. 121-35.

58. 1936 Melan, J., "Die Biegebruchspannungen des Eisenbetonbalkens," Beton und Eisen, Vol. 35 No. 19, Oct. 1936, pp. 315-17.

59. 1936 Emperger, F. v., "Der Beiwert n," Beton und Eisen, Vol. 35 No. 19, Oct. 1936, pp. 324-32.

60. 1936 Saliger, R., "Bruchzustand und Sicherheit im Eisenbetonbalken," Beton und Eisen, Vol. 35 Nos. 19 and 20, Oct. 1936, pp. 317-20 and 339-46.

61. 1936 Brandtzæg, A., "Forelesninger i jernbetong ved Norges tekniske høiskole," Tapirs forlag, Trondheim, Norway, 1937.

62. 1937 Hajnal-Konyi, K., "The Modular Ratio—A New Method of Design Omitting m," Concrete and Constructional Engineering, Vol. 32 Nos. 1, 2 and 3, Jan.-March 1937, pp. 11-26, 129-32 and 189-208.

63. 1937 Whitney, C. S., "Design of Reinforced Concrete Members Under Flexure and Combined Flexure and Direct Compression," ACI Journal, March-April 1937; Proceedings Vol. 33, pp. 483-98.

64. 1937 Lyse, I., "Der Beiwert n im Eisenbetonbau," Beton und Eisen, Vol. 36 No. 7, April 1937, pp. 124-25.

65. 1937 Roš, M., "Versuche und Erfahrungen an ausgeführten Eisenbeton-Bauwerken in der Schweiz," Eidg. Material-Prüfungsanstalt, Bericht No. 99, Zürich, 1937. 405 pp.

66. 1938 Saliger, R., "Der bildsame Bereich im Eisenbetonbalken," Beton und Eisen, Vol. 37 No. 1, Jan. 1938, pp. 15-20.

67. 1938 Richart, F. E. and Olson, T. A., "The Resistance of Reinforced Concrete Columns to Eccentric Loads," ACI Journal, March-April 1938; Proceedings Vol. 34, pp. 401-20.

68. 1938 Thomas, F. G., "Studies in Reinforced Concrete. VI. The Strength and Deformation of Reinforced Concrete Columns Under Combined Direct Stress and Bending," Department of Scientific and Industrial Research, Building Research Technical Paper No. 23, London, July 1938. 42 pp.

69. 1938 Whitney, C. S., "Eccentrically Loaded Reinforced Concrete Columns," Concrete and Constructional Engineering, Vol. 33 No. 11, Nov. 1938, pp. 549-61.

69a. 1938 Wilson, W. M., Kluge, R. W. and Coombe, J. V., "An Investigation of Rigid Frame Bridges, Part II," University of Illinois Engineering Experiment Station Bulletin No. 308, Dec. 1938. 75 pp.

70. 1939 Glanville, W. H. and Thomas, F. G., "Studies in Reinforced Concrete. V. Moment Redistribution in Reinforced Concrete," Department of Scientific and Industrial Research, Building Research Technical Paper No. 22, London, May 1939. 52 pp.

71. 1939 Habel, A., "Berechnung der Tragfähigkeit von Eisenbetonsäulen auf n-freier Grundlage," Beton und Eisen, Vol. 38 Nos. 13 and 15, July 1939, pp. 221 and 248.

72. 1939 Johnston, B. and Cox, K. C., "High Yield-Point Steel as Tension Reinforcement in Beams," ACI Journal, Sept. 1939; Proceedings Vol. 36, pp. 65-80.

73. 1939 "Regler for utførelse av arbeider i armert betong, N.S. 427," Oslo, Oct. 1939. 83 pp.

74. 1940 Whitney, C. S., "Plastic Theory in Reinforced Concrete Design," Proceedings ASCE, Dec. 1940; Transactions ASCE, Vol. 107, 1942, pp. 251-326.

75. 1941 Cox, K. C., "Tests of Reinforced Concrete Beams with Recommendations for Attaining Balanced Design," ACI Journal, Sept. 1941; Proceedings Vol. 38, pp. 65-80.

76. 1941 Andersen, P., "The Resistance to Combined Flexure and Compression of Square Concrete Sections," University of Minnesota Engineering Experiment Station, Technical Paper No. 29, 1941. 27 pp.

77. 1941 Guerrin, A., "Les théories nouvelles de la flexion dans les pièces en béton armé," Dunod, Paris, 1941. 450 pp.

78. 1942 Roš, M., "Festigkeit und Verformung von auf Biegung beanspruchten Eisenbetonbalken," Eidg. Material-Prüfungsanstalt, Bericht No. 141, Zürich, Oct. 1942.

79. 1943 Boase, A. J. and Morgan, C. E., "Balanced Design for Reinforced Concrete," ACI Journal, Feb. 1943; Proceedings Vol. 39, pp. 277-96.

80. 1943 Jensen, V.P., "The Plasticity Ratio of Concrete and its Effect on the Ultimate Strength of Beams," ACI Journal, June 1943; Proceedings Vol. 39, pp. 565-82.

81. 1943 Jensen, V. P., "Ultimate Strength of Reinforced Concrete Beams as Related to the Plasticity Ratio of Concrete," University of Illinois Engineering Experiment Station Bulletin No. 345, June 1943. 60 pp.

82. 1943 Evans, R. Harding, "The Plastic Theories for the Ultimate Strength of Reinforced Concrete Beams," Journal of the Institution of Civil Engineers, Paper No. 5376, London, Dec. 1943, pp. 98-121.

83. 1944 Bengtsson, B. Å., "Något om dimmensjoneringsmetoder för armerad betong," Betong, Vol. 29 No. 2, Stockholm, 1944, pp. 83-97.

84. 1944 Aas-Jakobsen, A., "Jernbetongtversnittets dimmensjonering," Betong, Vol. 29 No. 4, Stockholm 1944, pp. 288-95.

85. 1944 Shanley, F. R., "Basic Structures," John Wiley and Sons, Inc., New York, 1944. 392 pp.

86. 1944 Portland Cement Association, "Ultimate Design of Reinforced Concrete," Modern Developments in Reinforced Concrete No. 11, 1944. 19 pp.

87. 1944 Granholm, H., "En ny beräkningsmetod för armered betong," Transactions, Chalmers University of Technology, No. 38, Gothenburg, 1944. 88 pp.

88. 1945 Nylander, H., "Betongbalk belastad med excentrisk normalkraft, bereknad från brottstadiet," Betong, Vol. 30 No. 4, Stockholm, 1945, pp. 286-304.

89. 1945 Aas-Jakobsen, A., "Jernbetongstavers deformasjoner og knekking etter *n*-fri beregningsmetode," Tekniska Skrifter No. 114, Teknisk Tidskrifts Förlag, Stockholm, 1945. 19 pp.

90. 1946 Bjuggren, U., "Den armerade betongens verkningssätt i sprickstadiet vid böjning," Betong, Vol. 31 No. 3, Stockholm, 1946, pp. 182-211.

91. 1946 Richart, F. E., "The Structural Effectiveness of Protective Shells on Reinforced Concrete Columns," ACI Journal, Dec. 1946, Proceedings Vol. 43, pp. 353-63.

92. 1947 Ramaley, D. and McHenry, D., "Stress-Strain Curves for Concrete Strained Beyond the Ultimate Load," Laboratory Report No. SP-12, U. S. Bureau of Reclamation, March 1947. 22 pp.

93. 1947 "Building Code Requirements for Reinforced Concrete (ACI 318-47)," ACI Journal, Sept. 1947; Proceedings Vol. 44, pp. 1-64.

94. 1947 Hanson, R. and Rosenström, S., "Trykkforsök med slanka betongpelare," Betong, Vol. 32 No. 3, Stockholm, 1947, pp. 247-62.

95. 1947 Richart, F. E., Draffin, J. O., Olson, T. A. and Heitman, R. H., "The Effect of Eccentric Loading, Protective Shells, Slenderness Ratios, and Other Variables in Reinforced Concrete Columns," University of Illinois Engineering Experiment Station Bulletin No. 368, Nov. 1947. 128 pp.

96. 1947 Saliger, R., "Die neue Theorie des Stahlbetons auf Grund der Bildsamkeit im Bruchzustand," Second Edition, Franz Deuticke, Vienna, 1947. 110 pp.

97. 1948 Whitney, C. S., "Application of Plastic Theory to the Design of Modern Reinforced Concrete Structures," Journal of the Boston Society of Civil Engineers, Vol. 35 No. 1, Jan. 1948, pp. 30-53.

98. 1948 Aas-Jakobsen, A., "Gamle og nye dimmensjoneringsmetoder," Betong, Vol. 33 No. 2, Stockholm, 1948, pp. 41-74.

99. 1948 Saliger, R., "Von Gegenwartstand der Stahlbetontheorie," Österreichische Bauzeitung, Vol. 3 No. 11, Nov. 1948, pp. 170-77.

99a. 1948 Johansen, K. W., "The Ultimate Strength of Reinforced Concrete Slabs," Final Report, Third Congress, International Association for Bridge and Structural Engineering, Liège, 1948, pp. 565-70.

100. 1949 Brumer, M., "Comparative Designs of a Segmental Skewed Frame Concrete Bridge by the Straight Line and Plastic Theory Methods," ACI Journal, Jan. 1949; Proceedings Vol. 45, pp. 409-20.

101. 1949 Kleinlogel, A., "Zur Frage der zerstörungsfreien Prüfung von Beton im fertigem Bauwerk," Betonsteinzeitung, Wiesbaden, 1949, No. 2, pp. 17-21.

102. 1949 Chambaud, R., "Étude expérimentale de la flexion dans les pièces en béton armé," Annales de l'Institut Technique du Bâtiment et des Travaux Publics No. 61, Béton, Béton Armé No. 4, Paris, Feb. 1949. 36 pp.

103. 1949 Jones, R., "A Non-Destructive Method of Testing Concrete During Hardening," Concrete and Constructional Engineering, Vol. 44 No. 4, April 1949, pp. 127-29.

104. 1949 Blanks, R. F. and McHenry, D., "Plastic Flow of Concrete Relieves High-Load Stress Concentrations," Civil Engineering, Vol. 19 No. 5, May 1949, pp. 320-22.

105. 1949 Shanley, F. R., "Applied Column Theory," Proceedings ASCE, Vol. 75 No. 6, June 1949, pp. 759-88.

106. 1949 Baker, A. L. L., "A Plastic Theory of Design for Ordinary Reinforced and Prestressed Concrete Including Moment Re-Distribution in Continuous Members," Magazine of Concrete Research, Vol. 1 No. 2, London, June 1949, pp. 57-66.

107. 1949 Beyer, F. R., "Stresses in Reinforced Concrete Due to Volume Changes," ACI Journal, June 1949; Proceedings Vol. 45, pp. 713-22.

108. 1949 Chambaud, R., "Théorie élasto-plastique de la flexion dans les poutres en béton armé," Annales de l'Institut Technique du Bâtiment et des Travaux Publics No. 101, Béton, Béton Armé No. 10, Paris, Nov. 1949.

109. 1949 Hruban, K., "A Plastic Theory in the New Czechoslovakian Regulations," Concrete and Constructional Engineering, Vol. 44 No. 12, Dec. 1949, pp. 375-77.

110. 1949 Gebauer, F., "Die Plastizitätstheorie im Stahlbetonbau," Georg Fromme, Vienna, 1949. 184 pp.

110a. 1949 Danish Standard No. 411, "Dansk Ingeniørforenings Normer for Bygningskonstruktioner, 2 Beton- og jernbetonkonstruktioner," June 1949. 60 pp.

110b. 1949 Lundgren, H., "Cylindrical Shells," The Danish Technical Press, Copenhagen, 1949. 360 pp.

111. 1950 Hognestad, E. and Viest, I. M., "Some Applications of Electric SR-4 Gages in Reinforced Concrete Research," ACI Journal, Feb. 1950; Proceedings Vol. 46, pp. 445-54.

112. 1950 Lash, S. D. and Brison, J. W., "The Ultimate Strength of Reinforced Concrete Beams," ACI Journal, Feb. 1950; Proceedings Vol. 46, pp. 457-72.

113. 1950 Hadley, H. N., "When Concrete Becomes Discrete," Civil Engineering, Vol. 20 No. 4, April 1950, pp. 29-31.

114. 1950 Hognestad, E. and Siess, C. P., "Effect of Entrained Air on Bond Between Concrete and Reinforcing Steel," ACI Journal, April 1950; Proceedings Vol. 46, pp. 649-67.

The Engineering Experiment Station was established by the act of the Board of Trustees of the University of Illinois on December 8, 1903. Its purpose is to conduct investigations and make studies of importance to the engineering, manufacturing, railway, mining, and other industrial interests of the State.

The management of the Engineering Experiment Station is vested in an Executive Staff composed of the Director, the Associate Director, the Heads of the Departments in the College of Engineering, the Professor in charge of Chemical Engineering, and the Director of Engineering Information and Publications. This Staff establishes general policies governing the work of the Station, including the approval of material for publication. All members of the teaching staff of the College are encouraged to engage in scientific research.

To make the results of its scientific investigations available to the public, the Station publishes and distributes a series of bulletins. Occasionally it publishes circulars of timely interest presenting information of importance and a few reprints of articles appearing in the technical press written by members of the staff and others.

Above the title on the cover is given the number of the Engineering Experiment Station bulletin, circular, or reprint which should be used in referring to these publications.

For copies of publications or for other information address

THE ENGINEERING EXPERIMENT STATION,
UNIVERSITY OF ILLINOIS,
URBANA, ILLINOIS